Dissertation

zur Erlangung des Doktorgrades

der Naturwissenschaften

der Fakultät für Biologie

der Ludwig-Maximilian Universität München

Regulation of Synapse Number and Synaptic Plasticity by SynCAM1

vorgelegt von

Alexander Krupp

München im Juli 2010

Erstgutachter: Prof. Dr. Mark Hübener

Zweitgutachter: Prof. Dr. Andreas Herz

Tag der mündlichen Prüfung: 08. Oktober 2010

Die dieser Dissertation zugrunde liegende wissenschaftliche Arbeit erfolgte in der Zeit von August 2006 bis Juni 2010 unter der Anleitung von Dr. Valentin Stein am Max Planck Institut für Neurobiologie in Martinsried.

Ehrenwörtliche Versicherung:

Ich versichere hiermit ehrenwörtlich, dass ich diese Dissertation selbständig und ohne unerlaubte Beihilfe angefertigt habe. Ich habe mich dabei keiner anderen als der von mir ausdrücklich bezeichneten Hilfen und Quellen bedient.

Erklärung:

Hiermit erkläre ich, dass ich mich nicht anderweitig einer Doktorprüfung ohne Erfolg unterzogen habe. Die Dissertation wurde in ihrer jetzigen oder ähnlichen Form bei keiner anderen Hochschule eingereicht und hat noch keinen sonstigen Prüfungszwecken gedient.

München, im Juli 2010

Alexander Krupp

Preface

The present study was conducted as a collaboration of Elissa M. Robbins in the laboratory of Thomas Biederer at Yale University and myself in the laboratory of Valentin Stein at the Max Planck Institute of Neurobiology. For the benefit of being comprehensible, this thesis sometimes requires the presentation of data other people contributed to (e.g. the design and verification of one transgenic mouse line used). Whenever this is the case, the contribution of the individual researchers is stated in the figure legend.

Contents

List of Figures

List of Tables

Abbreviations

A	Ampere
ACh	acetyl choline
ACSF	artificial cerebrospinal fluid
AK	Alexander Krupp
AMPA	α-amino-3-hydroxy-5-methyl-4-isoxazole propionic acid
AMPAR	AMPA receptor
CA	*cornu ammonis*, region in the hippocampus
CADM	cell adhesion molecule
CAM	cell adhesion molecule
CaMKII	Ca^{2+}/calmodulin-dependent protein kinase II
CASK	calcium/calmodulin dependent serine protein kinase
CMV	cytomegalovirus
CNS	central nervous system
DIV	days *in vitro*
Dlg3	drosophila lethal discs large protein 3
Dox	doxycycline
E	*embryonic age in days*
EMR	Elissa M. Robbins
EPSP	excitatory postsynaptic potential
fEPSP	field EPSP
FERM	4.1-ezrin-radixin-moesin
GABA	γ-amino-butyric acid
GAD65	glutamate decarboxylase 65
GFP	green fluorescent protein
GluN	glutamate receptor subunit N, formally called NR (Collingridge et al., 2009)
GRIP1	Glutamate receptor-interacting protein 1
HEK	human embryonic kidney
Hz	Hertz
Ig	immunoglobulin
KO	knockout
KS	Kolmogorov-Smirnov
LP	lysis pellet
LTD	long-term depression
LTP	long-term potentiation
M	molar concentration
MAGUK	membrane associated guanylate kinase
mEPSC	miniature excitatory postsynaptic current
Mint1	Munc-18-interacting protein 1
MWM	Morris water maze
N-CAM	neuronal cell adhesion molecule
Necl-2	nectin-like molecule 2
NLGN	neuroligin
NMDA	N-methyl-D-aspartate
NMDAR	N-methyl-D-aspartate receptor
NRXN	neurexin

OE	mice that overexpress SynCAM1^{flag} conditionally
P	pellet
P	*postnatal age in days*
p55	synonym of membrane palmitoylated protein 1 (MPP1)
Pals2	proteins associated with Lin-7
PDZ	PSD-95, discs large, zona occludens1
PICK1	protein interacting with protein kinase Cα1
PKA	protein kinase A
PKC	protein kinase C
PP1	protein phosphatase 1
PPF	paired-pulse facilitation
PPR	paired-pulse ratio
PSD	postsynaptic density
PSD-95	postsynaptic density protein 95
PTX	picrotoxin
RA175	retinoic acid inducible protein 175
Ras1	Ras-related C3 botulinum toxin substrate 1
RT	room temperature, (22-24°C)
S	supernatant
Shank1	SH3 and multiple ankyrin repeat domains protein 1
SPM	synaptic plasma membranes
SynCAM	synaptic cell adhesion molecule
TARP	transmembrane AMPA receptor regulatory protein
TB	Thomas Biederer
TCM	trichlormethiazide
Tet	tetracycline
TRE	Tet-responsive element
TSLC1	tumor suppressor of non-small cell lung cancer
tTA	transcriptional transactivator
TTX	tetrodotoxin
vGLUT	vesicular glutamate transporter
VS	Valentin Stein
wt	wild-type

Summary

Synapses are asymmetric cell junctions with precisely juxtaposed presynaptic and postsynaptic sides that are organized by transsynaptic adhesion complexes. The molecular composition of these complexes, however, remains incompletely understood but is crucial to the understanding of synapse development. In this thesis, the immunoglobulin superfamily proteins SynCAM1 and SynCAM2 are shown to be expressed in neurons in the developing brain and to localize to excitatory and inhibitory synapses. SynCAM1 and SynCAM2 function as cell adhesion molecules and assemble with each other across the synaptic cleft to form a specific, transsynaptic SynCAM1/2 complex. Importantly, the results presented here demonstrate that SynCAM1 and SynCAM2 promote functional synapse formation as they increase the number of functional excitatory synapses.

In the developing brain, synaptogenesis is required for wiring neuronal circuits and to remodel networks in the adult brain. However, the contribution of SynCAM1 to synapse development in the developing brain remains incompletely understood. Motivated by the cell culture studies outlined above, the results of this thesis demonstrate that SynCAM1 regulates excitatory synapse formation and alters synaptic plasticity in genetically modified mice.

The analysis of an inducible transgenic mouse line and of knock-out mice demonstrates that elevated SynCAM1 increases excitatory synapse number, while its loss results in fewer synapses. In addition to promoting synaptogenesis, SynCAM1 is required to maintain this increase in synapse number. Moreover, SynCAM1 alters synaptic plasticity by regulating long-term depression. Animals that overexpress SynCAM1 do not exhibit this form of synaptic plasticity whereas loss of SynCAM1 results in more pronounced LTD. Furthermore, the organization of synapses by SynCAM1 affects spatial learning, with knock-out mice learning better than controls. The reciprocal effects of loss and increased expression of SynCAM1

reveal that this adhesion molecule contributes to the regulation of synapse number and plasticity, and impacts changes of neuronal networks in an activity-dependent manner. Taken together, these results demonstrate that SynCAM1 acts specifically in the brain as a synaptic cell adhesion molecule that regulates excitatory synapse number as well as synaptic plasticity and spatial learning.

1 Introduction

Once axons and dendrites have formed and reached their target regions, neurons establish connections with their respective partners. These highly specific intercellular junctions are called synapses, enable communication between neurons and provide the basis for brain function. Synaptic connections of individual neurons are thought to encode information and mediate memory formation. Adaption of the brain to the changing environment requires synapses to remain plastic throughout life. One fundamental question of synaptogenesis in the central nervous system remains to be addressed: How are the formation of new synapses, the integration into networks and the stability of existing synapses molecularly encoded?

The growth of axons and the physiology of synaptic transmission is relatively well understood. In contrast, the molecular processes underlying synapse formation and the specification of synapse diversity are less clear, as are the mechanisms mediating the assembly of synapses into neuronal circuits (Sudhof, 2008).

1.1 Three steps to synaptogenesis in the CNS

Cellular and molecular cues control three different phases of synapse formation (Holt and Harris, 1998; Gerrow and El-Husseini, 2006): In the early phase of synaptogenesis, axons and dendrites need to come in physical contact with each other which enables the interaction of cell surface proteins. During the following synapse assembly, the presynaptic release machinery as well as all postsynaptic proteins are recruited to the nascent synapse (Li and Sheng, 2003; Garner et al., 2006). In the third phase, synapses either become stable and undergo maturation (Fig. 1.1) or are eliminated.

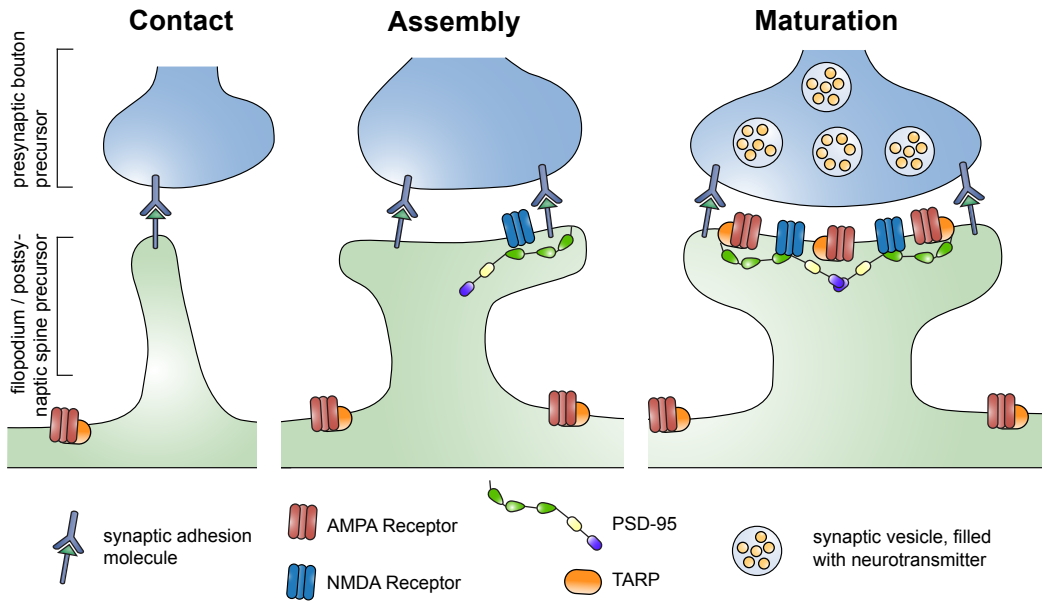

Figure 1.1: Three steps to form a synapse. Left to right, Contact formation: The cell membranes and surface-expressed cell adhesion molecules of a dendritic filopodium (green) and an axon (blue) come in physical contact. Assembly: Presynaptic vesicles filled with glutamate and the release machinery are formed. NMDA receptors as well as the postsynaptic density protein 95 (PSD-95) are recruited to the postsynaptic side. Maturation: The synapse becomes functionally active, often grows in size, now contains TARP-associated AMPA receptors and a larger PSD. The former filopodium has matured to a "spine".

1.1.1 Target recognition and initial contact formation

CNS synapse formation first requires axon growth to the respective target area and a subsequent process in which contacts between axons and dendrites are established. Two conceptionally different models of synapse formation have been proposed over the decades: Sotelo showed that spine development is independent of the presynaptic terminal in purkinje cells (Sotelo, 1990). Miller and Peters proposed a contradictary model that predicts the growth of spines from dendritic shafts, triggered by the axon terminal (Miller and Peters, 1981). Both models might be inspired by the first studies of synaptogenesis at the neuromuscular junction and might not fully reflect CNS synapse formation. However, technical advancements of high resolution microscopy of nascent synapses in tissue culture and in living animals provided data in favor of the so-called filopodia model of synaptogenesis (Yuste and Bonhoeffer, 2004): Early in development, dendrites are lined with highly motile filopodia. According to the filopodia model, local dendritic Ca^{2+} signals control the outgrowth of filopodia that

search their environment for axonal partners (Lohmann et al., 2005). Upon contact with an axon, a filopodium can retract or grow in a different direction if no synapse is formed with the respective axon. Alternatively, the filopodium can remain at the contact site and thereby define a site of synapse formation (Fig. 1.1). Very little is known about this early phase of synaptogenesis but it seems conceivable that surface molecules on the axonal and dendritic membranes mediate early axon-dendrite interactions, regulate subsequent cell signalling and thereby control synapse formation (Waites et al., 2005; Gerrow and El-Husseini, 2006).

1.1.2 Excitatory synapse formation

The transformation of an axo-dendritic contact into a synapse requires the recruitment of the presynaptic release machinery, of postsynaptic receptors, of receptor-associated proteins, and of signaling molecules to the developing synapse. At the same time, this site of initial contact of axon and dendrite undergoes morphological changes and gives rise to a presynaptic bouton and to a postsynaptic spine (Fig. 1.1).

Distinct axonal regions can give rise to presynaptic boutons and accommodate synaptic vesicles containing transmitters, the basis of chemical neurotransmission. Many molecules that are required to form a presynapse are preassembled in transport vesicles and delivered to the site of synapse formation in bulk. Resembling an 'instant presynapse', these transport vesicles contain synaptic vesicle precursors, or components of the presynaptic release machinery (Carroll et al., 1999; Shapira et al., 2003; Ziv and Garner, 2004). Fully functional presynapses contain two pools of synaptic vesicles: The vesicles can form the reserve pool that is not anchored to the synaptic membrane. Alternatively, vesicles can be docked at the active zone of the presynaptic membrane and comprise the so-called 'readily-releasable vesicle pool' (Sudhof, 2004). Vesicle docking requires recruitment and assembly of an extensive protein matrix to the presynaptic membrane. The SNARE complex of proteins plays a central role in vesicle docking, serves as a Ca^{2+} sensor, and mediates vesicle fusion (Sudhof and Rothman, 2009). How the recruitment of synaptic vesicles is triggered and whether cell adhesion molecules (CAMs) play a role therein remains to be investigated.

The most prominent neurotransmitters contained in synaptic vesicles in the CNS are glutamate, γ-amino-butyric acid (GABA), glycine, acetyl choline (ACh), dopamine and sero-

tonin. Of these, glutatmate is by far the most abundant neurotransmitter in the mammalian CNS and glutamatergic synapses are the main subject of this study.

Presynaptic boutons and postsynaptic spines are separated by the synaptic cleft, which is bridged by cell adhesion molecules to link the pre- and the postsynaptic side. Transsynaptic communication by CAMs might ensure that the transmitter released from the presynapse and the receptors at the postsynapse match. Synapses are surrounded by so-called 'puncta adherentia' that stabilize synaptic contacts and are presumably composed of CAMs (Spacek, 1985).

Formation of the postsynaptic side requires the recruitment of receptors and a variety of accessory scaffolding and signalling molecules. Accessory proteins as well as receptors are anchored to the postsynaptic side by a dense protein matrix (Han and Kim, 2008). This densely packed network of proteins appears dark in electron micrographs and was hence termed postsynaptic density (PSD). Apart from receptors and accessory proteins, many cell adhesion molecules are localized to the synapse and play important roles in synapse formation and synapse maintenance, as well as shaping synapse function (Kim and Sheng, 2004; Dalva et al., 2007).

In contrast to presynapse formation, most components of the postsynapse are not recruited in preassambled vesicles but individually. AMPA- and NMDA receptors are transported to the postsynapse by distinct kinesin family motors (Setou et al., 2000; Setou et al., 2002; Shin et al., 2003). At the postsynapse, NMDA receptors directly bind to PSD-95 and are thereby anchored at the postsynaptic membrane. Unlike NMDA receptors, AMPA receptors (AMPAR) are not anchored to the postsynapse via direct interactions with PSD-95 but via transmembrane AMPA receptor regulating proteins (TARPs) (Tomita et al., 2007). TARPs regulate AMPAR exit from the endoplasmic reticulum, subsequent trafficking and AMPAR function (Ziff, 2007).

Some findings suggest a role of the postsynaptic side in inducing presynapse differentiation, which was shown in co-culture experiments of neurons and non-neuronal cells that express neuroligin or SynCAM1. In these experiments, axons that contact the neuroligin or SynCAM1 expressing non-neuronal cells formed presynaptic structures (Scheiffele et al., 2000; Biederer et al., 2002). Thereby, neuroligin and SynCAM1 were identified as the first two adhesion molecules that induce presynaptic differentiation.

1.1.3 Synapse maturation

Once formed, synapses are in fact quite dynamic and the strength of existing synapses can still be modulated. The transformation of nascent synaptic contacts into functional synapses is termed 'synapse maturation' (Waites et al., 2005; Gerrow and El-Husseini, 2006). Developing glutamatergic synapses do initially not contain AMPA- but only NMDA receptors (Li and Sheng, 2003). In contrast to AMPARs, NMDARs are only permeable at positive membrane potentials (see 1.3.1) and synapses that only contain NMDAR can thus not be activated by glutamate release. They are therefore termed 'silent synapses' and can become physiologically active by the incorporation of AMPAR, which can for example be triggered by high frequency stimulation and might be one of the mechanisms underlying LTP (Liao et al., 2001). In early postnatal development, synapse maturation requires synaptic activity, which in turn results in the transformation of pure NMDAR based contacts that do not conduct ions at resting membrane potential, into conducting, AMPAR containing synapses (Durand et al., 1996). This early form of synapse maturation depends on activity and can be triggered experimentally by pairing presynaptic stimulation with postsynaptic depolarization. However, immature or 'silent' synapses are also observed at later stages of development (Kerchner and Nicoll, 2008).

During maturation, synapses grow in volume, the number of synaptic vesicles increases, and the PSD grows (Blue and Parnavelas, 1983). The enlarged PSD of mature synapses accomodates more receptors, which results in an increase in synaptic strength. One family of cell adhesion molecules, the neuroligins, were shown to mediate an increase in receptor density and thereby mediate synapse maturation (Varoqueaux et al., 2006). Despite the implication of CAMs in some aspects of synapse maturation, the intracellular signaling mechanisms that underly synapse maturation remain unclear.

1.2 Molecular mediators of synapse formation and plasticity

Recent evidence demonstrates that cell adhesion molecules play an important role in all phases of synaptogenesis. For instance, synaptically localized CAMs such as SynCAMs, neuroligins, neurexins, ephrins and Eph receptors, cadherins have been shown to influence various aspects of synaptogenesis (Yuste and Bonhoeffer, 2004; Dalva et al., 2007).

Table 1.1: Nomenclature and synonyms of SynCAM / CADM family members. Human genes are named according to the HUGO Gene Nomenclature Committee; mouse genes according to Mouse Genome Informatics provided by the Jackson Laboratory. Table modified from Biederer, 2006; Spiegel et al., 2007 .

gene name	CADM1	CADM2	CADM3	CADM4
protein name	SynCAM1	SynCAM2	SynCAM3	SynCAM4
old gene name				
human	IGSF4	IGSF4D	IGSF4B	IGSF4C
mouse	*Igsf4a*	*Igsf4d*	*Igsf4b*	*Igsf4c*
synonyms	Necl2 RA175 Tslc1 SgIGSF	Necl3	Necl1 TSLL1	Necl4 TSLL2

1.2.1 The family of synaptic cell adhesion molecules (SynCAMs)

SynCAMs comprise a family of four immunoglobulin family proteins that are only found in vertebrates and were identified in human, rodents, chicken and recently in zebrafish (Biederer, 2006; Pietri et al., 2008). SynCAM family proteins are composed of three Ig-like domains, a single transmembrane domain and a short cytosolic tail with a protein 4.1 interaction sequence and a PDZ class II binding motif (Biederer, 2006) (see Fig. 1.2). All four SynCAM family proteins share a high degree of 35 to 50% amino acid identity between the full-length proteins and are encoded by the *Cadm* (cell adhesion molecule) gene family (see Table 1.1) (Biederer, 2006). Most of the amino acid variability between the four family members is found in the extracellular domain. The juxtamembrane region of the extracellular domain is predicted to be O-glycosylated and the three Ig domains contain multiple N-glycosylation sites, which influence the binding specificity between SynCAM proteins (Fogel et al., 2007; Galuska et al., 2010).

SynCAM 1-4 are widely expressed in excitatory and inhibitory neurons of the developing and adult central nervous system (Thomas et al., 2008). Investigation of different brain regions in the developing and mature mouse brain indicates that each SynCAM exhibits a defined spatiotemporal expression pattern. This is particularly notable in the cerebellum, where SynCAMs display highly distinct expression patterns in cerebellar granule and Purkinje cells (Thomas et al., 2008). Guided by the recent analysis of the four SynCAM

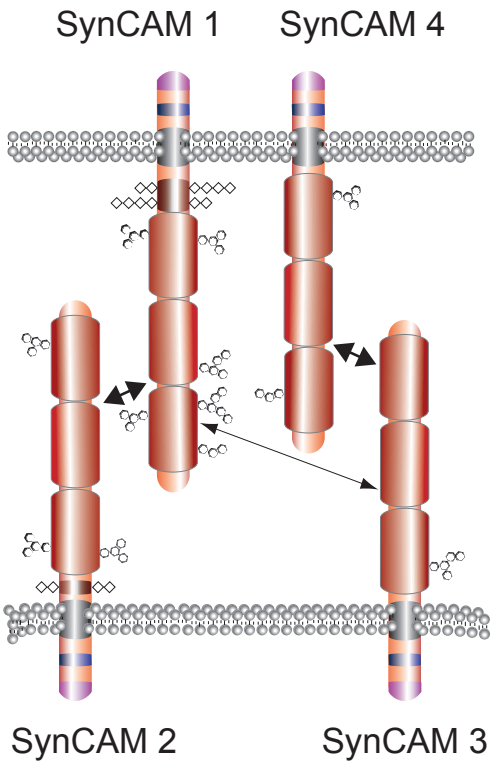

Figure 1.2: Structure and interaction of SynCAM family proteins. Model of heterophilic interactions between SynCAM family members. SynCAM1 and 2 as well as 3 and 4 form two strong cognate cell adhesion pairs (bold arrows). The heterophilic interaction of SynCAM1 and 2 is mediated by the Ig domains one and two of SynCAM1 and requires N-glycosylation (Fogel et al., 2007). In addition, SynCAM 1 and 3 can bind more weakly (light arrow). The additional homophilic interactions of SynCAM 1, 2, and 3 are not shown. Ig-like domains are represented as barrels, the 4.1 binding motif is shown in blue, the PDZ class II binding site in purple, predicted N-glycosylation domains of SynCAM1 and 2 are depicted in brown, the PDZ class II binding motif in purple, the 4.1 binding motif in blue, N-linked carbohydrates as hexagons, and O-linked carbohydrates as rhombi. Predicted glycosylation sites in SynCAM proteins are drawn to scale (Biederer, 2006). Figure modified from (Fogel et al., 2007).

family members that share the same domain organization (Biederer, 2006), SynCAM2 was considered as candidate heterophilic binding partner of SynCAM1 and their interaction was characterized (Fig. 3.1). Three prominent interactions are observed, mediated by the extracellular domains of SynCAMs 1/2, 1/3, and 3/4 (Fig. 1.2) (Fogel et al., 2007; Thomas et al., 2008). These expression and adhesion profiles of SynCAMs together with their previously reported functions in synapse organization indicate that SynCAM proteins contribute to CNS synapse formation. More specifically, it was not known whether they together confer synaptic adhesion and can contribute to synapse organization and function. In the first

part of this study, SynCAMs were identified as a family of neuronal adhesion molecules that prefer heterophilic over homophilic interactions, enabling them to cooperate in synapse organization (published in Fogel et al., 2007).

The best characterized member of this protein family is SynCAM1, which was identified in multiple contexts and will be the main subject of this study. Under the names Necl-2 (nectin-like molecule 2) and RA175 (retinoic acid inducible protein 175), SynCAM1 was described to mediate cell-adhesion and to be required for spermatid motility (Urase et al., 2001; Shingai et al., 2003) (see Table 1.1). In the nervous system, SynCAM1 can induce the formation of functional synapses in cell culture and is thought to play an important role in synaptogenesis (Biederer et al., 2002; Sara et al., 2005).

Presentation of SynCAM1 from non-neuronal cells to cultured hippocampal neurons drives neurons to develop fully functional excitatory presynaptic terminals at sites of contact (Biederer et al., 2002). Furthermore, SynCAM1 overexpression promotes excitatory neurotransmission (Biederer et al., 2002; Sara et al., 2005). However, the role of SynCAM1 in the intact brain with regard to synapse formation and to synapse function remained elusive. Furthermore, the function of SynCAM1 in the intact brain and its differential effects during development were unknown. Resolving the function of SynCAM1 in synapse formation and in synapse function was the overall goal of this project.

Some properties of SynCAM1 were characterized in the context of cancer research in which SynCAM1 is mostly named Tslc1 (tumor suppressor of non-small cell lung cancer) and serves as tumor suppressor in glioma and in non-small cell lung cancer (Kuramochi et al., 2001; Houshmandi et al., 2006). The cytoplasmic domain of SynCAM1 is critical for its tumor suppressor activity and cytosolic signaling proteins bind to this domain to mediate cell signaling (Mao et al., 2003).

Specifically, the membrane associated guanylate kinase (MAGUK) family proteins Dlg3 (drosophila lethal discs large protein 3), Pals2 (proteins associated with Lin-7), and CASK (calcium/calmodulin-dependent serine protein kinase) as well as Mint-1 and syntenin interact with SynCAM1 (Biederer et al., 2002; Kakunaga et al., 2005). These findings can advance the understanding of the contribution of MAGUKs to SynCAM1 signaling in the nervous system and could give insight into the role of SynCAM1 in synapse formation. MAGUK proteins are generally localized to synapses and regulate trafficking, targeting, and signaling of ion

channels to regulate synapse assembly and function. MAGUKs are thus potential mediators of the functions of SynCAM1 in the nervous system (Hsueh, 2006). For instance, CASK forms a CASK/Veli/Mint-1 protein complex that binds the C-terminal tail of the NMDAR subunit GluN2B and recruits NMDA receptors to the synapse, which is an important process in the early phase of synaptogenesis (Jo et al., 1999).

In addition to cell signaling, SynCAM1 interacts with the FERM domain protein 4.1B (also called Dal-1), which connects SynCAM1 to the actin cytoskeleton (Yageta et al., 2002). This interaction is triggered by activation of protein kinase C and induces colocalization of SynCAM1 with protein 4.1B in regions of actin cytoskeleton reorganization (Yageta et al., 2002). The latter finding might be related to the synaptogenic capacity of SynCAM1 as synaptogenesis requires changes of the actin cytoskeleton (Dillon and Goda, 2005).

In the second part of this study, it was demonstrated that the increased expression of SynCAM1 boosts the number of excitatory synapses in transgenic mice. Nicely complementing this finding, SynCAM1 knock-out mice exhibit fewer excitatory synapses. Furthermore, the synaptogenic capacity of SynCAM1 is not restricted to a narrow time window in early development since SynCAM1 retains its synaptogenic potential in juvenile animals. SynCAM1 expression is required to sustain the SynCAM1-induced increase in synapse number. In addition to synapse formation, SynCAM1 also impacts synaptic plasticity and overexpression of SynCAM1 decreases long-term depression and impairs spatial learning. Again, loss of SynCAM1 has the complementary effect and increases long-term depression and promotes learning. In summary, the present study defines SynCAM-mediated synaptic adhesion to regulate synapse number, synaptic plasticity, and to impact spatial learning. Thus, SynCAM1 plays a central role in synaptogenesis and in synaptic plasticity in the CNS.

1.2.2 The neuroligin-neurexin adhesive pair

Neuroligin (NLGN) and Neurexin (NRXN) family proteins play an important role in synapse formation and function. Neuroligins are mainly localized at the postsynaptic side (NLGN1-4) (Ushkaryov et al., 1992; Rudenko et al., 1999). Postsynaptic neuroligins interact with presynaptic neurexins via their extracellular domains and three of the four known neurexins (NRXN 1-3) have been reported in mammals. Each of these neurexins is transcribed from

dual promoters that enable the expression of two distinct isoforms: a long α isoform and a short β isoform with the short β isoform binding to neuroligins (Sudhof, 2008). Neurexins have been found on both, inhibitory and excitatory presynapses (Ushkaryov et al., 1992; Ullrich et al., 1995; Dean et al., 2003; Graf et al., 2004) but can also be found postsynaptically (Kattenstroth et al., 2004; Taniguchi et al., 2007).

Similar to SynCAM family proteins, neuroligin expression in non-neuronal cells induces presynaptic differentiation upon contact with neurons (Scheiffele et al., 2000). Neuroligins interact with β neurexins that are linked to the presynaptic release machinery (Futai et al., 2007), induce clustering of voltage–gated calcium channels and mediate changes in the actin cytoskeleton (Hata et al., 1996; Butz et al., 1998; Biederer and Sudhof, 2000; Atasoy et al., 2007). Postsynaptically, neuroligins regulate spine number as well as synapse density, and cluster NMDA receptors in cell culture via binding to PSD-95 (Chih et al., 2005). In cultured neurons, overexpression of neuroligins 1 and 2 specifically promotes the maturation of excitatory and inhibitory synapses, respectively (Chubykin et al., 2007). Accordingly, deletion of either protein decreases synaptic responses. Some observations of neuroligin function in cell culture studies could not be reproduced *in vivo* and it remains to be shown whether these results reflect the function of neuroligins in the intact brain.

In addition to these cell culture experiments, it is known from fixed tissue that neuroligins are expressed in a cell–type specific manner: Neuroligins 1 and 4 are exclusively found at excitatory and neuroligin 2 only at inhibitory synapses (Song et al., 1999; Graf et al., 2004; Varoqueaux et al., 2006; Chubykin et al., 2007). In contrast, neuroligin 3 is found in both cell types (Budreck and Scheiffele, 2007). Following up on these results from experiments in cell culture, analysis of the role of neuroligin *in vivo* revealed that even in triple knockout animals of neuroligin 1-3, synaptogenesis still occurred. Despite normal synaptogenesis, these animals died after birth from imbalanced cerebellar transmission and subsequent respiratory failure, which is attributed to impaired synapse maturation in these animals (Varoqueaux et al., 2006). In addition, neuroligins are implicated in the assembly of the synaptic machinery. Binding of neurexin to postsynaptic neuroligin induces clustering of PSD-95 and NMDA but not AMPA receptors at the postsynapse (Graf et al., 2004).

In summary, neuroligins induce synapse formation when overexpressed *in vitro* but not *in vivo*. Mice lacking neuroligins 1-3 exhibit deficits in synapse maturation but do not show

alterations in synapse number. Hence, neuroligins do most likely not play a prominent role in synaptogenesis but affect maturation of excitatory as well as inhibitory synapses.

1.2.3 Ephrins and Eph receptors

Eph receptors and their ephrin ligands guide axons during neural development and regulate synapse formation and neuronal plasticity. Ephrins and Eph receptors possess repulsive effects in axon guidance (Drescher et al., 1995). EphB receptor signaling regulates filopodia motility and thereby mediates the capability of a neuron to sense its environment for putative axonal partners to form a synapse with (Kayser et al., 2008). Ephrins and Eph receptors are furthermore implicated in NMDAR clustering and in synapse formation (Dalva et al., 2000; Klein, 2009), in synaptic plasticity (Grunwald et al., 2004), and mediate interactions between neurons and glia (Filosa et al., 2009). Different from SynCAMs, neither ephrins nor Eph receptors were shown to induce the formation of synapses.

More specifically, EphB2 receptors interact with the GluN1 subunit of NMDA receptors. In detail, stimulation of EphB2 with soluble ephrinB resulted in EphB2 and subsequent NMDA receptor clustering at the postsynaptic membrane (Dalva et al., 2000). Furthermore, EphB2 activation triggers the phosphorylation of the cell surface proteoglycan syndecan-2 and subsequent spine morphogenesis (Ethell et al., 2001). The importance of EphB receptors in spine morphogenesis is highlighted by a study describing the triple knockout of EphB1, 2, and 3 that results in the loss of normal spine morphology and in a decrease in functional synapse number (Henkemeyer et al., 2003). Surprisingly, the total number of dendritic protrusions remains unchanged in the triple KO; however, the length of the individual protrusions increases and the morphology is reminiscent of filopodia-like structures that are mainly found in early synapse development.

The filopodia-like structures in the EphB triple KO are devoid of AMPARs and NMDARs which supports the notion that they represent immature structures which might indicate a maturation defect and imply EphR signalling in synapse maturation (Kayser et al., 2006). The phenotype of the triple KO animals can be partially rescued by expression of the EphB2 extracellular domain, which might mean that EphB2 kinase activity is dispensable for proper spine differentiation. It is noteworthy that the single knockout of any of

these three EphB receptors did not result in this phenotype which indicates redundancy and complementation within the EphB receptor family (Kayser et al., 2006).

1.2.4 Integrins

Integrins are transmembrane proteins that are expressed in all vertebrate tissues except red blood cells and mediate the interaction of cells with the surrounding extracellular matrix and with neighboring cells. Upon binding of a target molecule to their extracellular domain, integrins interact with the actin cytoskeleton and can mediate cell migration, cell adhesion, differentiation and other aspects of cell signalling.

In the nervous system, integrins are implicated in neuron-glia interactions (Gleeson and Walsh, 2000; Forster et al., 2002), in the maturation of synapses (Chavis and Westbrook, 2001), in the modulation of synaptic transmission (Kramar et al., 2003; Lin et al., 2003; Cingolani et al., 2008), and in the regulation of synaptic plasticity (Chun et al., 2001; Chan et al., 2003). The effects of integrins on synapse maturation have been demonstrated in various studies. For instance, the loss of β1-integrin causes defects in the formation of the presynaptic release machinery (Huang et al., 2006). Using NMDAR subunit composition as a measure of synapse maturation, it was shown that blocking integrin activation keeps synaptic NMDAR composition in an immature state (Chavis and Westbrook, 2001). Similarly, integrins directly mediate synaptic transmission through modifications of the physiological properties of AMPA and NMDA receptors by altering their permeability for Ca^{2+} (Lin et al., 2003; Bernard-Trifilo et al., 2005; Chan et al., 2006; Cingolani et al., 2008). Since an increase of the intracellular Ca^{2+} concentration can induce synaptic plasticity and is mediated by NMDARs, integrins are a potential modulator of synaptic plasticity. Indeed, LTP is impaired in mice with reduced integrin expression or function (Chun et al., 2001; Chan et al., 2003; Chan et al., 2006; Huang et al., 2006). In summary, integrins are important players in the formation and in controlling the function of synapses with regard to synapse maturation and plasticity.

1.2.5 Cadherins

Cadherins are a class of molecules that is implicated in neuronal target recognition in mammals (Shapiro and Colman, 1999). At least 80 cadherin isoforms have been described and matching cadherins between axons and dendrites is believed to promote selective adhesion between appropriate partners. All three major subtypes of cadherins are expressed in the brain: classical cadherins, cadherin-related proteins, and protocadherins. The expression pattern of cadherins and of their intracellular binding partner catenin varies with cell type and developmental status (Benson and Tanaka, 1998; Togashi et al., 2002; Jontes et al., 2004), which is often interpreted to reflect their importance for synaptic connectivity. For instance, overexpression of dominant negative N-cadherin lacking the extracellular domain causes spine loss and the formation of filopodia-like structures in cultured hippocampal neurons (Togashi et al., 2002). This effect was less prominent in older neurons, suggesting differential effects of cadherins in development. Nevertheless, synapse initiation is not blocked but merely delayed by the expression of a dominant negative cadherin, indicating a role of cadherins in target recognition but not in synapse induction (Bozdagi et al., 2004). The same study revealed that blocking cadherin function results in smaller synapses that are functionally impaired. This observation suggests that cadherins stabilize synapses and are involved in structural and functional maturation but are not required for induction of synapse formation.

The contribution of protocadherins to synapse maturation was addressed in a study of mutant mice with a deletion of all 22 γ-protocadherins. These animals are not viable and die from neuronal apoptosis which makes the detailed analysis of the phenotype impossible (Wang et al., 2002). Introducing an additional mutation that prevents apoptosis revealed that loss of all γ-protocadherins results in fewer and smaller synapses (Weiner et al., 2005) and highlights the importance of γ-protocadherins for synapse maturation and maintenance. The mechanism underlying cadherin function was addressed in a study presenting a recombinant N-cadherin ectodomain to cadherin expressing cells and revealed that ligand binding induces Rac1 (Ras-related C3 botulinum toxin substrate 1) dependent anchoring of N-cadherin to the actin cytoskeleton (Lambert et al., 2002). This association of cadherins with the cytoskeleton might enable the transduction of mechanical forces across the cell

membrane and thereby contribute to neuron morphogenesis. In summary, cadherins represent an important adhesive pair that supposedly controls contact specificity and synapse maturation and maintenance in a Ca^{2+}-dependent manner. However, protocadherins are not essential for synaptogenesis itself as demonstrated by the cited KO study.

1.3 Synaptic transmission and plasticity

Chemical transmission between neurons requires the release of neurotransmitter from the presynapse. The released transmitter then diffuses across the synaptic cleft and binds to receptors on the postsynaptic side. Transmitter binding to ionotropic receptors induces a conformational change of the receptor that causes the receptor pore to open to conduct ions across the cell membrane. Alternatively, transmitter binding to metabotropic receptors can directly activate cell signaling.

1.3.1 Glutamatergic synaptic transmission

Action potentials depolarize the presynaptic membrane and lead to membrane-depolarization and opening of voltage dependent Ca^{2+} channels. The resulting influx of Ca^{2+} into the presynapse triggers vesicle fusion and transmitter release. The transmitter diffuses across the synaptic cleft and binds to receptors at the postsynaptic side.

The most abundant neurotransmitter in the CNS is glutamate and the two glutamate receptor subclasses of AMPA– and NMDA receptors are most relevant to this thesis. Fast glutamatergic transmission in the CNS is mediated by AMPA receptors, which conduct cations across the membrane. AMPA receptors are tetrameric complexes composed of four subunits, termed GluA1-4 (Hollmann and Heinemann, 1994; Collingridge et al., 2009). Each of these subunits has three transmembrane domains and one re-entrant loop. These loops form the pore of the receptor. The extracellular domains of the receptor form the ligand-binding domain. Binding of glutamate to at least two of the four binding sites induces a conformational change of the receptor that results in opening of the channel pore. While the ligand is still bound, AMPA receptors desensitize rapidly by another conformational switch, and recover slowly from this desensitization.

AMPAR are heterotetrameric, mostly formed of a symmetric 'dimer of dimers' of

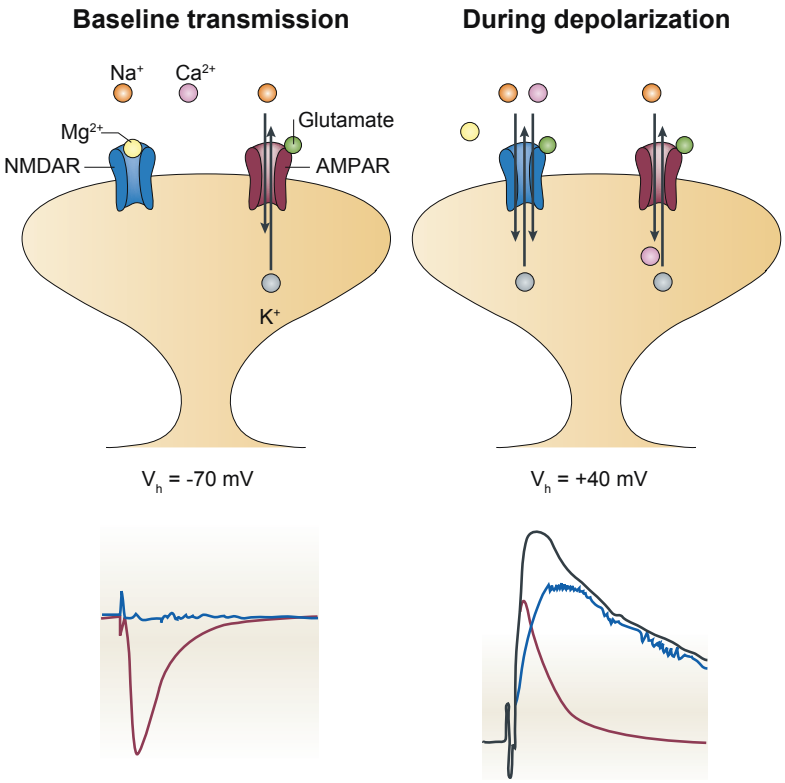

Figure 1.3: Physiological properties of AMPAR and NMDAR. AMPAR and NMDAR are permeable to Na^+ and K^+, with reversal potentials close to 0 mV. NMDARs additionally exhibit important interactions with divalent cations: whereas Ca^{2+} is highly permeant, mediating the important signalling functions of these receptors, Mg^{2+} gets stuck in the pore, producing voltage-dependent NMDAR blockade at negative membrane potentials (blue trace in bottom left panel). Thus, at the resting membrane potential (left-hand panels), synaptic glutamate will evoke an excitatory postsynaptic current (EPSC) that is mediated almost entirely by AMPARs (bottom left panel, red trace). Depolarized potentials will relieve the Mg^{2+} blockade, and EPSCs will subsequently contain contributions from both AMPARs and NMDARs (bottom right panel, black trace). Using selective antagonists to one or the other receptor, these components can be isolated: the AMPAR component is represented by the red trace in the bottom right panel; the NMDAR component is represented by the blue trace. Figure adopted from Kerchner et al., 2008.

GluA2 and either GluA1, GluA3 or GluA4. These GluA2 containing receptors mainly conduct Na^+ and K^+ and are impermeable to Ca^{2+}. In contrast, GluA2 lacking receptors are Ca^{2+} permeable and can be blocked by endogenous polyamines at positive membrane potentials. GluA2 lacking AMPAR are hence called 'inwardly rectifying', which means that they pass less outward current than inward current.

In the adult hippocampus, two populations of AMPA receptors predominate: receptors

composed of GluA1/GluA2 and GluA2/GluA3 (Wenthold et al., 1996). Although the majority of AMPA receptors in the CNS are GluA2-containing, significant expression of GluA2-lacking receptors has been observed. Since GluA2-lacking receptors are Ca^{2+}-permeable, they have been implicated in the processes of synaptic plasticity and excitotoxicity.

NMDA receptors are another class of heterotetrameric glutamate receptors in the CNS. NMDARs are composed of two obligatory GluN1 subunits and of two GluN1, GluN2A-D, GluN3A or GluN3B subunits. In contrast to AMPARs, ionotropic NMDA receptors do not conduct ions at resting membrane potential because their channel pore is blocked by Mg^{2+} at negative membrane potentials. Thus, NMDA receptors require previous membrane depolarization to release the so-called Mg^{2+} block and become permeable. The NMDA receptor therefore functions as a 'molecular coincidence detector'. The important kinetic differences between the two receptor subtypes are outlined in Fig. 1.3: Whereas AMPAR-mediated currents activate quickly and decay within milliseconds, NMDAR-mediated currents activate more slowly and decay over hundreds of milliseconds. Since NMDA receptors are an important mediator of Ca^{2+} influx into the cell, they are implicated in Ca^{2+} mediated synaptic plasticity and in cell signalling.

Immature synapses mainly contain NMDA receptors, whereas AMPA receptors are incorporated into the postsynaptic membrane during synapse maturation (Durand et al., 1996). Comparatively small AMPA currents therefore represent a less mature state of the synapse. The ratio of AMPA and NMDA currents is thus used as a measure of synaptic strength and synapse maturation (see Fig. 1.3).

In contrast to action potential driven release, spontaneous vesicle fusion occurs in an action potential independent manner and spontaneously released glutamate can trigger miniature excitatory postsynaptic currents (mEPSCs). Assuming a constant probability of transmitter release, the frequency of mEPSCs is used as a measure of the number of synaptic inputs a cell receives, whereas mEPSC amlitude is thought to reflect postsynaptic receptor density (Raghavachari and Lisman, 2004). In this study, mEPSC recordings were employed to determine the effects of SynCAM1 on excitatory synapse number.

1.3.2 Synaptic plasticity

The brain needs to adapt to an ever changing environment throughout life. This adaption is mediated by changing synaptic transmission and neuronal connectivity between neurons in order to modify properties of the respective networks. Synaptic plasticity requires the strengthening and weakening of existing synaptic connections as well as the formation of new synapses and loss of unused synapses. In all cases, synaptic plasticity requires contact specificity and transsynaptic communication that is most likely mediated by CAMs.

The experimental paradigms used to study plasticity are inspired by the "Hebbian rule" which says that cells that fire together, also wire together (Hebb, 1949). Hence, increased synaptic activity results in strengthening of synaptic connections whereas paradigms representing low activity resulted in synapse weakening. LTP as well as LTD induction require neuronal activity and the NMDAR mediated influx of Ca^{2+} into the cell. Electrically induced LTP and LTD require distinct kinetics of Ca^{2+} influx: Induction of LTP requires a brief increase of the intracellular [Ca^{2+}] whereas weaker but prolonged increases of the intracellular [Ca^{2+}] result in LTD induction.

Following induction, LTP has two phases: An early phase, in which receptors are recruited to the synapse (Plant et al., 2006; Adesnik and Nicoll, 2007) and a late phase with altered protein synthesis, increase in spine size and gain of the number of spines (Engert and Bonhoeffer, 1999; Kelleher et al., 2004). Conversely, LTD can cause the loss of receptors from the synapse, a decrease in spine size and a decline in spine number (Dudek and Bear, 1992; Kandler et al., 1998; Carroll et al., 1999; Becker et al., 2008).

The form of LTD induced in this study depends on Ca^{2+} influx into the cell through NMDARs and potentially on additional release of Ca^{2+} from internal stores. Biochemical studies have indicated that LTD correlates with dephosphorylation of postsynaptic PKC and PKA substrates that might be mediated by protein phosphatase 1 (PP1) (Malenka and Bear, 2004). In addition, LTD is associated with the selective dephosphorylation of Ser-845 of the GluA1 intracellular domain (Lee et al., 1998). Dephosphorylation of Ser-845 might contribute to LTD expression because it decreases the open probability of AMPARs (Banke et al., 2000). Another mechanism underlying LTD is the rapid internalization of AMPARs in a dynamin- and clathrin-dependent mechanism (Carroll et al., 1999; Ehlers, 2000). Receptor

modification as well as internalization results in a decrease of synaptic strength. Another hypothesis postulates the existence of receptor slots at the postsynaptic membrane (Malinow and Malenka, 2002). According to the slot hypothesis, LTD induction would result in loss of slot proteins from the postsynaptic side, cause a decrease in the number of available slots and thereby decrease the number of AMPARs and synaptic strength. However, this hypothesis has not been proven experimentally but PSD-95 is a good candidate to serve as slot protein. Finally, the induction of LTD can result in the loss of synaptic contacts and thereby weaken synaptic transmission (Becker et al., 2008; Bastrikova et al., 2008). In summary, LTD induction causes the loss of AMPARs from synapses and the loss of entire synapses. LTD thereby mediates a decrease in synaptic strength and connectivity.

We are only beginning to understand the role of CAMs in synaptic plasticity. The contribution of integrins to synaptic plasticity is understood to some degree (Chun et al., 2001; Chan et al., 2003; Chan et al., 2006). Integrin signalling has been implicated in the regulation of NMDAR physiology (Lin et al., 2003; Bernard-Trifilo et al., 2005; Shi and Ethell, 2006) and in the abundance and subunit composition of AMPARs (Cingolani et al., 2008). Mice lacking EphB2 receptors exhibit defects in LTP and postsynaptic ephrinsBs are required for hippocampal LTP (Grunwald et al., 2001; Grunwald et al., 2004). Furthermore, interactions of ephrins and metabotropic glutamate receptors affect the induction of LTD (Piccinin et al., 2010). This thesis contributes to the understanding of CAMs in LTD and identifies SynCAM1 as a cell adhesion molecule that modulates long-term depression.

1.4 The hippocampus as a model system

The hippocampus is part of the limbic system and is buried deep within the medial temporal lobe. The hippocampus comprises three structures that serve distinct functions: Most inputs into the hippocampus originate in the entorhinal cortex and terminate in the gyrus dentatus. The excitatory neurons of the gyrus dentatus are called granule cells and their somata are located in the stratum granulosum. They form axonal projections, called mossy fibers, onto pyramidal cells of region three of the cornu ammonis (CA3). CA3 pyramidal cells send their axons, called Schaffer collaterals, through the stratum radiatum and project onto pyramidal cells in region one of the cornu ammonis (CA1). Finally, CA1 cells project to the subiculum

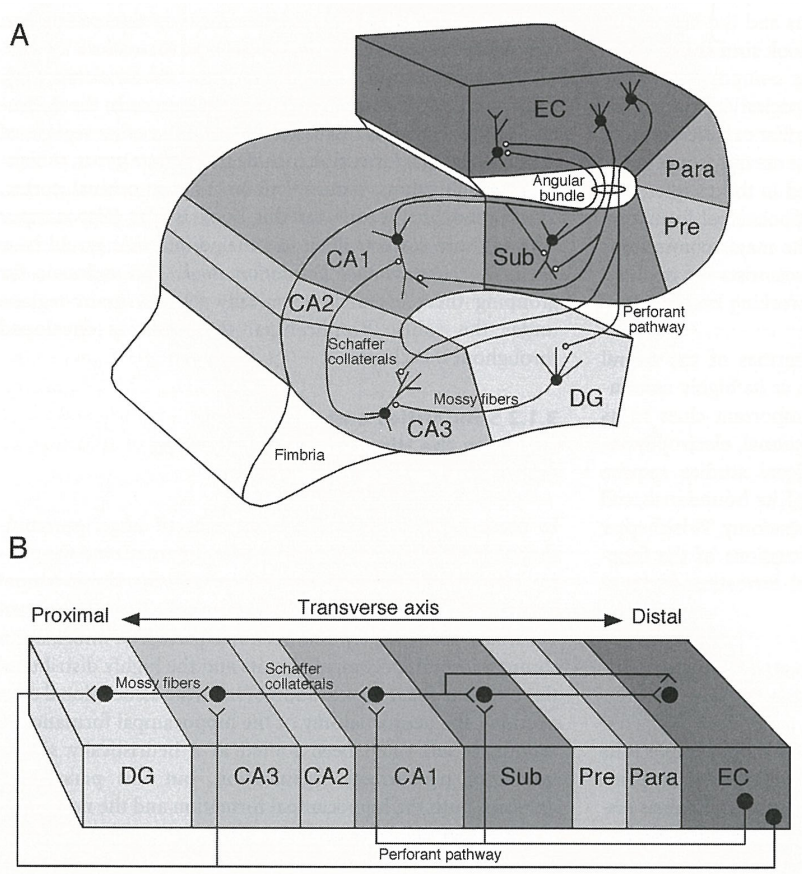

Figure 1.4: Connectivity and projections in the hippocampus. A. Neurons in layer II of the entorhinal cortex project to the dentate gyrus and the CA3 field of the hippocampus proper via the perforant pathway. Neurons in layer III of the entorhinal cortex project to the CA1 field of the hippocampus and to the subiculum via the perforant and alvear pathways. The granule cells of the dentate gyrus project to the CA3 field of the hippocampus via mossy fiber projections. Pyramidal neurons in the CA3 field of the hippocampus project to CA1 via Schaffer collaterals. Pyramidal cells in CA1 project to the subiculum. Both CA1 and the subiculum project back to the deep layers of the entorhinal cortex. **B**. Projections along the transverse axis of the hippocampal formation; the dentate gyrus is located proximally and the entorhinal cortex distally. Figure adapted from Sprouston and McBain, 2007.

that represents the output region of the hippocampus (Fig. 1.4).

The hippocampus plays an important role in long-term memory and in spatial navigation. These functions were extensively studied in rodents, enabled correlating synaptic plasticity and learning, and led to the identification of place cells that fire when the animal passes through a specific environment (Whitlock et al., 2006; Kemp and Manahan-Vaughan, 2007; Treves et al., 2008). However, the hippocampus did not receive too much attention in the early days of neurobiology. The first experimental studies using the hippocampus were

published in the 1950s and it suddenly became of interest in 1957 when its role in memory formation was demonstrated in a spectacular way: Scoville and Milner had removed the hippocampi of the now famous patient H.M. to treat epilepsy and observed loss of recent memory in the patient (Scoville and Milner, 1957). Since that time, the knowledge about this structure has increased tremendously and a PubMed search for "hippocampus" currently yields almost 100,000 published articles. The reasons for this success story are manifold: The hippocampus serves as an ideal model to study synapse formation and physiology in the CNS for its excellent morphological and functional characterization. The synaptic connectivity as well as the morphology of the individual cells, their axonal projections and dendritic trees are well characterized. The Schaffer collateral – CA1 synapse is often referred to as "canonical synapse" meaning that it can be used as a model of many (but definetely not all) excitatory connections in the forebrain. The laminar structure of the hippocampus makes it reasonably easy to handle experimentally since axonal projections and postsynaptic targets are mostly found within the same plane. In this study, the canonical synapse formed by Schaffer collaterals and CA1 dendrites was used to characterize the role of the cell adhesion molecule SynCAM1 in synapse formation and function.

In this study, the function of the synaptic cell adhesion molecule SynCAM1 in synaptogenesis was analyzed. A SynCAM1 knockout as well as a SynCAM1^{flag} overexpressing mouse model was characterized physiologically and morphologically with respect to synapse formation and to synaptic plasticity. I found that increasing SynCAM1-mediated synaptic adhesion by SynCAM1^{flag} overexpression increases the number of functional synapses whereas SynCAM1 knockout animals exhibit a decrease in the number of synapses. Furthermore, SynCAM1 retains its synaptogenic potential throughout development and its continuous expression is required to maintain the increase in synapse number. Interestingly, SynCAM1^{flag} overexpressing mice do not show LTD whereas KO mice with decreased synaptic adhesion exhibit increased LTD. Finally, SynCAM1 overexpression, which results in increased synaptic adhesion and decreased plasticity, correlates with abrogated spatial learning whereas KO animals with decreased adhesion and increased synaptic plasticity learn better than the resprective controls.

2 Material and Methods

2.1 Material

Chemicals and media used in this study are listed in the following two tables. Chemicals were dissolved either in distilled water or dimethyl sufoxide (DMSO).

2.1.1 Chemicals

Chemical	**Supplier**
2-Amino-2-hydroxymethyl-propane-1,3-diol (Tris, Trizma base)	Sigma
2-chloroadenosine	Sigma
Adenosine 5'-triphosphate magnesium salt (MgATP)	Sigma
Agarose	Inivitrogen
Aprotinin	Sigma
Bovine albumin powder	Sigma
Calcium chloride dihydrate ($CaCl_2$)	Merck
Calcium nitrate tetrahydrate ($Ca(NO_3)_2$)	Merck
Cesium chloride (CsCl)	Sigma
Cesium methane-sulfonate ($CsMeSO_4$)	Sigma
D(+)Glucose monohydrate	Merck
Dimethyl sufoxide (DMSO)	Merck
Doxicycline hyclate	Fargon
Ethidiumbromide Solution	Fluka Chemie
Ethyl-3-aminobenzoate methanesulfonate salt	Sigma
Fetal bovine serum	Biochrom
GeneRuler 1kb DNA-ladder	Fermentas
Gentamycin	Sigma
Glacial acetic acid	Merck
Glutaraldehyde	Polyscience
Guanosine 5'-triphosphate sodim salt hydrate (NaGTP)	Sigma
Horse serum	Gibco
Isoflurane	Baxter

Chemical	**Supplier**
Magnesium chloride hexahydrate ($MgCl_2$)	Merck
Magnesium sulfate heptahydrate ($MgSO_4$)	Merck
Mineral oil	Sigma
N-2-Hydroxyethylpiperazine-N'-2-ethane sulfonic acid (HEPES)	Biomol
Paraformaldehyde (PFA)	Merck
Penicillin	Gibco
Picrotoxin	Sigma
Potassium chloride (KCl)	Merck
Restriction endonucleases	Fermenatas
Potassium dihydrogen phosphate (KH_2PO_4)	Merck
QX-314	Alomone Labs
Sodium chloride (NaCl)	Merck
Sodium dihydrogen phosphate monohydrate (NaH_2PO_4)	Merck
Sodium hydrogen carbonate ($NaHCO_3$)	Merck
Sucrose	Merck
Tetrodoxin citrate (TTX)	BioTrend
Titriplex II (EDTA)	Merck
Titriplex VI (EGTA)	Merck
Trichlormethiazide (TCM)	Sigma
Trypsin/EDTA	Gibco
α-chymotrypsin	Sigma

2.1.2 Media and solutions

Name	Recipe
BHK cells medium	Glasgow MEM BHK-21 medium (Gibco), 10 % Fetal bovine serum, 1 % Penicilin/Streptomycin
ACSF	in mM: 119 NaCl, 2.5 KCl, 1.3 $MgSO_4$, 1 NaH_2PO_4, 26.2 $NaHCO_3$, 4 $CaCl_2$, 4 $MgCl_2$, 11 glucose
Slice-preparation medium	MEM medium (Gibco), 1 % Penicilin/Streptomycin, 1 % 1M Tris/HCl pH 7.2
Slice-culturing medium	50 % MEM medium (Gibco), 25 % HBSS (Gibco), 25 % Horse serum, 0.5 % L-Glutamine 200 mM
sucrose-ACSF	in mM: 87 NaCl, 26 $NaHCO_3$, 75 sucrose, 25 glucose, 2.5 KCl, 1.25 NaH_2PO_4, 7 $MgCl_2$
PBS (10x)	100 mM Na_2HPO_4, 20 mM KH_2PO_4, 1.37 M NaCl, 27 mM KCl
TAE (50x)	in 1 l: 242 g Tris, 57.1 ml glacial acetic acid, 100 ml 0.5M EDTA (pH 8.0)

2.2 Methods

2.2.1 Molecular cloning

Sequences encoding full-length SynCAM1 and SynCAM2 (splice product 2) were kindly provided by Thomas Biederer (Biederer, 2006). PCR products were subcloned into the eukaryotic expression vector pCMV5 for heterologous expression. To generate vectors for Semliki forest viral particle production and expression in neurons, sequences encoding wild-type, full-length SynCAM1 and 2 were PCR amplified and subcloned into pSCA (DiCiommo and Bremner, 1998).

2.2.2 Cultures of hippocampal neurons

Primary hippocampal cultures for electrophysiological analyses were prepared from embryonic day 18 (E18) to E19 Sprague Dawley rats. Neurons were grown in neurobasal B27 medium for 7 to 9 DIV and transduced using the Semliki forest virus system to coexpress full-length, wild-type SynCAM proteins and soluble GFP. Twelve to 24 h posttransduc-

tion, whole cell recordings of mEPSCs (see 2.2.4.3) were performed from transduced neurons identified by their GFP expression.

2.2.3 Transgenic and KO SynCAM1 Mouse Models

2.2.3.1 Transgenic mouse generation

Genetically modified mice were generated by Biederer and co-workers. This is the first publication of the SynCAM1^{flag} overexpressing mouse line. The transgenic design is relevant for this thesis and is consequently described here. To generate the transgenic cassette, the pTRE vector (Clontech) was modified after filling in the unqiue XhoI site to generate a new PvuI site, and the coding sequence for mouse SynCAM1 was subcloned from pCMV3333644 (Biederer et al., 2002) after EcoRI digest and filling in into the XbaI site of the modified pTRE. A NheI site was generated using the PCR mutagenesis kit (Stratagene) to generate pTRE mSynCAM1(420)*NheI, with the bracketed number indicating the amino acid into whose codon the restriction site was introduced. A cassette of two flag epitopes flanking a central tetracysteine motif was inserted into this NheI site using the annealed oligos TMA02183 (ctagcgctgactacaaggacgacgatgacaaatgctgtccaggatgctgtgactacaaggacgacgatgacaagcttg) / TMA02184 (ctagcaagcttgtcatcgtcgtccttgtagtcacagcatcctggacagcatttgtcatcgtcgtccttgtagtcagcg). This inserted the flagepitope containing cassette in the middle of the cytosolic SynCAM1 sequence to facilitate the immunohistochemical detection and biochemical purification of the transgenic SynCAM1^{flag} while minimally interfering with its intracellular protein interaction motifs (Biederer, 2006). The resulting pTRE mSynCAM1(420)flagC4flag vector was digested with PvuI/NgoMIV to obtain a 2.88 kb fragment including the TRE and coding sequences that was injected into BL6SJLF1/J ES cells. The founder of the transgenic line reported here had 5 copies of the transgene inserted. These transgenic x TRE-SynCAM1$^{flag\ +/-}$ mice were crossed to mice overexpressing the transcriptional transactivator tTA from a CaMKII promoter (Mayford et al., 1996).

All experiments except for electrophysiological analyses were performed on CaMKII-tTA $^{+/-}$ x TRE-SynCAM1$^{flag\ +/-}$ mice maintained in this BL6SJLF1/J background. For electrophysiological recordings of littermates, transgenic males were backcrossed to C57BL/6 females for at least 4 generations to obtain offspring. Non-overexpressing littermates carrying

only the CaMKII-tTA $^{+/-}$ transgene while being TRE-SynCAM1$^{flag\ -/-}$ served as controls in this study. Where indicated, CaMKII-tTA $^{+/-}$ x TRE-SynCAM1$^{flag\ +/-}$ mice treated with the tTA inhibitor doxycycline served as additional control. All analyses were performed with littermates to control for their genetic background.

2.2.3.2 SynCAM1 KO mouse model

SynCAM1 KO mice were reported previously (Fujita et al., 2006) and have a mixed BL6/129Sv genetic background. All analyses were performed only with littermates to control for differences in genetic background.

2.2.3.3 Animal breeding

Mice were group-housed with a 12 hour light-dark cycle with constant temperature. To suppress SynCAM1^{flag} overexpression, 1 g/l doxycycline hyclate (Fargon, Barsbüttel, Germany) and 5 g/l sucrose were added to the drinking water. To temporally control SynCAM1 overexpression, the drinking water was changed to doxycycline containing or doxycycline-free water as described in the respective experiments. To administer doxycycline to pups from birth, the drug was added to the drinking water of their mouse dams from E14. Doxycycline-containing water was protected from light and replaced with a fresh batch every 2-3 days to account for the potential instability of the drug.

2.2.4 Electrophysiological procedures

2.2.4.1 Slice preparation

Animals were anesthetized with Isoflurane and decapitated. The hippocampus was removed and transversally sliced (400 μm) with a vibratome (Leica VT1200S). Slices were stored in artificial cerebrospinal fluid (ACSF) gassed with carbogen (95% O2; 5% CO2).

P14-P19 animals: The brain was removed from the skull and chilled for 1 min in cooled (4°C) artificial cerebrospinal fluid (ACSF) containing in mM: 125 NaCl; 2.6 KCl; 1.4 $MgSO_4$; 2.5 $CaCl_2$; 1.1 NaH_2PO_4; 27.5 $NaHCO_3$ and 11.1 D-glucose; pH 7.2, 310 mosm/kg. Slices were equilibrated in a custom made submerged chamber in ACSF continuously gassed with carbogen for 30 min at 32°C, and subsequently kept at RT.

P27-P29 animals: The brain was removed from the skull and chilled for 4 min in sucrose-supplemented artificial cerebrospinal fluid (sucrose-ACSF) containing in mM: 87 NaCl; 26 $NaHCO_3$; 75 sucrose; 25 glucose; 2.5 KCl; 1.25 NaH_2PO_4; 7 $MgCl_2$. 400 μm horizontal slices of the entire brain were prepared in ice-cold sucrose-ACSF. Slices were kept in a custom made interphase chamber in ACSF continuously gassed with carbogen at RT. Miniature EPSCs in the conditional overexpression study were recorded from animals at an age of P27 to P29.

2.2.4.2 Field potential recordings

Field potentials were obtained from P15 to P19 animals. To avert recurrent excitation, Schaffer collaterals were severed between CA3 and CA1. Synaptic responses were evoked by stimulating the Schaffer collaterals at 0.03-0.1 Hz with 0.2 ms pulses. Field EPSPs (fEPSPs) were recorded in the stratum radiatum of the CA1 region using glass microelectrodes (Science Products, Hofheim, Germany) filled with ACSF. Data was acquired using a Multiclamp 700B amplifier (Axon Instruments), digitized on a Digidata 1322A (Axon Instruments) and stored on a personal computer. All experiments were performed at room temperature (22-24°C). fEPSP slopes were used as a measure of dendritic activity and determined between 20-80% of the maximum field amplitude (see 2.2.7 for detailed description of data analysis). At least 20 min of stable baseline were recorded prior to the induction of synaptic plasticity.

Long-term potentiation (LTP) was induced by two trains of 0.2 ms pulses at 100 Hz for 1 s with an intertrain interval of 20 s. Post-induction responses were monitored for 60 min.

Long-term depression (LTD) was induced by low-frequency stimulation (1 Hz for 15 min). Post-induction responses were monitored for 60 min.

Representations of LTP and LTD traces omit stimulus artifacts for clarity and show post-induction traces recorded 55-60 min after induction.

2.2.4.3 Whole-cell recordings

Pyramidal CA1 neurons were visualized using an BX51WI microscope (Olympus) and differential infrared video microscopy. Slices were constantly superfused with gassed ACSF.

Miniature EPSCs were obtained from P14 to P15 or P27 to P29 animals. Evoked EPSCs were obtained from P15 to P19 animals. Recording electrodes had a resistance of 3 - 5 MΩ and were pulled from borosilicate glass (Science Products, Hofheim, Germany). The internal pipette solution contained (in mM): 150 CsGluconate, 8 NaCl, 2 MgATP, 10 HEPES, 0.2 EGTA, and 5 QX-314 ([2-[(2,6-dimethylphenyl)amino]-2-oxoethyl]-triethylazanium bromide), pH 7.2, 290 mosm/kg. EPSCs were evoked on Schaffer collaterals with glass electrodes filled with ACSF.

AMPA/NMDA ratio: AMPA EPSCs were recorded at -70 mV, the NMDA component was recorded at +40 mV. To determine the AMPA/NMDA ratio, the maximum amplitude of the AMPA current was divided by the NMDA component (taken 70 ms after the stimulus).

Paired-pulse facilitation (PPF): Two AMPA EPSCs were evoked with an interstimulus interval of 40 ms. The amplitude of the second AMPA EPSC was divided by the amplitude of the first AMPA EPSC to determine the paired-pulse ratio.

Miniature EPSCs were recorded in voltage clamp at -70 mV in ACSF perfusion (in mM: 125 NaCl; 2.6 KCl; 1.4 $MgSO_4$; 4 $CaCl_2$; 2.7 $MgCl_2$; 1.1 NaH_2PO_4; 27.5 $NaHCO_3$ and 11.1 D-glucose) supplemented with tetrodotoxin (TTX, 0.2 μM), picrotoxin (PTX, 100 μM), and trichlormethiazide (TCM, 250 μM) to increase mEPSC frequency. mEPSCs were detected off-line and statistically analyzed with a custom written MATLAB routine (MathWorks) (see 2.2.7 for detailed description of data analysis).

2.2.5 Biochemical procedures

Frozen tissue samples were rapidly homogenized using microtip-aided sonication. Brain homogenates were subfractionated by the method of Jones and Matus (Jones and Matus, 1974) with modifications (Biederer et al., 2002). For co-immunoprecipitation experiments, forebrain membrane extracts were prepared in 1% Triton X-100 (Biederer et al., 2002) and incubated with Protein G agarose-conjugated flag M2 antibodies. SDS-polyacrylamide gel electrophoresis and immunoblotting were performed using standard procedures. Quantitative immunoblotting was performed on an Odyssey Imaging System (Li-Cor, Lincoln, NE, USA) and signals were calibrated against purified epitopes (Fogel et al., 2007).

2.2.5.1 Antibodies

Immunoblotting was performed with specific antibodies against SynCAM1 (YUC8. 1:1000), SynCAM2 (YU524, 1:1000), SynCAM3 (YU525, 1:1000), and SynCAM4 (YU591, 1:1000) that were described previously and detect these proteins at apparent molecular weights of 100 kDa, 62-76 kDa, 49 kDa, and 67 kDa, respectively (Fogel et al., 2007). Apparent molecular weights are higher than predicted from the open reading frames due to N-glycosylation (Fogel et al., 2007). For simultaneous detection of SynCAMs 1-3, a pleioSynCAM antibody (T2412, 1:2000) was utilized, which was raised in rabbits against the SynCAM1 carboxyl-terminal sequence that recognizes this conserved sequence in SynCAM1, 2 and 3, but not 4 (Fogel et al., 2007). Antibodies to flag (clone M2, F1804; 1:2000) were obtained from Sigma-Aldrich (St. Louis, MO, USA), to N-cadherin (1:2000) from BD Biosciences (San Jose, CA, USA), to NCAM from Sigma-Aldrich (clone OB11; 1:400), to CASK (clone K56A/50, 1:1000) from NeuroMab (UC Davis, CA, USA), and to synaptophysin (clone 7.2; 1:10,000) from Synaptic Systems (Gottingen, Germany). Monoclonal antibodies to actin (clone JLA20, developed by Jim Jung-Ching Lin) were obtained from the Developmental Studies Hybridoma Bank maintained by the University of Iowa and used for immunoblotting at 1:100.

For immunolocalization in brain sections, antibodies were employed against flag (M2, 1:2000), the synaptic markers vGlut1 (Millipore AB5905) and vGlut2 (Millipore AB5907) (used in combination at each 1:1000), GAD65 (Millipore AB5082, 1:1000), and the neuronal nuclei marker NeuN (Millipore MAB377, 1:300).

2.2.5.2 Sample preparation

For preparation of brain tissue, animals were anesthetized with isoflurane (Baxter) and decapitated. The brain was removed from the skull and chilled in phosphate buffered saline (PBS, 4°C). To obtain tissue samples, brain regions were dissected quickly and immediately frozen in liquid nitrogen. Frozen tissue samples were rapidly homogenized using microtip-aided sonication in Hepes pH 7.4 (50 mM), urea (8.0 M), and PMSF (0.5 mM). For preparation of subcellular fractions, fresh brain homogenates were subfractionated by the method of Jones and Matus (Jones and Matus, 1974) with modifications (Biederer et al., 2002). For co-immunoprecipitation experiments, crude membrane preparations were prepared (Biederer

et al., 2002) and solubilized on ice by dounce homogenization in 1% Triton X-100 (Roche) in a homogenization buffer composed of Hepes pH 7.4 (25 mM) and sucrose (320 mM), followed by centrifugation. After preclearing of solubilized membrane extracts against unconjugated Protein G agarose beads (Invitrogen), detergent extracts from overexpessors and controls were incubated with Protein G agarose-conjugated flag M2 antibody. Beads were collected, washed 3 times with extraction buffer, and eluted with SDS sample buffer for immunoblotting analysis. Protein concentrations were determined using the Pierce BCA assay. SDS polyacrylamide gel electrophoresis and immunoblotting were performed using standard procedures. For quantitative immunoblotting, an Odyssey Imaging System (Li-Cor, Lincoln, NE, USA) was used and signals were calibrated against known amounts of purified epitopes (Fogel et al., 2007).

2.2.5.3 Immunohistochemistry

Immunohistochemistry was performed on cryosections of P21 mouse brains, and stained sections were imaged with a Zeiss LSM 510 META laser scanning confocal microscope. Golgi staining of hippocampal pyramidal neurons was performed using the FD Rapid Golgi Stain Kit (FD NeuroTechnologies, Ellicott City, MD) according to the manufacturer's instructions. Differential interference contrast images of secondary and tertiary CA1 apical dendrites were acquired and spines of Golgi-stained sections were classified and quantitatively analyzed as described (Li et al., 2004; Knott et al., 2006).

2.2.5.4 Golgi staining

Golgi staining of hippocampal pyramidal neurons was performed using the FD Rapid Golgi Stain Kit (FD NeuroTechnologies, Ellicott City, MD) according to the manufacturer's instructions. Briefly, freshly dissected brains were incubated in the impregnation solution for 3 days at room temperature in the dark. Brains were vibratome sectioned to 100 μm thickness, developed, and permanently mounted. Differential interference contrast images of secondary and tertiary CA1 apical dendrites were acquired at 63x. CA1 dendrites and spines of Golgi-stained sections were quantitatively analyzed as described (Li et al., 2004). Spines were classified as described (Knott et al., 2006) as mushroom spines with head diameters

that are much greater than their neck diameters, thin spines that have lengths much larger than their diameters and similar diameters of both head and neck, stubby spines that are short and have similar diameters of both head and neck, and undefined protrusions.

2.2.5.5 Electron microscopy

Mice were perfused with 10 mM HEPES buffer followed by fixation with 2.5% glutaraldehyde (GA) and 2% paraformaldehyde (PFA) in 0.1 M sodium cacodylate (pH 7.4). Coronal sections of 100 μm thickness from the CA1 stratum radiatum of hippocampus were cut using a vibratome. Approximately 1000 μm^2 of CA1 stratum radiatum from each sample was imaged by random sampling. Quantifications were compared using Mann-Whitney statistical test. Morphometric classification of synapses and analysis of ultrastructural parameters were performed as described (Gray, 1959; Rosahl et al., 1995). Quantifications were performed blind to the genotype. Only littermates were analyzed to control for their same genetic background.

2.2.6 Behavioral studies

The series of behavioral tests was performed by Biederer and co-workers using cohorts of male mice, with animals first subjected to open field recordings, followed by the novel object recognition test, the Morris water maze, and finally the elevated plus maze. Different cohorts were tested for visual cliff avoidance and latency to a hidden cookie. Locomotor activity was controlled by videotracking swim speed and distance in an open field box. Morris water maze training and probe trials were conducted in a water-filled circular tank, with visual cues mounted on the tank wall. Path length, time spent in each quadrant, and latency to find the escape platform were tracked by video as described (Rabenstein et al., 2005). Statistical analyses were performed using Student's t-test and errors stated in the text and figure legends correspond to the standard error of mean unless indicated otherwise.

2.2.6.1 Sensory and motor controls

To assess vision, visual cliff avoidance was performed by placing adult male mice into the visual cliff apparatus suspended by their tails headfirst so that front paws were first to be

placed on the elevated beam (n=9 littermate tTA controls and n=9 transgenic overexpressors, aged 3-5 months; 6 trials total). Direction of entry was alternated between trials to correct for possible left-right bias. To record latency, time was started when all four paws contacted the beam and stopped when mice stepped onto either solid flooring (score=1) or the visual cliff (score=0). Mice that did not choose a side within 5 min were excluded from further testing (1 of 9 controls). Choice scores and latency to choice were compared across genotypes with t-tests. To test for proper olfaction, adult male mice were subjected to a hidden cookie test (n=11 littermate tTA controls and n=12 transgenic overexpressors, aged 11-12 months). Prior to testing, subjects were food deprived overnight. A 1 cm x 1 cm x 0.5 cm cookie cube colored similar to the bedding was hidden under corncob bedding in one corner of a clean mouse cage. Subjects were placed in the center of the cage and latency to finding the hidden cookie was recorded, as defined by making nasal or oral contact. Mice that did not find the cookie within 5 min were excluded from further testing (2 of 11 controls). Latency to cookie finding was analyzed by genotype with t-tests. Locomotor activity was measured in an open field using automated tracking software (Panlab SMART). Mice were placed in a 50 cm x 50 cm x 20 cm plexiglas enclosure with opaque walls and allowed to explore it freely for 20 min. Walk speed was measured by the tracking software and analyzed by genotype with t-tests. Distance traveled during the 20 min duration was binned in 5 min intervals and habituation to the open field environment was analyzed by genotype with t-tests. Swim speed was obtained during the Morris water maze training as described below using the same tracking software.

2.2.6.2 Morris water maze training and probe trial

Morris water maze studies were performed as described (Rabenstein et al., 2005). Adult male mice received four training trials per day during their light cycle for 10 days (n=11 littermate tTA controls and n=12 transgenic overexpressors, aged 4-5 months) or 20 days (n=8 wild-type littermate controls and n=9 KO mice, aged 6-12 months). KO and respective control animals were aged to facilitate the detection of learning improvements as described in the results. Animals were tested in a water-filled circular white plastic tank (diameter 100 cm, water temperature 21-22°C). A clear plastic platform (10 cm x 10 cm) was submerged 0.5 cm

under water and placed in the same location in the tank over the training days. For analysis, the tank was divided into four equal quadrants, with animals starting one training trial in each quadrant on all training days. The order of starting quadrants was randomized, and mice were placed facing the tank's edge. Salient visual cues of different shape and color were mounted on the tank wall. Path length, time spent in each quadrant, and latency to find the platform were measured by a SMART video tracking system (San Diego Instruments, San Diego, CA). Animals that did not find the platform within 60 sec were manually placed onto the platform. All animals were allowed to remain on the platform for 15 sec. The intertrial interval was 5 min. On day 11 (transgenic overexpressor and control cohorts) or day 21 (aged KO and control cohorts), the probe trial was performed. The platform was removed, and the mice were placed in the middle of the tank and allowed to swim for 60 sec. Time spent in each quadrant was recorded. On day 12 or 22, respectively, the platform was moved to a different quadrant and marked with a flag. Training in the visible platform task was the same as in the hidden platform procedure, and was performed over 6 consecutive days (transgenic and control cohorts) or 5 days (KO and control cohorts) with the marked platform being moved to a new quadrant at each day of training. Failure rates were calculated based on the number of times animals failed to reach the platform in a time span of 60 seconds. Statistical analysis of swim-time data was performed using two-way ANOVA for repeated measures.

2.2.7 Data and statistical analysis

Data analysis was performed using MATLAB (The Mathworks, Aachen, Germany, program version: 7.8.0.347 (R2009a)). Graphs were layouted using Prism (Graph Pad Software, La Jolla, USA, program version: 5.03).

2.2.7.1 Semi-automatic mEPSC detection

The available tools for mEPSC detection and analysis (e.g. the template search in the Clampfit program (Axon Instruments)) were inconvenient to use, prone to user errors and detected many false positive events. Therefore, a MATLAB-based analysis tool for semi-automated mEPSC detection and analysis was developed. mEPSCs were detected by analyzing onset slope(differential), amplitude threshold, and mEPSC decay kinetics to identify potential

mEPSC events. All events were manually evaluated (accept/reject) by the user to enable complete control of the analysis process. Statistical analysis of event properties is implemented in MATLAB and does not require the error-prone manual transfer of the aquired data to other programs for analysis.

Subsequent to mEPSC evaluation, the time between individual events (interevent interval), the amplitudes of the individual events, the decay constant and other mEPSC parameters are statistically analyzed and plotted as cumulative histograms. Histograms of all cells of the same conditions were averaged and data are reported as mean and SEM, which are also presented as error bars in the figures. Distributions of different datasets are tested for difference using the Kolmogorov-Smirnov significance test.

2.2.7.2 Synaptic plasticity

Manual analysis of plasticity experiments is inflexible to modification of the analysis criteria (e.g. changing bin size), very monotonous (which make it prone to user errors), and can never be as objective as a routine with clearly defined analysis parameters. Hence, a MATLAB based program was developed to ensure maximum precision and complete user control in analysis of long-term plasticity experiments.

This "PlasticityAnalysis" tool determines the slope of the dendritic field between 20 and 80% of the maximum field amlitude. The slopes can be binned over time and the time-course of all individual experiments is plotted. All recordings of one experimental condition are subsequently averaged, and data are reported as mean and SEM, which are also presented as error bars in the figures. Differences between experimental conditions were analyzed by comparing the means at 55-60 min after the induction of plasticity between experimental conditions.

3 Results

3.1 SynCAM1 and SynCAM2 overexpression induces excitatory synapse formation in neuronal cultures

SynCAM family proteins have been known to induce the formation of functional presynaptic specializations in co-culture systems (Biederer et al., 2002). Whether SynCAM family members would only exert this effect in heterologous systems or also induce the formation of functional synaptic contacts in neurons remained elusive. To elucidate the role of SynCAMs in interneuronal contact formation, SynCAM1 and SynCAM2 were overexpressed in dissociated hippocampal neurons using a Semliki Forest virus expression system.

Based on previous findings, it was hypothesized that SynCAM overexpressing neurons could form more synaptic contacts. Postsynaptic neurons overexpressing SynCAM proteins would therefore receive more synaptic inputs than non-overexpressing control neurons. Experimentally, the number of functional synapses onto a cell can be analyzed by recording miniature postsynaptic currents. This approach exploits the fact that functional synapses exhibit action potential independent vesicle release. At glutamatergic synapses, the transmitter elicits miniature excitatory postsynaptic currents (mEPSCs), which can be measured by whole cell recordings. The frequency of mEPSC events is a measure for the number of synapses onto the respective neuron.

Dissociated hippocampal neurons were transfected with SynCAM1 or SynCAM2 using a Semliki Forest virus. All transfected cells coexpressed soluble GFP with control neurons only expressing GFP. mEPSCs of GFP positive neurons were recorded 12-24 h post infection.

mEPSC recordings from SynCAM1 and SynCAM2 overexpressing neurons revealed significant increases in mEPSC frequencies compared to control neurons that only expressed GFP (GFP controls n=15, 0.10 $\pm$ 0.02 Hz; SynCAM1 n=11, 0.21 $\pm$ 0.04 Hz; SynCAM2

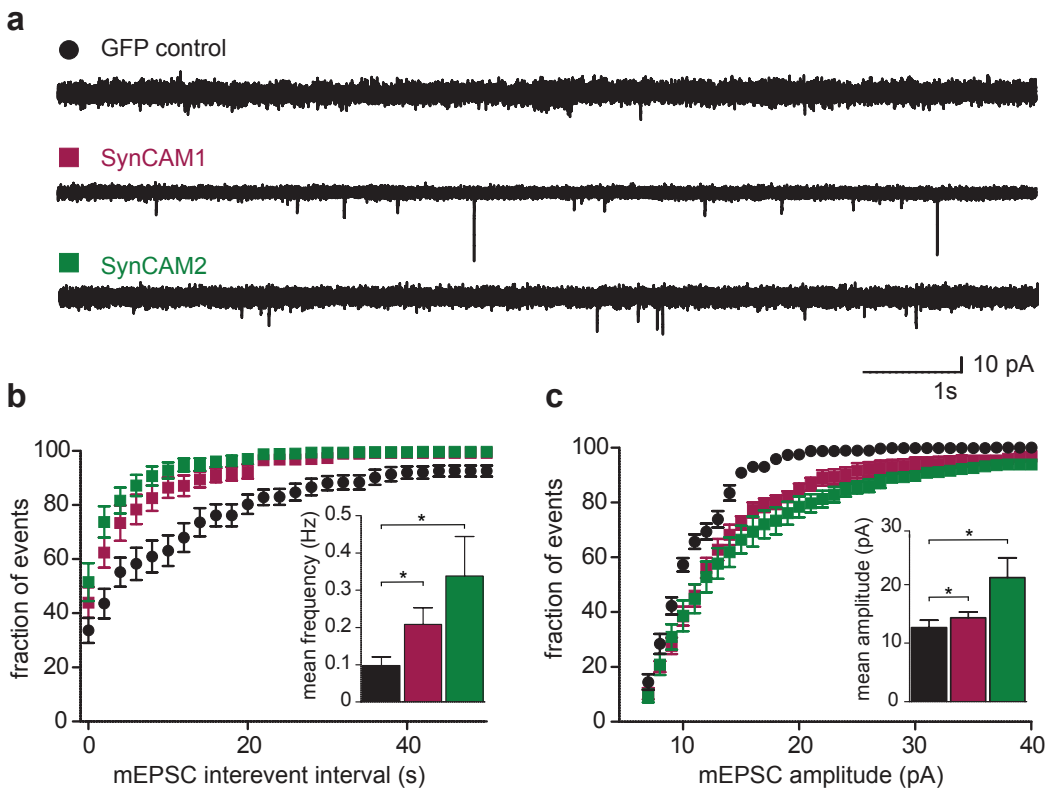

Figure 3.1: **a**, Representative whole cell recordings of mEPSCs from dissociated hippocampal neurons at 8-10 DIV. Neurons overexpressed GFP as a control (black; n=15 cells), SynCAM1 (purple; n=11 cells), or SynCAM2 (green; n=9 cells). Legend and color scheme in panel (a) also apply to (b) and (c). **b**, Cumulative distribution of mEPSC interevent intervals. The bar graph inset depicts mean mEPSC frequencies. **c**, Cumulative distribution of mEPSC amplitudes. The bar graph inset depicts mean mEPSC amplitudes. Experimental design, experiments and analyses by AK.

n=9, 0.3 ± 0.11 Hz; Kolmogorov-Smirnov $p < 0.005$ for SynCAM1 vs. GFP control, and $p < 0.001$ for SynCAM2 vs. GFP control). This result confirms the hypothethis that SynCAM1 and SynCAM2 induce excitatory synapse formation in neurons. In contrast to mEPSC frequency, mEPSC amplitude is a measure of receptor density (Raghavachari and Lisman, 2004). Overexpression of SynCAM1 and SynCAM2, caused an increase in mEPSC amplitude (GFP controls n=15, 12 ± 1.2 pA; SynCAM1 n=11, 14 ± 1.0 pA; SynCAM2 n=9, 21 ± 3.4 pA; Kolmogorov-Smirnov $p < 0.01$ for SynCAM1 vs. GFP control, and $p < 0.005$ for SynCAM2 vs. GFP control), suggesting a higher receptor density. However, the effect on mEPSC amplitude did not occur upon overexpression of $SynCAM1^{flag}$ in the intact brain (Fig. 3.4) and might be specific for cultured neurons. Taken together, these results confirm

the hypothesis that SynCAM1 and SynCAM2 overexpression in neurons induces excitatory synapse formation.

3.2 Roles of SynCAM1 in the intact brain

Based on the insights into the molecular and physiological functions of SynCAM1 in cultured neurons, I hypothesized that SynCAM1 serves similar roles in the intact brain. Furthermore, the analysis of the normally developing brain would extend the understanding from molecular questions to roles of SynCAM1 in a more physiological context. To understand the funtions of SynCAM1 in brain development, I analyzed the neurological phenotypes of a knockout (KO) and of a conditionally overexpressing mouse line (OE), respectively.

3.2.1 Mouse models for knockout and conditional SynCAM1 overexpression

The non-neuronal phenotype of SynCAM1 KO animals has been described previously (Fujita et al., 2006; van der Weyden et al., 2006). While these mice are infertile due to impaired maturation of spermatids, their neuronal phenotypes had not been analyzed.

In adition to the analysis of the SynCAM1 KO phenotype, I performed a complementary study of SynCAM1 overexpression (OE). Biederer and co-workers generated a mouse line carrying a transgene encoding flag-epitope tagged SynCAM1 (SynCAM1^{flag}) under the control of a Tet-responsive element (TRE), which is designed to allow exogenous control of protein expression (Mansuy and Bujard, 2000). This line was crossed to mice expressing the transcriptional transactivator tTA driven by the CaMKII promoter, which is active in excitatory forebrain neurons (Mayford et al., 1996) (Fig. 3.2a). Hence, overexpressing mice carry two transgenes; one encodes the transcriptional transactivator tTA under control of the CaMKII-promoter to drive excitatory forebrain neuron expression under temporal control, the other encodes SynCAM1^{flag} under control of a Tet-responsive element. Upon tTA binding to the TRE, constitutive expression of SynCAM1^{flag} is driven from a cytomegalovirus (CMV) promoter. Doxycycline (Dox) inhibits tTA binding to the TRE and thereby represses overexpression. This transgenic TRE-SynCAM1^{flag} x CaMKII-tTA mouse model constitutes a Tet-Off system (Mansuy and Bujard, 2000). Correspondingly, the tTA inhibitor doxycycline was administered to repress SynCAM1^{flag} expression and allowed precise temporal

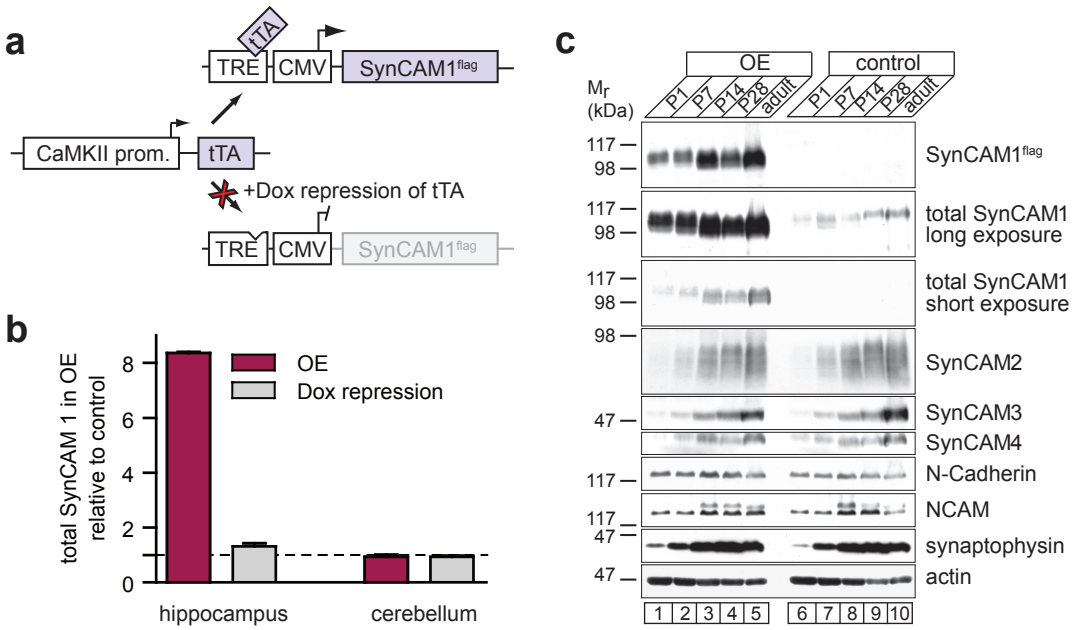

Figure 3.2: A transgenic mouse model for SynCAM1^{flag} overexpression, **a** Tet-Off design for the generation of a SynCAM1 transgenic mouse line that conditionally overexpresses flag-epitope tagged SynCAM1 (SynCAM1^{flag}) in forebrain neurons. **b**, SynCAM1^{flag} overexpression (OE) is restricted to the forebrain and was efficiently shut down by doxycyclin (Dox repression). Animals either continuously overexpressed SynCAM1^{flag} until P28 in the absence of the tTA inhibitor doxycycline (OE), or were treated from P14-28 with doxycycline to repress transgenic expression (Dox repression). **c**, Developmental profile of OE and control SynCAM1 expression. Equal amounts of total forebrain homogenate prepared at the indicated developmental stages were analyzed by immunoblotting. SynCAM1^{flag} overexpression in transgenic mice increases postnatally, following the profile of endogenous SynCAM1. The profiles of the other SynCAM family members and the control proteins tested are unaffected. Actin served as loading control. Transgenic design and verification performed by Biederer and co-workers (a,c). Experimental design and dissection in (b) performed by AK, western blotting by EMR.

control of SynCAM1 overexpression. Littermates carrying only the CaMKII-tTA transgene did not exhibit altered SynCAM1 protein levels (data not shown) and served as controls for transgenic overexpressors.

SynCAM1^{flag} overexpression (OE) as well as doxycycline-mediated repression of overexpression (Dox repressed) were verified by quantitative immunoblotting (Fig. 3.2b). Brain regions were dissected at P28 and SynCAM1 levels comprised of endogenous and transgenic protein were analyzed by quantitative immunoblotting of equal amounts of hippocampus and cerebellum homogenate. The amounts of SynCAM1 were normalized to the signals of non-overexpressing littermates carrying only the tTA transgene. Transgenic overexpression

increased total SynCAM1 levels 8-fold in the hippocampus, without altering its expression in the cerebellum where the CaMKII promoter is inactive. Feeding doxycycline to the animals efficiently repressed SynCAM1^{flag} expression and thereby provided a powerful tool for temporal expression control (Fig. 3.2b). The transgenic protein expression followed the developmental increase of endogenous SynCAM1 in postnatal forebrain, without altering the expression profile of other synaptic proteins, including other SynCAM family members (Fig. 3.2c).

tTA drove the neuronal expression of SynCAM1^{flag} throughout the forebrain of double transgenic mice. The expression pattern of SynCAM1^{flag} was assessed by immunostaining of a hippocampal section obtained at P21 with antibodies against the flag epitope. Similar to the distribution of the endogenous protein (Thomas et al., 2008), SynCAM1^{flag} was localized to the stratum radiatum of the CA1 area and to mossy fiber terminals in the CA3 area (Fig. 3.3a, top panel) (Fogel et al., 2007). To analyze subcellular localization, hippocampal sections were prepared from transgenic mice at P21, and triple labeling was performed using anti-flag antibodies to detect SynCAM1^{flag} as well as antibodies directed against excitatory (vGLUT1/2) and inhibitory (GAD65) presynaptic markers (Fig. 3.3a, bottom panels). Both panels show the same CA1 stratum radiatum section with the indicated labels. Closer analysis revealed that the majority of vGlut1/2-positive excitatory synapses expressed SynCAM1^{flag} (Fig. 3.3a, bottom left), whereas SynCAM1^{flag} was not detected at inhibitory synapses marked by GAD65 (Fig. 3.3a, bottom right). While subsynaptic resolution is not achieved by immunostaining, this finding agreed with previous immuno-electron microscopic analyses showing that SynCAMs are endogenously present at both pre- and postsynaptic sites of excitatory synapses (Biederer et al., 2002). Native protein interactions were maintained in the synaptic membranes of these overexpressing animals as the *trans* adhesion partner SynCAM2 co-immunoprecipitated with SynCAM1^{flag} (Fig. 3.3b). Subcellular fractionation confirmed the enrichment of SynCAM1^{flag} in synaptic plasma membranes purified from the forebrain of adult transgenic overexpressors, similar to endogenous SynCAM1 in control animals (Fig. 3.3c,d). Accordingly, total SynCAM1 amounts were increased 8-fold in synaptic plasma membranes purified from the forebrain of adult transgenic overexpressors (Fig. 3.3d). N-cadherin served as control for synaptic membranes, and synaptophysin as a marker for synaptic vesicles. SynCAM1, 2, and 4 signals in the crude synaptic vesicle

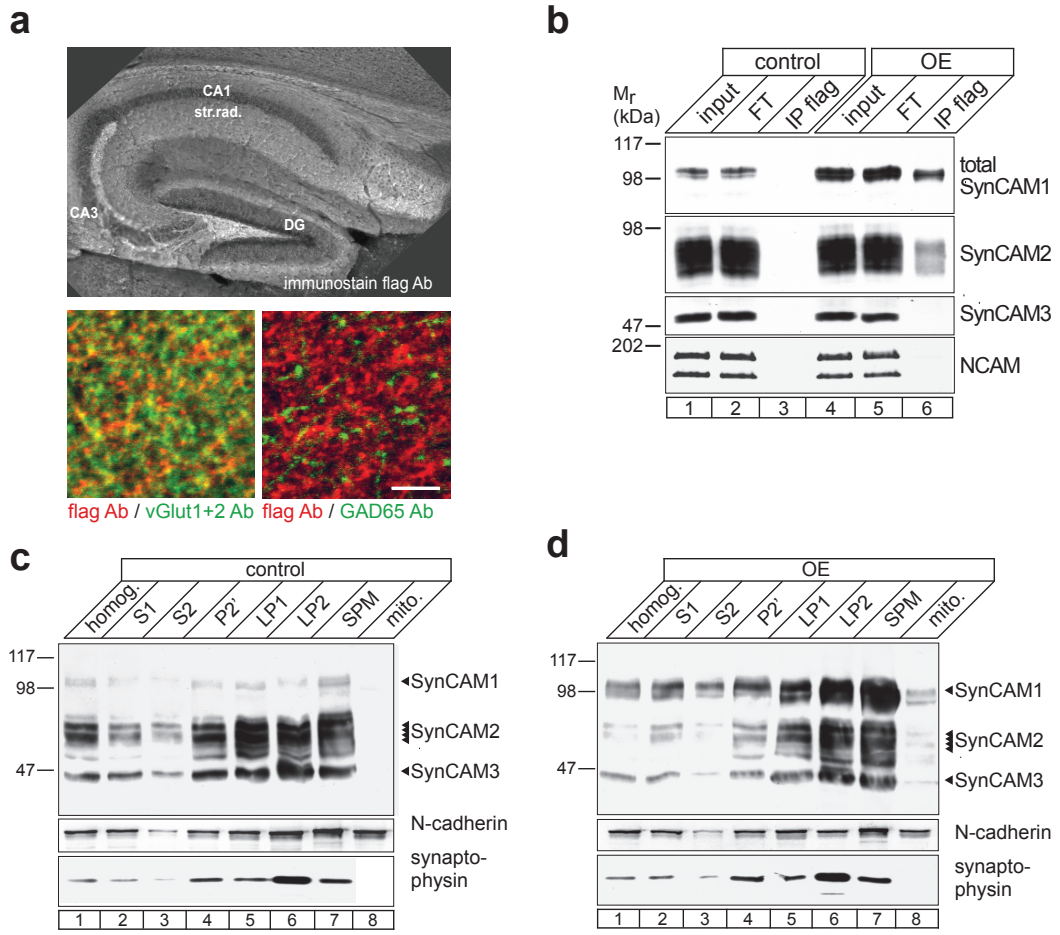

Figure 3.3: SynCAM1^{flag} subcellular localization and native interaction. a top, Transgenically expressed SynCAM1^{flag} is properly localized to synaptic areas in the hippocampus. CA, hippocampal fields; DG, dentate gyrus. bottom, SynCAM1^{flag} is sorted to excitatory but not inhibitory synapses. SynCAM1^{flag} (red channel) co-localizes with the majority of vGLUT-positive excitatory synapses (bottom left, green channel), but is not present at GAD65-positive inhibitory synapses (bottom right, green channel). Scale bar, 5 μm. **b**, Endogenous SynCAM2 is co-immunoprecipitated with overexpressed SynCAM1^{flag}, demonstrating its formation of the native SynCAM1/2 complex. Immunoprecipitation of SynCAM1^{flag} was performed from a crude membrane preparation obtained from adult transgenic overexpressor forebrains (lanes 4-6). Brain preparations of non-overexpressing tTA control animals served as negative control (lanes 1-3). Samples were immunoblotted with antibodies against the indicated proteins, with SynCAM3 and NCAM serving as negative controls and being absent from the immunoprecipitates. **c, d**, Subcellular fractionation of transgenic brains from adult control animals (c) and animals overexpressing SynCAM1^{flag} (d). S, supernatant; P, pellet; LP, lysis pellet; SPM, synaptic plasma membranes. Experiments performed by Biederer and co-workers.

fraction are due to the contamination of this preparation with other membranous material. These biochemical results were consistent with the immunohistochemical analysis that con-

firmed the correct subcellular sorting of SynCAM1^{flag} to synaptic regions, while cell body layers lacked staining (Fig. 3.3a, top). Together, this transgenic SynCAM1 mouse model replicated key properties of endogenous SynCAM1 expression and biochemistry, and was suited to identify roles of SynCAM1 in the postnatal brain.

3.2.2 SynCAM1 increases the number of functional excitatory synapses

I have previously shown that SynCAM1 induces the formation of excitatory synapses, *in vitro* (Fig. 3.1, published in Fogel, Krupp, et al., 2007). Whether SynCAM1 also controls synapse number in the intact brain, remained unanswered. Due to its excellent functional and morphological characterization, the Schaffer collateral – CA1 synapse was used as a model to study synapse formation and physiology. The question whether SynCAM1 expression levels affect functional synapse number was addressed using whole-cell voltage clamp recordings of miniature excitatory postsynaptic currents (mEPSC). mEPSCs are not action potential driven but represent spontaneous vesicle release and thereby reflect the number of synaptic inputs the recorded cell receives. Thus, mEPSC frequency is used as a measure of synapse number (Raghavachari and Lisman, 2004).

mEPSC frequencies were analyzed for three SynCAM1^{flag} expression conditions: Animals not carrying the SynCAM1^{flag} trangsgene (tTA control), animals that carried the SynCAM1^{flag} transgene and were constantly treated with doxycycline to repress the overexpression (OE^{never}), and animals that constantly overexpressed SynCAM1^{flag} (OE^{always}). Indeed, animals continuously overexpressing SynCAM1^{flag} exhibited a strong increase in mEPSC frequency compared to tTA controls (Fig. 3.4a,b). Upon continuous SynCAM1^{flag} overexpression, the distribution of mEPSC interevent intervals is shifted to the left compared to littermate tTA controls and doxycycline-repressed mice (OE^{never}), demonstrating a strongly increased mEPSC frequency (Kolmogorov-Smirnov $p < 0.001$ for OE^{always} vs. tTA control, and $p < 0.001$ for OE^{always} vs. OE^{never}, $p > 0.1$ for control vs. OE^{never}). This observation is also reflected in the average mEPSC frequency (tTA controls n=14, 0.9 ± 0.2 Hz; OE^{always} n=11, 1.9 ± 0.3 Hz; OE^{never} n=12, 0.8 ± 0.1 Hz) (Fig. 3.4b inset). mEPSC amplitude was not affected (tTA control 14.6 ± 0.5 pA, n=11; control Dox repressed 13.4 ± 0.5 pA, n=11 (not depicted) OE^{always} 14.0 ± 0.7 pA, n=14; OE^{never} 13.8 ± 0.4 pA,

n=12) (Fig. 3.4c). The transgenic design allowed analysis of animals in which SynCAM1^{flag} overexpression was continuously repressed by administering doxycycline (Figs. 3.2, 3.8a). Recordings from these mice (OE^{never}) showed that mEPSC frequencies and amplitudes of these animals were indistinguishable from those of control littermates that did not carry the SynCAM1^{flag} transgene (Fig. 3.4a-c). The efficient repression of SynCAM1^{flag} overexpression by doxycycline was thereby confirmed and unspecific effects of transgene insertion were excluded. This SynCAM1-induced increase in excitatory synapse number agreed with the previously demonstrated synaptogenic effect of SynCAM1 in cultured hippocampal neurons (Biederer et al., 2002; Fogel et al., 2007; Sara et al., 2005) and demonstrated the synaptogenic function of SynCAM1 for the first time in the intact brain.

In contrast to the overexpression of SynCAM1, its loss in SynCAM1 KO mice caused a strong reduction in mEPSC frequency compared to wild-type littermates (Kolmogorov-Smirnov $p < 0.001$), which is also reflected in the average mEPSC frequency (wild-type control, n=16, 3.5 ± 0.7 Hz; KO, n=8, 1.5 ± 0.2 Hz) (Fig. 3.4d,e). mEPSC amplitudes of SynCAM1 KO mice (12.6 ± 0.5 pA; n=16) are not significantly changed compared to wild-type mice (wild-type 13.1 ± 0.7 pA, n=8). Differences between mouse strains presumably accounted for the higher mEPSC frequency in KO control groups compared to transgenic SynCAM1 controls. Taken together, these electrophysiological data revealed that SynCAM1 regulates the formation of functional excitatory synapses.

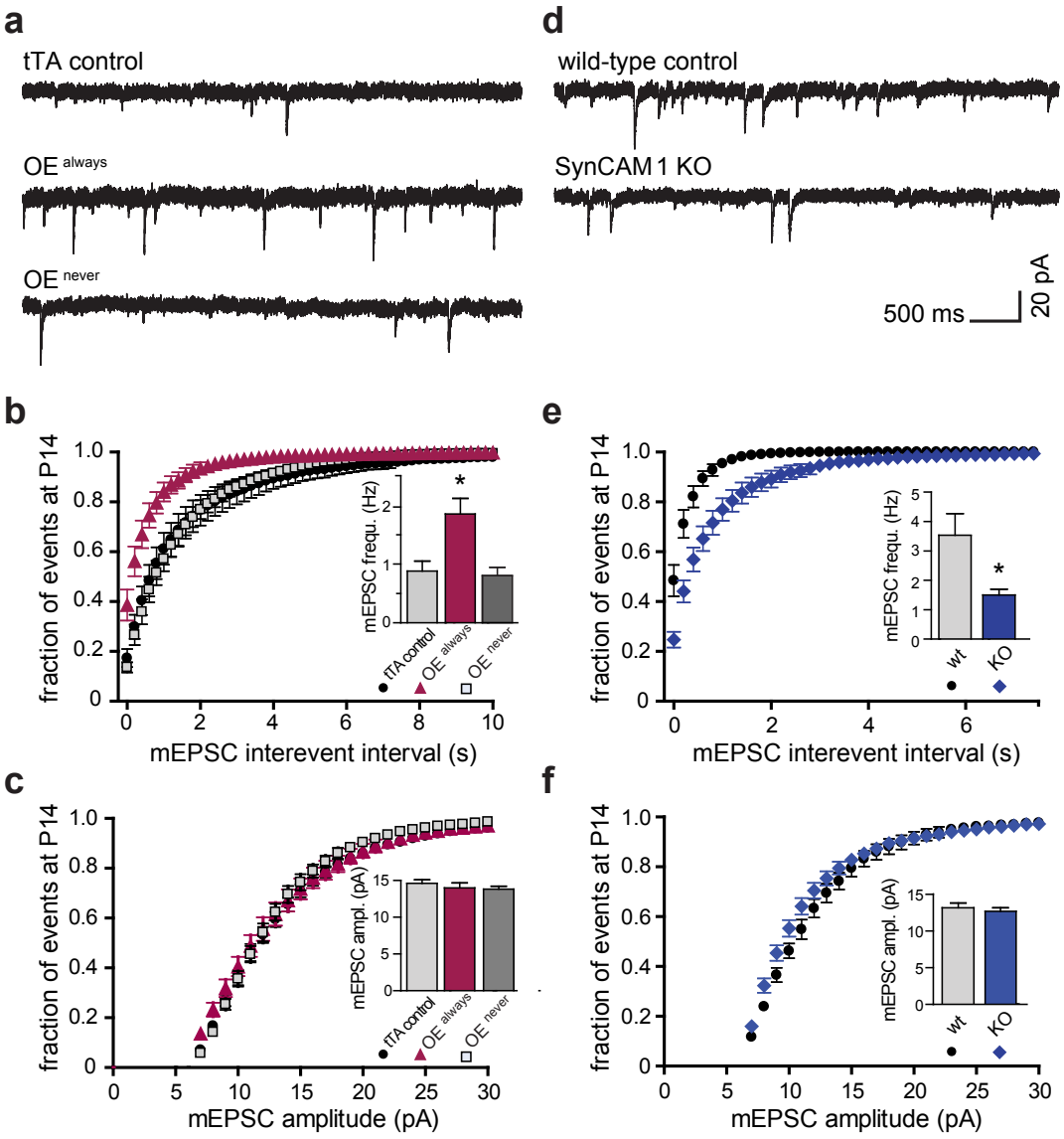

Figure 3.4: SynCAM1 induces functional excitatory synapses. **a-c**, mEPSCs recordings from P15-19 hippocampal CA1 pyramidal neurons. Littermates carrying only the tTA transgene (tTA control) served as controls. OE^{always}, continuous $SynCAM1^{flag}$ overexpression; OE^{never}, continuously repressed overexpression. **a**, Representative whole-cell recordings. Scale bar in (d) applies to (a,d). **b**, $SynCAM1^{flag}$ overexpression increases excitatory synapse number. Cumulative distribution of mEPSC interevent intervals. The bar graph inset depicts mean mEPSC frequencies. **c**, Cumulative distribution of mEPSC amplitudes. mEPSC amplitudes remain unaltered under $SynCAM1^{flag}$ overexpression. **d-f**, mEPSCs recordings from P14 to P15 hippocampal CA1 pyramidal neurons of wild-type littermate controls and SynCAM1 KO mice. **d**, Representative whole-cell recordings. **e**, Loss of SynCAM1 decreases excitatory synapse number. Cumulative distributions of mEPSC interevent intervals show that mEPSC frequency is strongly reduced in SynCAM1 KO mice compared to wild-type littermates. The inset shows mean mEPSC frequencies. **f**, mEPSC amplitudes of SynCAM1 KO mice are not significantly changed compared to wild-type mice. Experimental design, experiments and analyses by AK.

3.2.3 Ultrastructural verification: SynCAM1 regulates the number of asymmetric synapses

To complement my physiological findings, Robbins and colleagues determined SynCAM1 effects on the density and ultrastructure of asymmetric (Gray type I, excitatory) and symmetric (Gray type II, inhibitory) synapses in the CA1 stratum radiatum area of the hippocampus, using electron microscopy. Notably, the density of asymmetric, excitatory synapses in mice overexpressing SynCAM1^{flag} was increased by 26 ± 3 % (tTA littermate control, 3.0 ± 0.11 per 10 μm^2, n=180 images, n=848 synapses; OE, 3.8 ± 0.11 per 10 μm^2, n=180, n=1087 synapses; n=3 adult male mice each) (Fig. 3.5b). As expected, inhibitory synapse number

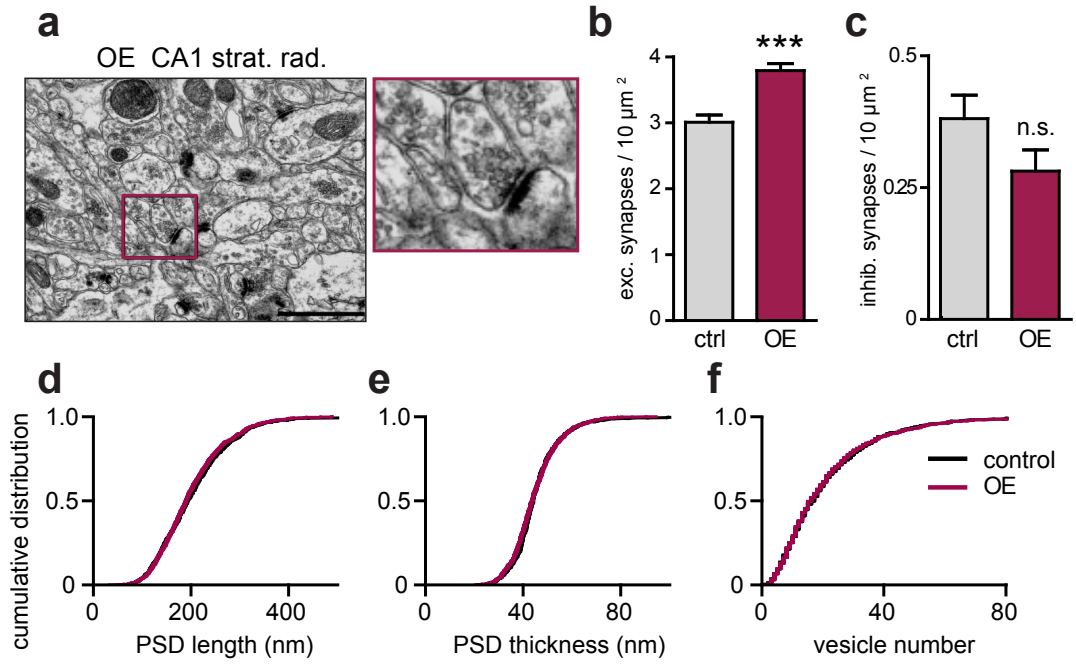

Figure 3.5: SynCAM1 overexpression increases synapse number. **a**, Left panel, representative electron micrograph of the hippocampal CA1 stratum radiatum of transgenic mice overexpressing SynCAM1^{flag} (magnification 26,500x). Right panel, enlargement of one asymmetric synapse boxed in the left panel. Scale bar, 1 μm. **b**, Transgenic mice overexpressing SynCAM1^{flag} exhibit a 26 ± 3% higher density of asymmetric, excitatory synapses in the hippocampal CA1 stratum radiatum than littermate controls as determined after electron microscopy. **c**, Symmetric, inhibitory synapse density in the CA1 stratum radiatum is not affected by SynCAM1^{flag} overexpression. **d**, Cumulative distribution of PSD length of asymmetric synapses. **e**, PSD thickness is not altered by SynCAM1^{flag} overexpression as shown by cumulative distribution analysis. **f**, SynCAM1^{flag} overexpression does not affect synaptic vesicle number per sectioned presynaptic terminal area as shown by cumulative distribution analysis. Experiments by EMR and TB.

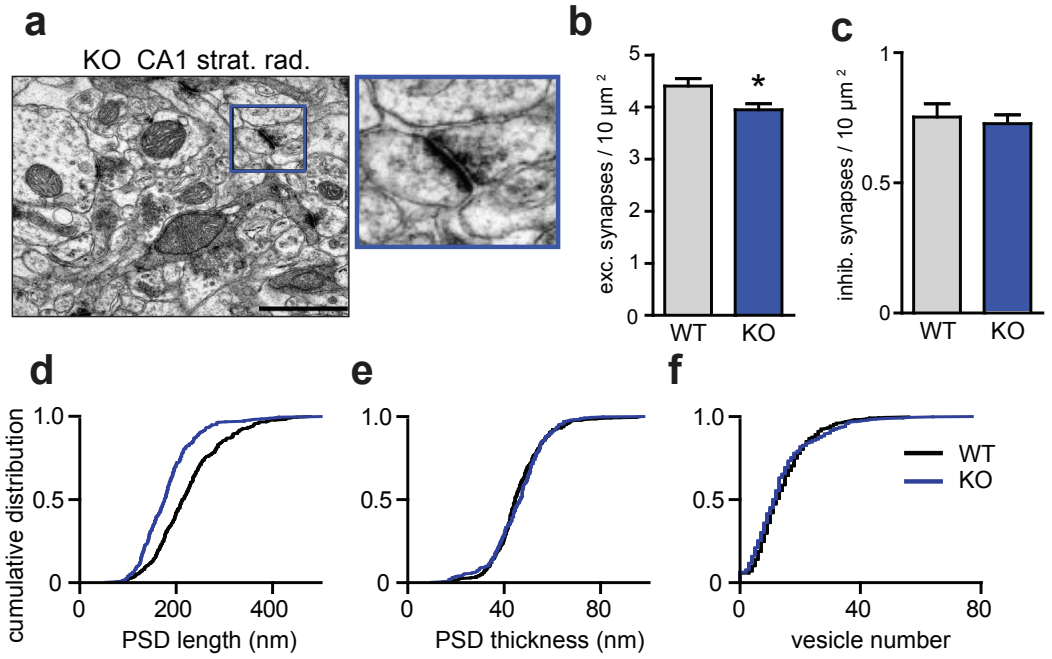

Figure 3.6: SynCAM1 KO decreases synapse number. **a**, Left panel, representative electron micrograph of the hippocampal CA1 stratum radiatum of SynCAM1 KOmice (magnification 26,500x). Right panel, enlargement of one asymmetric synapse boxed in the left panel. Scale bar, 1 μm. **b**, KO mice lacking SynCAM1 exhibit a 10 $\pm$ 3% decrease in the density of asymmetric, excitatory synapses in the hippocampal CA1 stratum radiatum compared to controls. **c**, The density of symmetric, inhibitory synapses in the CA1 stratum radiatum is not affected by the lack of SynCAM1. **d**, SynCAM1 KO mice show a 19 $\pm$ 2% decrease in PSD length as shown by cumulative distribution analysis. **e**, PSD thickness is not affected by the lack of SynCAM1 as shown by cumulative distribution analysis. **f** Lack of SynCAM1 does not alter synaptic vesicle number per sectioned presynaptic terminal area as shown by cumulative distribution analysis. Tissue preparation by AK, EM analyses by EMR and TB.

was not significantly affected (tTA littermate control, 0.39 $\pm$ 0.05 per 10 μm^2, n=180 images, n=68 synapses; OE, 0.28 $\pm$ 0.04 per 10 μm^2, n=180 images, n=50 synapses; n=3 adult male mice each) (Fig. 3.5c). The absence of an effect of SynCAM1 on inhibitory synapse number was consistent with previous cell culture studies (Fogel et al., 2007), and with the transgenic design that restricted SynCAM1 overexpression to excitatory forebrain neurons similar to its endogenous expression pattern (Thomas et al., 2008). Morphometric scoring of synapses in electron micrographs did not reveal differences in PSD length in mice overexpressing SynCAM1^{flag} (tTA littermate control 204 $\pm$ 2.6 nm, n=846 asymmetric synapses; OE 200 $\pm$ 2.1 nm, n=1087; Kolmogorov-Smirnov p=1) (Fig. 3.5d). Also, PSD thickness was not altered by SynCAM1^{flag} overexpression (tTA littermate control 45.3 $\pm$ 0.4, n=846 asymmet-

ric synapses; OE 44.8 ± 0.3, n=1087; Kolmogorov-Smirnov p=1) (Fig. 3.5e). The number of synaptic vesicles per excitatory presynaptic terminal was unchanged after SynCAM1^{flag} overexpression, as well (tTA littermate control 21.1 ± 0.59, n=793 asymmetric synapses; OE 21.1 ± 0.60, n=1018; Kolmogorov-Smirnov p=1) (Fig. 3.5f). These results demonstrate a specific effect of SynCAM1^{flag} overexpression on excitatory synapse number in the living animal.

Secondly, the question whether the loss of SynCAM1 reveals endogenous functions in organizing synapse number was addressed. Electron microscopy demonstrates that the number of excitatory synapses in SynCAM1 KO mice was significantly reduced by 10 ± 3% (wild-type littermate control, 4.40 ± 0.14 per 10 μm^2, n=120 images, n=825 synapses, n=2 male mice; KO, 3.95 ± 0.11 per 10 μm^2, n=180 images, n=1110 synapses, n=3 male mice) (Fig. 3.6b). As in SynCAM1^{flag} overexpressors, the number of inhibitory synapses was not affected in SynCAM1 KO mice (wild-type littermate control, 0.75 ± 0.05 per 10 μm^2, n=120 images, n=24 synapses, n=2 male mice at 2 months of age; KO, 0.72 ± 0.03 per 10 μm^2, n=180 images, n=40 synapses, n=3 male mice) (Fig. 3.6c). The higher synapse density in the wild-type control groups compared to the transgenic controls described above was presumably due to mouse strain differences (Crusio, 2009). Interestingly, the PSD length was reduced in SynCAM1 KO mice by 19 ± 2% (wild-type littermate control 224 ± 3.7 nm, n=391 synapses; KO 182 ± 3.5 nm, n=302; $p < 0.001$) (Fig. 3.6d), suggesting that endogenous SynCAM1 contributes to the postsynaptic structural organization of excitatory synapses. The thickness of the PSD (wild-type littermate control 45.9 ± 0.6 nm, n=391 synapses; KO 45.8 ± 0.7 nm, n=302; p=1) (Fig. 3.6e) and the number of synaptic vesicles (wild-type littermate control 13.9 ± 0.5, n=391 synapses; KO 13.0 ± 0.6, n=302; p=1) (Fig. 3.6f) were not affected in SynCAM1 KO mice. The unaltered mEPSC amplitude in the KO mice (Fig. 3.4f) indicated that the density of AMPA receptors is not altered in their shortened PSD, as mEPSC amplitude reflects postsynaptic AMPA receptor density rather than the total receptor number (Raghavachari and Lisman, 2004). These results demonstrated that the other SynCAM family members and unrelated synapse organizing proteins did not compensate, or only partially compensated, for the roles of SynCAM1 in regulating excitatory synapse number and morphology.

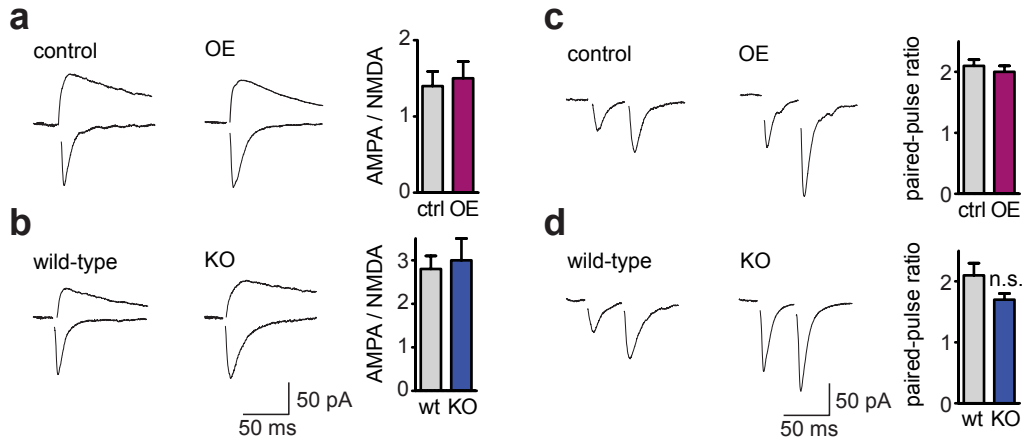

Figure 3.7: Basal synaptic transmission is unaltered in SynCAM1^{flag} overexpressors and SynCAM1 KO mice. a,b Synaptic strength does not depend on SynCAM1 protein levels. Left, representative traces of AMPA and NMDA currents from CA1 pyramidal neurons of mice aged P15 to P19. AMPA / NMDA ratios are neither altered by SynCAM1^{flag} overexpression (a) nor by loss of SynCAM1 (b), respectively. Scale bar in (b) applies to (a,b). **c,d** PPR does not depend on SynCAM1 expression levels. PPR was neither altered upon SynCAM1^{flag} overexpression (c) nor by the lack SynCAM1 (d). Scale bar in (d) applies to (c,d). Experimental design, experiments and analyses by AK.

3.2.4 Synaptic strength and presynaptic facilitation are not affected by SynCAM1

Does SynCAM1 affect other functional synaptic properties? To assess synaptic strength, I analyzed the α-amino-3-hydroxy-5-methyl-4-isoxazole propionic acid (AMPA) receptor and N-methyl-D-aspartate (NMDA) receptor components of evoked excitatory postsynaptic currents (EPSCs). Compared to littermate controls, the AMPA/NMDA ratio was neither altered in SynCAM1^{flag} overexpressing mice (tTA littermate control 1.4 $\pm$ 0.2, n=7; OE 1.5 $\pm$ 0.2, n=8; $p > 0.5$) (Fig. 3.7a) nor in KO animals (wild-type littermate control 2.8 $\pm$ 0.3, n=12; KO 3.0 $\pm$ 0.5; n=13; $p > 0.6$) (Fig. 3.7b). To assess presynaptic properties and short-term plasticity I performed paired-pulse facilitation (PPF) experiments. I found that the paired-pulse ratio (PPR), a measure of changes in the probability of transmitter release, was unchanged after SynCAM1 overexpression (tTA littermate control 2.1 $\pm$ 0.1, n=17; OE 2.0 $\pm$ 0.1, n=15; $p > 0.5$) or loss (wild-type littermate control 2.1 $\pm$ 0.2, n=17; KO 1.7 $\pm$ 0.1; n=11; $p > 0.1$) (Fig. 3.7d). These experiments showed that synaptic strength and short-term plasticity of synapses are unaffected by SynCAM1 expression levels.

With the exception of the shortened PSD in the SynCAM1 KO, these experiments and the ultrastructural analyses in figures 3.5, 3.6, demonstrate that SynCAM1 does not affect the structural and functional properties of excitatory synapses.

3.2.5 SynCAM1 increases and maintains excitatory synapse number

As my results demonstrated that SynCAM1 overexpression increases excitatory synapse number, I asked at which point in synapse development SynCAM1 acts to exert this effect. I considered two hypotheses: Either SynCAM1 acts during development to drive an increase in synapse number, but is then dispensable for sustaining this effect. In this case, the SynCAM1-mediated increase in synapse number would persist beyond a shutdown of its overexpression. Alternatively, SynCAM1 could be continuously required to determine excitatory synapse number, possibly by initially promoting dendrite outgrowth and then stabilizing transient synapses. In that case, the gain in synapse number would be lost after ending SynCAM1 overexpression.

To distinguish between these hypotheses, I utilized the temporal expression control afforded by the previously described transgenic mouse line (see 3.2.1). First, I confirmed the efficient functional repression of SynCAM1^{flag} expression by doxycycline feeding using mEPSC recordings. When animals were continuously fed doxycycline to repress overexpression mEPSC frequencies were indistinguishable between tTA control and OE^{never} (tTA control 0.9 $\pm$ 0.1 Hz, n=11; OE^{never} 1.3 $\pm$ 0.1 Hz, n=12) (Fig. 3.9a,b). Furthermore, feeding control animals with doxycycline had no effect on functional synapse number (1.0 $\pm$ 0.1 Hz, n=8) (Fig. 3.9a,b). Accordingly, this model system afforded efficient functional repression of SynCAM1^{flag} overexpression. Moreover, doxycycline had no effect on mEPSC frequency, permitting further analyses.

My earlier results showed that SynCAM1 overexpression increases mEPSC frequency at the peak of synaptogenesis around P14 (Fig. 3.4b). I next asked whether the increase in synapse number would be maintained at later stages of development an whether SynCAM1 only acts early in development or can still induce synpase formation in juvenile animals after P14. I therefore analyzed excitatory synapse numbers by mEPSC recordings from acute hippocampal slices of juvenile mice at P28. Three different SynCAM1^{flag} overexpression

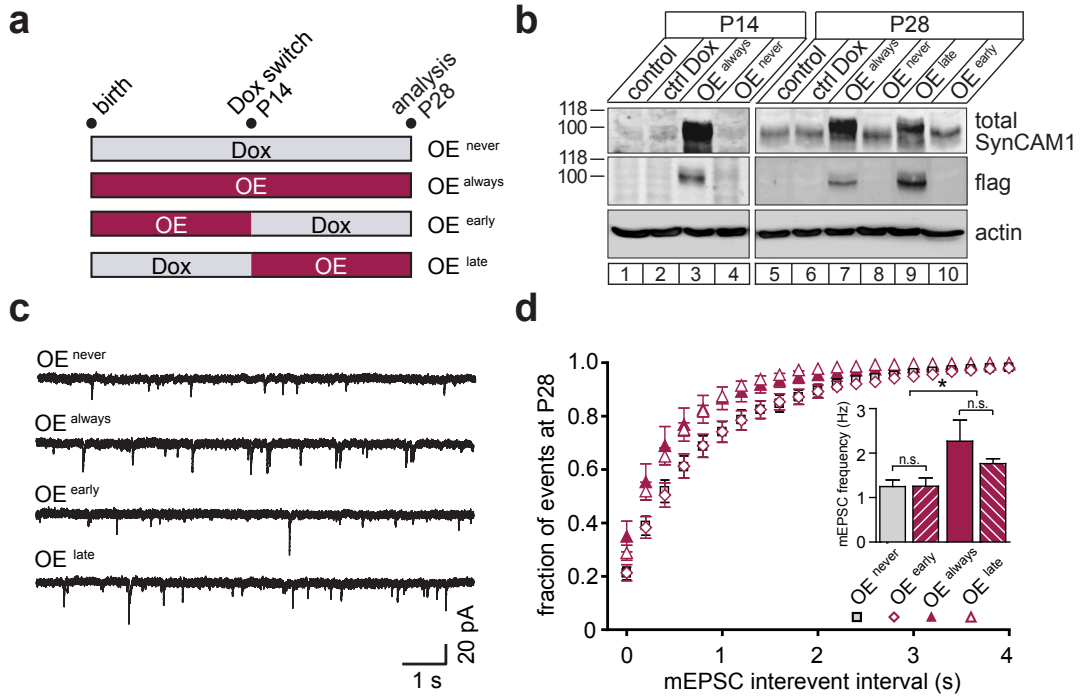

Figure 3.8: Continuous presence of SynCAM1 is required to maintain increased synapse number. **a**, Experimental design. Overexpression of SynCAM1^{flag} in transgenic mice was either continuously repressed by doxycycline (OE^{never}), or animals continuously overexpressed SynCAM1^{flag} until P28 (OE^{always}). Two other cohorts were either treated from P14 with doxycycline to repress overexpression from this time point (OE^{early}), or were removed from preceding doxycycline-mediated repression at P14 (OE^{late}) to turn overexpression on. **b**, Immunoblot analysis of hippocampal homogenates. SynCAM1^{flag} protein levels were probed at P14 and P28 in hippocampi obtained from animals treated as described in (a). Actin served as a loading control. **c**, Representative mEPSC recordings from P28 hippocampal CA1 pyramidal neurons of transgenic overexpressors following the experimental treatments described in (a). **d**, SynCAM1-induced increases in synapse number require its continuous presence. Cumulative distributions of mEPSC interevent intervals at P28. Compared to littermate control animals, the continuous overexpression of SynCAM1^{flag} (OE^{always}) causes an increase in mEPSC frequency at P28. Continuous repression (OE^{never}) of SynCAM1^{flag} expression reduces mEPSC frequencies to control levels. Early overexpression of SynCAM1^{flag} until P14 initially increases mEPSC frequencies at P14 (Fig. 3.4 a,b), and subsequent repression of SynCAM1^{flag} returns mEPSC frequencies to control levels by P28 (OE^{early}). When overexpression is turned on at P14 (OE^{late}) mEPSC frequencies are indistinguishable from those of continuously overexpressing animals (OE^{always}). See Tab. 3.1 for statistical analyses and Fig. 3.9 for additional control experiments. Experimental design, experiments and analyses by AK (a,c,d). Experimental design and tissue preparation by AK, western blotting by EMR (b).

conditions were analyzed: Animals overexpressed SynCAM1 either constitutively (OE^{always}), or only within the first two weeks of postnatal development (OE^{early}), or selectively in the third and fourth postnatal week (OE^{late}) (Fig. 3.8a). Three controls were analyzed in

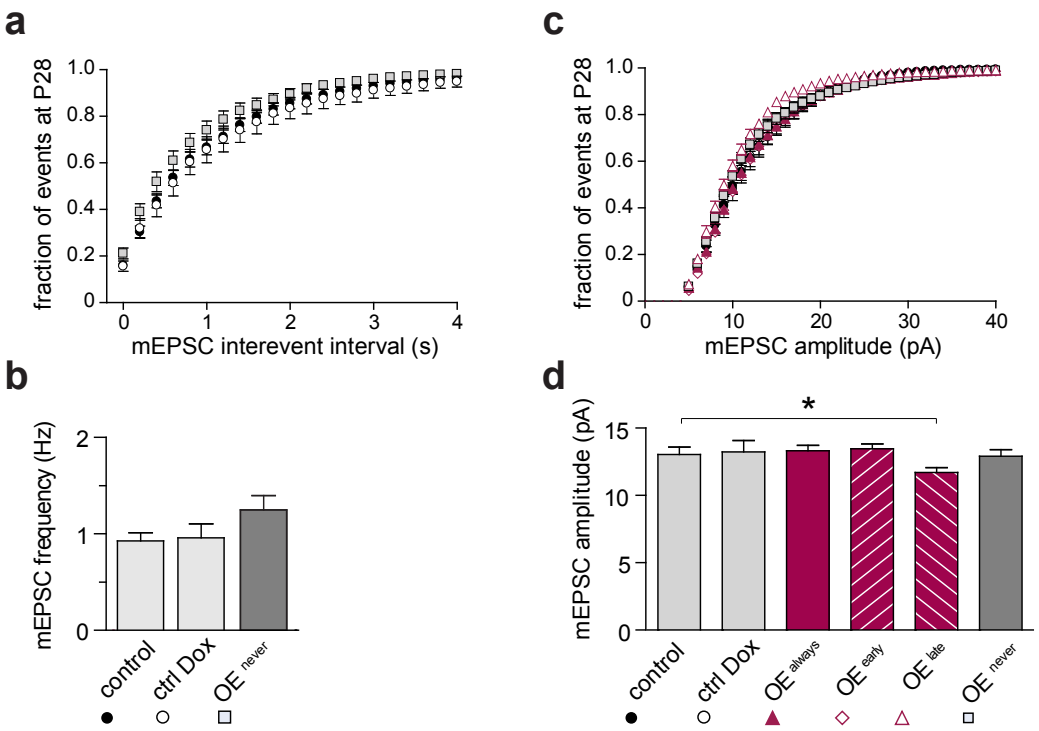

Figure 3.9: Control experiments of conditional SynCAM1^{flag} overexpression. **a**, Cumulative distributions of mEPSC interevent intervals at P28. Doxycycline efficiently represses SynCAM1^{flag} overexpression effects. For symbol legends, see (b). **b**, Mean mEPSC frequencies of the conditions shown in (a). Miniature EPSC frequencies of untreated control animals (tTA control) are indistinguishable from those of continuously repressed mice (OE^{never}). Doxycycline treatment of animals that only carry the tTA transgene (ctrl Dox) has no effect on mEPSC frequencies compared to untreated tTA control animals. **c**, Cumulative distributions of mEPSC amplitudes at P28 were indistinguishable between most SynCAM1^{flag} expression conditions (Table 3.1). Only after late SynCAM1^{flag} expression (OE^{late}), mEPSC amplitudes were slightly decreased compared to all other conditions. For symbol legends, see (d). **d**, Mean mEPSC amplitudes of the conditions shown in (c). Note that only the slight reduction in mEPSC amplitude of OE^{late} was significantly different from tTA controls, but not when compared to the other conditions. This could be due to the high sensitivity of the Kolmogorov-Smirnov test used to test for statistical difference of mEPSC distributions. Experimental design, experiments and analyses by AK.

parallel to these SynCAM1^{flag} overexpression conditions. In one cohort of mice, SynCAM1^{flag} overexpression was repressed by continuously administering doxycycline (OE^{never}). A second and third cohort comprised animals lacking the SynCAM1^{flag} transgene. This second group of mice remained untreated, while the third group was treated with doxycycline to exclude nonspecific effects of this drug on synapse number. Immunoblotting of hippocampal lysates obtained after these treatments confirmed the repression and late expression of SynCAM1^{flag}

Table 3.1: Summary of Kolmogorov-Smirnov significance tests. Cumulative distributions of mEPSC interevent intervals (Figs. 3.8b, 3.9a) and amplitudes (Figs. 3.8c, 3.9c) were tested for significance using the Kolmogorov-Smirnov test. P values are given in the table. Significance level for KS test was 0.01.

a

intervals					
	OE^{always}	OE^{late}	OE^{early}	OE^{never}	ctrl Dox
OE^{late}	1				
OE^{early}	0.001	0.001			
OE^{never}	0.001	0.001	1		
ctrl Dox	0.001	0.001	1	1	
ctrl tTA	0.001	0.001	1	1	1

b

amplitudes					
	OE^{always}	OE^{late}	OE^{early}	OE^{never}	ctrl Dox
OE^{late}	1				
OE^{early}	1	0.025			
OE^{never}	1	1	0.1		
ctrl Dox	1	1	1	1	
ctrl tTA	1	0.01	1	0.05	0.1

(Fig. 3.8b). mEPSC frequencies and amplitudes were indistinguishable under all control conditions (frequencies: tTA control 0.9 ± 0.1 Hz, n=11; OE^{never} 1.3 ± 0.1 Hz, n=12; amplitudes: OE^{late} 11.7 ± 0.4 pA, n=7; OE^{always} 13.3 ± 0.4 pA, n=8; OE^{early} 13.5 ± 0.4 pA, n=11; OE^{never} 12.9 ± 0.5 pA, n=12; tTA control 13.0 ± 0.5 pA, n=11; ctrl Dox 13.2 ± 0.9 pA, n=8) (Fig. 3.9b,d). Distributions of mEPSC interevent intervals and amplitudes were compared using the Kolmogorov-Smirnov (KS) test with an assumed significance level of $p < 0.01$ as summarized in table 3.1.

As observed at P14 (Fig. 3.4b), the continuous overexpression of $SynCAM1^{flag}$ caused a similarly strong increase in mEPSC frequency at P28 (Fig. 3.8d). This reflected a SynCAM1-driven increase in excitatory synapse number not only at the peak of synaptogenesis during the second postnatal week, but also at later stages. Notably, when SynCAM1 was only overexpressed until P14, but was then shut down (OE^{early}), mEPSC recordings at P28 revealed that the increase in synapse number that had been observed at P14 was lost by P28 (Fig. 3.8c,d).

Interestingly, when the overexpression of $SynCAM1^{flag}$ was repressed until P14 and switched on at P14 (OE^{late}), I observed at P28 an increase in mEPSC frequency that was statistically indistinguishable from the frequency recorded after continuous overexpression (Fig. 3.8d, also see 4.6 for discussion of seeming difference in means). Taken together, these results demonstrated that SynCAM1 does not only induce synapse formation in early stages

of development but also increases synapse number in more mature brains. Furthermore, the continuous presence of SynCAM1 is required to maintain the increase in synapse number and its withdrawl results in the loss of the gained synapses. Hence, these findings were in agreement with my second hypothesis that SynCAM1 is required to sustain the increase in excitatory synapse number.

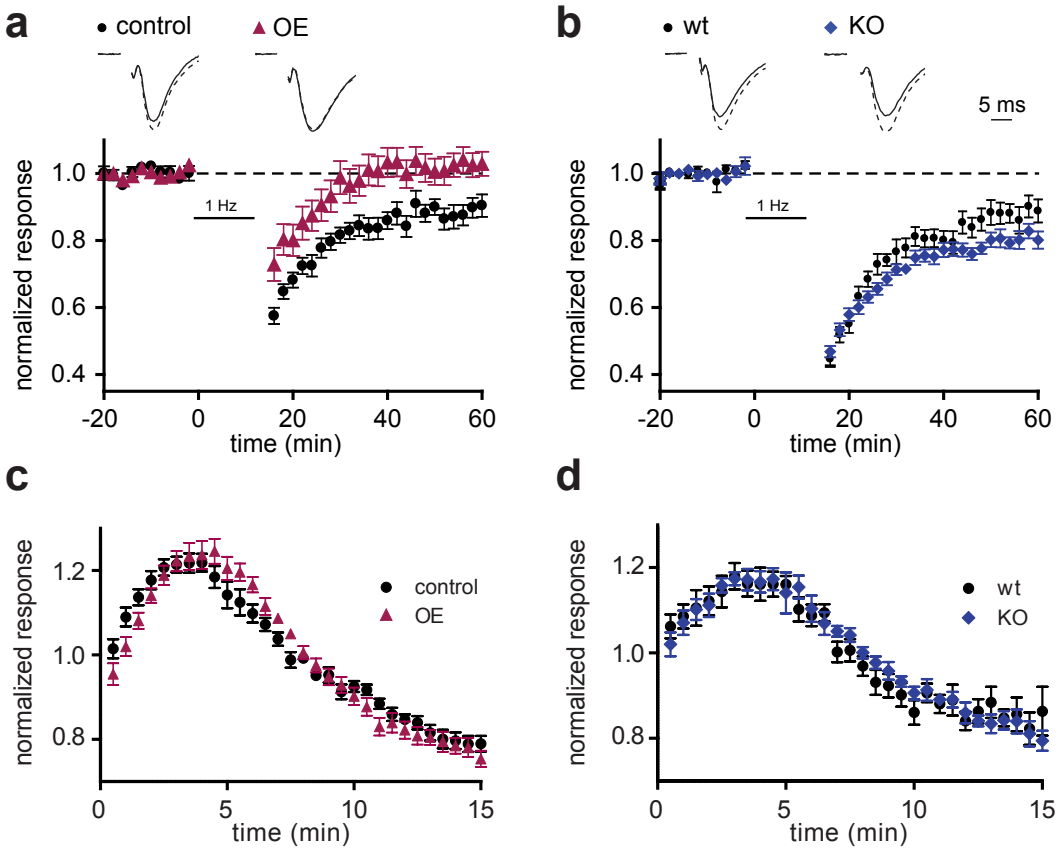

Figure 3.10: Expression level of SynCAM1 changes LTD. Extracellular field potential recordings (fEPSP) were obtained before and after induction of LTD in SynCAM1^{flag} overexpressors (a,c) and KO mice (b,d). Representative traces (a,b,top) depict normalized average fEPSP recordings before (dotted line) and 55-60 min after (solid line) LTD induction. Stimulus artifacts were omitted for clarity. Scale bar in (b) applies to (a,b). **a**, LTD is not observed in SynCAM1^{flag} overexpressors, while tTA littermate control animals exhibit normal levels of LTD. **b**, Loss of SynCAM1 leads to an increased level of LTD. Horizontal bars depict the time of LTD induction. **c,d**, fEPSP responses during LTD induction are neither affected by SynCAM1^{flag} overexpression (c) nor by loss of SynCAM1 (d), respectively. Experimental design, experiments and analyses by AK.

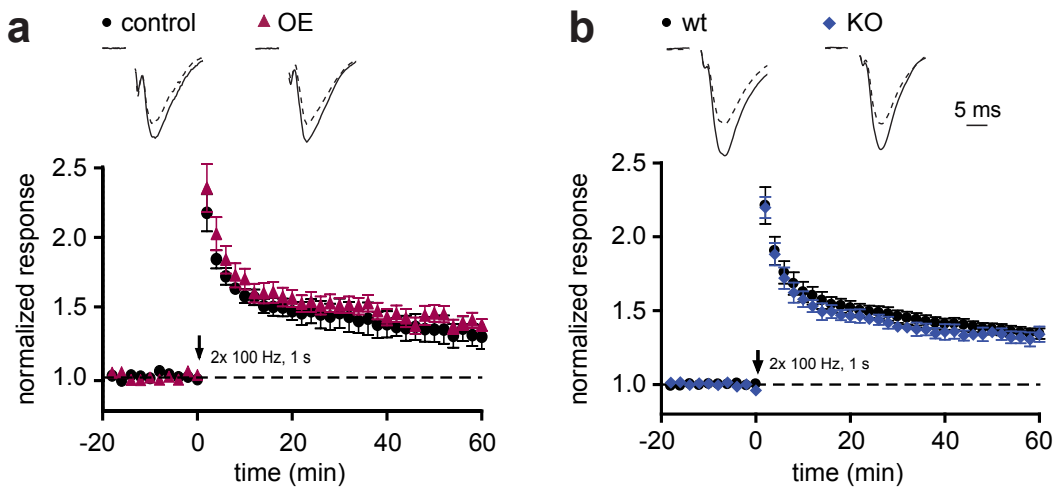

Figure 3.11: SynCAM1 does not affect long-term potentiation. a,b Extracellular field potential recordings (fEPSPs) were obtained before and after induction of LTP in SynCAM1^{flag} overexpressors (a) and KO mice (b). Representative traces (top) depict normalized average fEPSP recordings before (dotted line) and 55-60 min after LTP induction (solid line). Stimulus artifacts were omitted for clarity. Overexpression (a) or loss (b) of SynCAM1 do not impact LTP. Scale bar in (b) applies to (a,b). Stimulus artifacts were omitted for clarity. Arrow depicts time of LTP induction. Experimental design, experiments and analyses by AK.

3.2.6 Long-term depression is regulated by SynCAM1 expression level

Trans-synaptic interactions may not only alter synapse formation and development but also synaptic plasticity. I therefore addressed whether SynCAM1 affects neuronal connectivity not only through controlling excitatory synapse number, but also through effects on synaptic plasticity. I first tested the roles of SynCAM1 in long term depression (LTD), a plasticity mechanism that decreases synaptic strength after low-frequency stimulation. Intriguingly, mice overexpressing SynCAM1^{flag} fail to exhibit LTD in extracellular field potential recordings from the CA1 area of the hippocampus (tTA littermate control 0.90 $\pm$ 0.01, n=15; OE 0.99 $\pm$ 0.01, n=20; $p < 0.001$) (Fig. 3.10a). Conversely, LTD was expressed more strongly in SynCAM1 KO mice (wild-type littermate control 0.88 $\pm$ 0.01, n=10; KO 0.82 $\pm$ 0.01, n=17; $p < 0.001$)(Fig. 3.10b).

SynCAM1 expression might not necessarily influence LTD expression but could also influence the induction itself. Both mechanisms of action would be indistinguishable by analysis of LTD expression, only. However, the timecourses of the induction of LTD were indistinguishable between the KO or overexpressor and the respective controls (Fig. 3.10c,d).

Effects of SynCAM1 on LTD induction could therefore be excluded confirming the effect of SynCAM1 on LTD expression.

To test whether SynCAM1 also alters the ability to strengthen synaptic transmission in an activity-dependent manner, long term potentiation (LTP) was measured. I observed no effects of SynCAM1^{flag} overexpression or loss of SynCAM1 on LTP (Fig. 3.11a, tTA littermate control 1.29 ± 0.09, n=6; OE 1.37 ± 0.05, n=10; $p > 0.05$; Fig. 3.11b, wild-type littermate control 1.34 ± 0.06, n=4; KO 1.35 ± 0.04, n=10; $p > 0.05$). Together, these experiments demonstrate that SynCAM1 does not alter the strengthening of synaptic transmission by LTP. In contrast, SynCAM1 strongly affects the weakening of synaptic connections by LTD.

3.2.7 SynCAM1 affects spatial learning

As higher cognitive tasks involve synaptic plasticity, SynCAM1 expression may alter experience-dependent behavior. This question was first addressed in the SynCAM1^{flag} overexpressing mice that lack LTD. Locomotor function of these mice was unaltered, as measured by swim speed (n=11 male tTA control, n=12 male OE mice per genotype, aged 3-5 months) (Fig. 3.12a). These control experiments confirmed that their motor functions as well as vision are unaffected (data not shown), permitting behavioral studies. These mice were analyzed in the Morris water maze paradigm, a hippocampus-dependent task of spatial reference learning. The animals' motivation to reach a submerged, but visibly marked platform in a water tank was unaltered (data not shown). Yet, SynCAM1^{flag} overexpressors failed to properly learn the quadrant location when the platform was hidden (Fig. 3.8b), and did not locate the correct maze quadrant when subjected to a probe trial (tTA littermate control 46.7 ± 3.1% , n=11 male mice; OE 29.0 ± 6.8% , n=12 male mice; $p < 0.05$; mice were 4-5 months of age) (Fig. 3.12b). This surprising impairment of spatial learning and memory was not due to a general hippocampal dysfunction, as these animals performed normally in a novel objection recognition task (data not shown). To extend this analysis beyond cognitive tasks, anxiety-related behavior was also assessed. Testing the SynCAM1^{flag} overexpressing animals in the elevated plus maze identified no alteration in the number of entries into an exposed maze arm, indicative of unchanged anxiety levels (Robbins and Biederer, personal

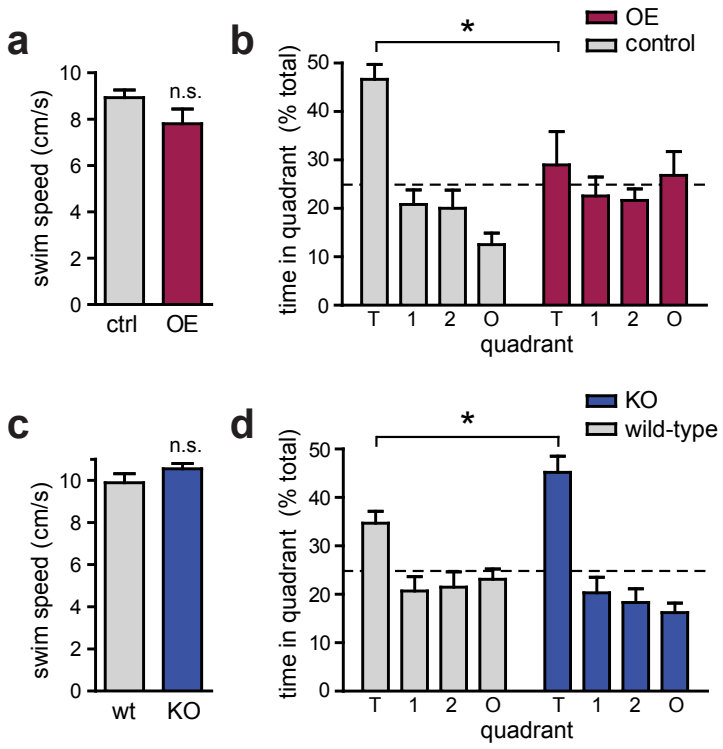

Figure 3.12: Spatial learning is impaired by SynCAM1 overexpression and enhanced by its loss. **a**, Locomotor activity, measured by swim speed, is not altered in SynCAM1^{flag} overexpressing **b**, Hippocampus-dependent memory is impaired in SynCAM1^{flag} overexpressing mice. Following training in the Morris water maze, a probe trial was performed to measure the time spent by trained animals in the target quadrant that contained the escape platform during training. SynCAM1^{flag} overexpressing mice exhibit no preference for the correct target quadrant T after training. O, opposite quadrant; 1, 2, adjacent quadrants. The dotted line at 25% indicates chance level. **c**, Swim speed is not altered in SynCAM1 KO animals. **d**, SynCAM1 KO mice exhibit improved performance in the Morris water maze compared to controls. KO mice spent more time in the target quadrant T, demonstrating increased spatial learning. Differences of time spent in quadrant T by SynCAM1 transgenic controls in (b) and wild-type controls in (d) are likely due to differences in age. Experimental design, experiments and analyses by EMR (a,b) and AKG (c,d).

communication).

In contrast to SynCAM1^{flag} overexpressors, LTD was enhanced in SynCAM1 KO animals; this led to the hypothesis that learning might be altered and possibly improved in these mice. To facilitate the detection of putative changes, behavioral studies were performed in adult mice that exhibit a reduced capability to learn. Motor functions were normal in these mice (n=8 male wild-type control, n=9 male KO mice, aged 6-12 months) (Fig. 3.12b), and no changes in anxiety-related behavior were identified in the KO mice (data not shown).

Further, the animals' motivation to reach the visibly marked platform in a water tank was unaffected (data not shown). Notably, SynCAM1 KO mice learned the location of the quadrant in the Morris water maze that contains the hidden platform significantly faster than wild-type littermate controls (data not shown). Even more surprisingly, the lack of SynCAM1 enhanced spatial memory as tested in a probe trial of these trained mice (wild-type littermate control 34.7 ± 2.5%, n=7 male mice; KO 45.2 ± 3.3%, n=9 male mice; $p < 0.05$; mice were 6-12 months of age) (Fig. 3.12d).

4 Discussion

The goal of this thesis was to identify the function of SynCAM1 in neurons of the CNS. This task was experimentally addressed with initial experiments in cell culture, which motivated the subsequent analyses of two genetically modified mouse models that either lacked SynCAM1 (KO line) or in which SynCAM1^{flag} can be conditionally overexpressed under temporal control of a Tet off system.

The results presented in this thesis reveal that SynCAM1 and SynCAM2 can interact homophilically or form heteromers of SynCAM1 and SynCAM2 to regulate excitatory synapse formation *in vitro*. In the intact brain, overexpression of SynCAM1 increases the number of functional excitatory synapses and is required to maintain this increase in synapse number during development. Furthermore, SynCAM1 is endogenously required to control excitatory synapse number. In addition to the effect on synapse number, overexpression of SynCAM1^{flag} impairs LTD and loss of SynCAM1 facilitates LTD. Finally, SynCAM1 KO mice that exhibit a decrease in excitatory synapse number and enhanced plasticity show improved performance in spatial learning. Conversely, SynCAM1^{flag} overexpressing mice with more excitatory synapses and impaired LTD fail in spatial learning tasks. Taken together, my results demonstrate that SynCAM1 modulates synapse number, regulates synaptic plasticity and impacts spatial learning.

4.1 Heterophilic adhesion of SynCAM1 and SynCAM2

The interaction of cell adhesion molecules across the synaptic cleft regulates synapse formation (Akins and Biederer, 2006; Dalva et al., 2007). In the first part of this study, the adhesive properties of SynCAM family proteins were demonstrated and the strongest interaction between the synaptically localized proteins SynCAM1 and 2 was identified (published

in Fogel, Krupp, et al., 2007).

The heterophilic interaction of SynCAM1 and 2 is mapped to the Ig domains 1 and 2 of both proteins and is regulated by N-glycosylation. The trans-interaction of the first two Ig like domains of SynCAM1 and SynCAM2 suggests an extended SynCAM complex that is likely found at the synaptic cleft. Binding among SynCAM family proteins is highly specific and SynCAM1 and 2 can either interact homophilically or form SynCAM1 and 2 heteromers. The capability of SynCAM2 to induce the formation of functional synapses is reported for the first time in this study (Fig. 3.1) whereas the interaction of the two remaining family members SynCAM3 and 4 is essential for myelination in the PNS (Spiegel et al., 2007; Maurel et al., 2007). Furthermore, all four SynCAM family proteins are thought to serve distinct functions since their expression as well as their glycosylation is differentially regulated in development.

To assess the function of SynCAM1 and 2, the respective SynCAM protein was overexpressed in neuronal cultures. Synaptic inputs onto this overexpressing neuron were recorded physiologically to determine alterations at the postsynaptic side of the overexpressing neurons. Upon overexpression of SynCAM1 and SynCAM2 mEPSC frequency is increased, reflecting an increase in excitatory synapse number (Fig. 3.1). In this system, the overexpressing cell always represented the postsynaptic side of the analyzed synapses. I can hence conclude that SynCAM1 and 2 increase the number of synapses when they are expressed postsynaptically. In contrast to other synaptically localized cell adhesion molecules, SynCAM1 and SynCAM2 do not alter basal synaptic transmission, neuron morphology, or dendritic arborization but exclusively affect synapse number.

Heterophilic binding of SynCAM1 and 2 is controlled by glycosylation (Fogel et al., 2007). This form of posttranslational modification may serve to regulate SynCAM1 and 2 interaction and thereby define distinct roles of these proteins in different periods of development (see Fogel, Krupp, et al., 2007). A recent study confirms this observation, identifies SynCAM1 as a target of polysialysation and implicates it in the formation of synapses between neurons and glial NG2 cells (Galuska et al., 2010). These results identify synaptic adhesion and glycosylation as one way to regulate synapse formation. Based on these findings, it is tempting to speculate about intracellular targets of SynCAM signaling, which will be discussed in paragraph 4.5. These promising results from cell culture experiments

motivated the more detailed analysis of the functions of SynCAM1 in the intact brain.

4.2 SynCAM1 regulates synapse number in the intact brain

Previous studies have shown that SynCAM1 induces the formation of presynaptic specializations in a co-culture system (Biederer et al., 2002) and that SynCAM1 exhibits a synaptogenic capacity in neuronal cultures (Sara et al., 2005). Furthermore, these data demonstrate that the synaptogenic effects of SynCAM1 are mediated by the protein's first and second immunoglobulin (Ig) domains and are regulated by glycosylation *in vitro* (Fogel et al., 2007).

In the developing brain, overexpression of SynCAM1^{flag} increases the number of excitatory synapses whereas the loss of SynCAM1 results in a lower number of excitatory synapses (see results 3.2.2). Both effects were observed using physiological (Fig. 3.4), as well as morphological analyses (Figs. 3.5, 3.6). These findings are consistent with previous studies *in vitro* (Biederer et al., 2002; Sara et al., 2005) and extend the knowledge of the function of SynCAM1 to its roles in the developing brain.

It is remarkable that SynCAM1 KO mice exhibit a significant decrease in excitatory synapse number since complementation by the remaining family members SynCAM2-4 seemed likely. However, the single KO of SynCAM1 already causes a significant decrease in synapse number in the presence of SynCAM2-4. This result indicates that SynCAM1 plays a critical role in synapse formation that cannot be fully compensated by other mechanisms. Furthermore, this study demonstrates that SynCAM1 is not essential for the formation of all excitatory synapses since synapse formation is still possible in SynCAM1 KO mice.

SynCAM1 and other cell adhesion molecules differ in the function of the respective protein at the synapse. Therefore, this study was extended to the analysis of parameters associated with synapse maturation and synaptic transmission. The expression level of SynCAM1 affects none of the parameters associated with synaptic transmission or synapse maturation, such as the AMPA/NMDA and the paired-pulse ratio (Fig. 3.7), PSD thickness and presynaptic vesicle number (Figs. 3.5, 3.6). The length of the PSD remains unchanged upon SynCAM1 overexpression (Fig. 3.5) and is slightly decreased in SynCAM1 knockout animals with reduced synaptic adhesion (Fig. 3.6). The shortened PSD might reflect a destabilization of the PSD upon loss of SynCAM1-mediated adhesion. However, no other parameter

associated with synapse maturation is altered upon loss or overexpression of SynCAM1. In contrast to other cell adhesion molecules, these results support the conceptionally interesting interpretation that SynCAM1 mediates the formation but not the maturation of excitatory synapses.

The relevance of SynCAM1 in synaptogenesis *in vivo* is further highlighted by the results of a gene chip analysis that was performed after induction of synaptic plasticity (Lyckman et al., 2008). One would predict increased transcription of genes involved in synapse formation after the induction of synaptic plasticity. *Cadm1*, the gene encoding the SynCAM1 protein, was the only synaptogenesis-related gene with an upregulation of transcription after the induction of synaptic plasticity (Lyckman et al., 2008). This compensatory upregulation of *Cadm1* transcription further illustrates the importance of SynCAM1 in synapse formation *in vivo*.

EphB receptors are implicated in the regulation of filopodia motility, in interactions with NMDARs, in the recruitment of synaptic machinery and in synapse maturation (Kayser et al., 2008; Dalva et al., 2000; McClelland et al., 2009). Similarly, the adhesion molecules NLGN1-3 mediate synapse maturation without affecting synapse formation (Varoqueaux et al., 2006). Knockout animal models for ephrins and Eph receptors as well as for neuroligins do not show pronounced deficits in synapse formation when any single molecule is knocked out. Instead, the importance of EphB receptors in synapse formation and of neuroligins in synapse maturation becomes apparent from triple knockout studies in both cases (Henkemeyer et al., 2003; Varoqueaux et al., 2006). The absence of obvious phenotypes in single KO lines of these molecules suggests complementing effects between family members. In contrast, the present study demonstrates that the single knockout of only one of the four SynCAM family members is sufficient to attenuate excitatory synapse formation (see chapter 3.2.2), which underlines the biological relevance of SynCAM1 in synapse formation.

The selective effect of SynCAM1 on synapse number is distinct from phenotypes of animal models for other cell adhesion molecules, that are also involved in synapse maturation and in the modulation of synaptic transmission (Chavis and Westbrook, 2001; Varoqueaux et al., 2006; Kayser et al., 2008; Wittenmayer et al., 2009). According to the filopodia model of synapse formation (see Fig. 1.1), I hypothesize that SynCAM1–mediated synaptic adhesion is important in early phases of synapse development that might be related to the

initial stabilization of axo-dendritic contacts. The protein's adhesive properties as well as the absence of effects on parameters of maturation and synaptic transmission support the interpretation that SynCAM1 mediates initial axo-dendritic contact formation and might also affect the stability of existing synapses.

Regarding the roles of synaptic molecules in the formation, maturation and function of excitatory synapses, SynCAM1 selectively regulates synapse formation without affecting most of the structural measures of maturation and none of the functional synaptic parameters. In summary, this thesis identifies SynCAM1 as a specific regulator of excitatory synapse formation but not of synapse maturation in the intact brain. Importantly, the loss of SynCAM1 cannot be fully compensated by other adhesion molecules.

4.3 Role of SynCAM1 during development

The overexpression of SynCAM1 increases the mEPSC frequencies of cultured neurons at 10 days *in vitro* (DIV) but has no effect in cultured neurons aged 14 DIV, suggesting differential developmental effects (Sara et al., 2005). The tet-off transgenic design of the SynCAM1^{flag} overexpressing mice allowed analyzing synaptic functions of a specific cell adhesion molecule at different stages of development in the living animal for the first time.

Most excitatory circuitry in the mouse hippocampus is formed in the first 14 days of postnatal development. Hence, the effect of overexpression of SynCAM1^{flag} in this early phase of development and in the juvenile period between P14 and P28 were analyzed separately. Using temporal control of SynCAM1^{flag} everexpression, I have demonstrated that the function of SynCAM1 is not restricted to early brain development. Instead, SynCAM1 still induces synapse formation in animals at the age of two to four weeks. Furthermore, it would have been conceiveable that SynCAM1 is only required for the induction of synaptogenesis and is dispensable afterwards. This is not the case as the continuous expression of SynCAM1 is required to maintain an increase in synapse number and ending overexpression results in a decrease of synapse number (Fig. 3.8).

These results indicate that SynCAM1 is generally required to regulate synapse number at early and late stages of brain development. One of the roles of SynCAM1 might be the stabilization of synaptic contacts between the pre– and the postsynapse by its adhe-

sive properties. This "adhesion" model would agree with the phenotypes observed in both animal models — with loss of adhesion in the KO mice resulting in a contact destabilization and strengthened adhesion upon SynCAM1^{flag} overexpression resulting in more stable transsynaptic interaction. Consequently, initial contacts between axon and dendrite would be stabilized in the presence of SynCAM1 and give rise to a functional synapse. In contrast, these contacts would only be transient in the absence of the protein and would not result in the formation of a synapse (Fig. 4.1). Accordingly, SynCAM1 might control the "success rate" of excitatory synapse formation througout development and serve as a "molecular glue" of excitatory synapse formation (see Fig. 4.1).

4.4 Synaptic plasticity

Synaptic plasticity is thought to be one of the mechanisms required for the adaptation of the brain to an ever changing environment. This adaptation requires the strengthening and weakening of existing synaptic connections as well as the formation of new synapses and loss of unused synapses (Malenka and Bear, 2004). LTP and LTD are experimental paradigms that allow studying these processes.

Synaptic plasticity in both of these paradigms, is mediated by similar mechanisms acting in opposite directions: Induction of LTP leads to the recruitment of more receptors to the postsynapse, to receptor modification by phosphorylation, and to the formation of additional synapses (Malenka and Bear, 2004). Consequently, LTP results in increased synaptic strength and in increased synapse number (Bredt and Nicoll, 2003; Malenka, 2003). Conversely, LTD results in loss of receptors from existing synapses, increased protein phosphatase activity and in loss of entire synapses to weaken synaptic transmission (Mulkey et al., 1993; Carroll et al., 1999; Becker et al., 2008; Bastrikova et al., 2008).

The influence of cell adhesion molecules on synaptic plasticity has been addressed in numerous studies, mostly implicating them in long-term potentiation. Integrins have been characterized in particular detail with respect to LTP and were found to be required for LTP expression (Chan et al., 2003) and consolidation (Chun et al., 2001). β3 integrins can furthermore control AMPAR subunit composition and receptor internalization as well as synaptic strength (Cingolani et al., 2008). They also modulate AMPAR and NMDAR

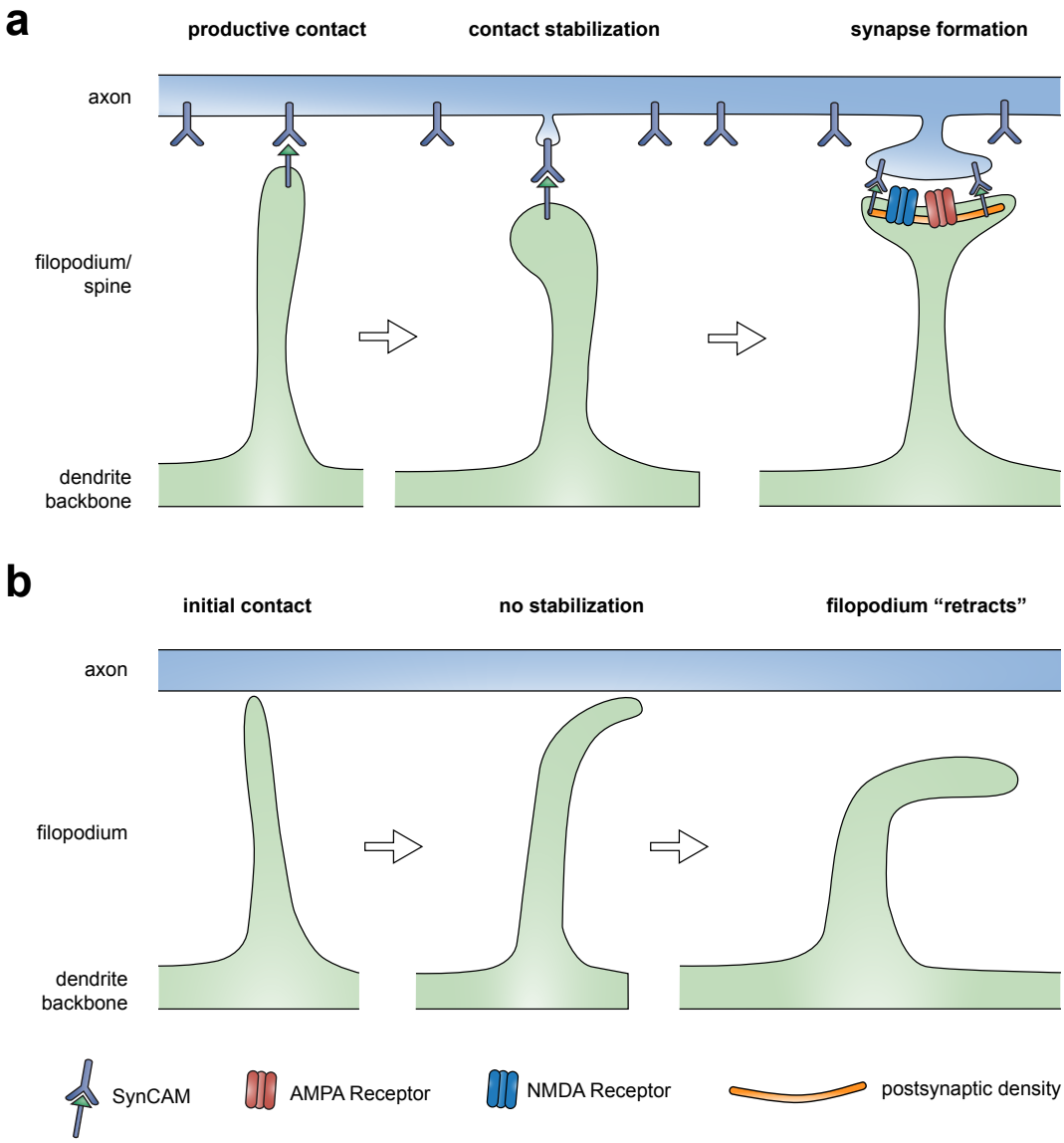

Figure 4.1: ”Synaptic glue” model of synapse formation. Formation of excitatory synapses in the CNS partially depends on the presence of SynCAM1 (depicted in light blue). SynCAMs mediate intracellular adhesion between axon (light blue) and dendrite (light green). **a**. A dendritic filopdium contacts an axon and SynCAM proteins on both membranes form an adhesive pair (prductive contact). SynCAM-mediated adhesion stabilizes the axo-dendritic contact and enables the formation of an excitatory synapse. **b**. A dendritic filopodium contacts an axon. In the absence of SynCAM1, this initial contact cannot be stabilized because no productive interaction forms between both cells. Consequently, the dendritic filopodium is not retained at the axon and retracts.

function and influence dynamics of the actin cytoskeleton which ultimately contributes to structural plasticity (Kramar et al., 2003; Lin et al., 2003). Differential effects on LTP have

also been reported for ephrins and Eph receptors. In EphB2 KO mice, protein synthesis dependent LTP, LTD and depotentiation are impaired (Grunwald et al., 2001). Furthermore, postsynaptic ephrinB2 and ephrinB3 as well as EphA4 are required for LTP (Grunwald et al., 2004). Additionally, loss and functional impairment of these two ephrinBs abrogates LTD. Neuron-glia communication between EphA4 and ephrinA3 also modulates LTP through the regulation of glial glutamate transport (Filosa et al., 2009). Furthermore, the PSD-95 binding adhesion molecule neuroligin 1 was shown to be required for LTP (Kim et al., 2008).

However, LTP is not affected by loss or overexpression of SynCAM1 (Fig. 3.11). Instead, this is the first study to show an effect of a synapse-inducing adhesion molecule on LTD (Fig. 3.10). This thesis demonstrates that LTD is impaired in SynCAM1^{flag} overexpressing animals whereas it is more pronounced in SynCAM1 knockout animals than in control animals. This data suggests that increasing cell adhesion by SynCAM1^{flag} overexpression prevents synaptic depression whereas a decrease in synaptic adhesion in the KO model increases the potential to undergo LTD.

4.4.1 Mechanisms underlying LTD

The experimental paradigm used in this study induces a form of LTD that requires the influx of Ca^{2+} ions into the cell through NMDA receptors (Dudek and Bear, 1992; Oliet et al., 1997). NMDA receptor dependent LTD requires the activation of protein phosphatases that dephosphorylate serine residues of the GluA1 and GluA2 subunits of AMPA receptors, which results in receptor internalization and synapse loss and thereby decreases synaptic transmission (Malenka, 2003; Malenka and Bear, 2004; Wang et al., 2005; Lee, 2006). LTD has an induction, an expression and a maintenance phase with the induction phase being particularly dependent on phosphatase activity (Mulkey et al., 1993). LTD induction was not altered by SynCAM1 (Fig. 3.10 c,d), leading to the conclusion that SynCAM1 does not affect phosphatase activity. AMPA receptor internalization upon induction of LTD is mediated by a dynamin- and clathrin-dependent mechanism (Carroll et al., 1999; Ehlers, 2000; Lee et al., 2002; Wang and Linden, 2000). Furthermore, the interaction of the AMPA receptor subunits GluA2/3 with PDZ domain proteins was shown to regulate LTD (Kim et al., 2001). As discribed earlier, the interaction of SynCAM1 with PDZ class II domain

proteins has been reported (Biederer et al., 2002) and could be a link between SynCAM1 and LTD.

The PDZ domain protein PICK1 plays a central role in signal transduction upon induction of synaptic plasticity (Seidenman et al., 2003; Terashima et al., 2008). PICK1 is present at synaptic and extrasynaptic sites of neurons to regulate synaptic strength and AMPA receptor subunit composition (Daw et al., 2000; Terashima et al., 2004). It shows promiscuous binding to PDZ binding motif containing proteins like PKCα, GluA2 and GluA3 (Kim and Sheng, 2004). PICK1 furthermore serves as a Ca^{2+} sensor and thereby controls AMPAR internalization in response to NMDAR mediated Ca^{2+} influx (Hanley and Henley, 2005). Importantly, loss of PICK1 and inhibition of its PDZ domain interaction occludes LTD (Terashima et al., 2008; Thorsen et al., 2010), showing the protein's requirement for LTD induction.

These functions of PICK1 mimic the phenotype described in this study (see Fig. 3.10) and suggest a mechanistic similarity. It is noteworthy that SynCAM1 is dynamically expressed in the visual cortex in response to the induction of synaptic plasticity: Under baseline conditions, transcription of SynCAM1 in the visual cortex is downregulated after the second postnatal week (Lyckman et al., 2008). Ocular dominance plasticity is a form of synaptic plasticity in the visual system that also involves the formation of new synapses. Intriguingly, induction of ocular dominance plasticity resulted in the adaptive upregulation of SynCAM1 transcription (Lyckman et al., 2008), which underlines the involvement of SynCAM1 in synapse formation and synaptic plasticity *in vivo*.

Taken together, SynCAM1 does not affect LTP and has no influence on LTD induction. Instead, SynCAM1^{flag} overexpression prevents LTD expression and loss of SynCAM1 facilitates this form of plasticity. Two ways in which SynCAM1 could modulate LTD expression are conceivable: SynCAM1 might anchor receptors at the postsynaptic side and thereby prevent LTD whereas the loss of receptors might be facilitated in SynCAM1 KO animals. Alternatively, the adhesive properties of SynCAM1 could stabilize synaptic contacts and thereby prevent LTD upon SynCAM1^{flag} overexpressing or cause a facilitation of LTD in the SynCAM1 KO model. SynCAM1 overexpression or loss could alter the ability of pre- and postsynaptic sites to shrink or to detach, which is an important component of this form of plasticity (Zhou et al., 2004; Nagerl et al., 2004; Becker et al., 2008). Taken together, I

hypothesize that SynCAM1 influences synapse stability and is directly or indirectly involved in glutamate receptor internalization to regulate LTD.

4.4.2 Learning and synaptic plasticity

LTP and LTD are often described as a cellular correlate of learning and memory and correlations of LTP and LTD with learning and memory have been reported in many studies (Pastalkova et al., 2006; Whitlock et al., 2006; Kemp and Manahan-Vaughan, 2007). Although one study described the induction of LTP in the hippocampus in response to inhibitory avoidance learning (Whitlock et al., 2006), it might be an inappropriate simplification that learning requires LTP and that LTP is generally induced by learning. Instead, the notion that synaptic plasticity, be it reflected in LTP, LTD or other experimental paradigms, is generally involved in learning appears more correct (Malenka and Bear, 2004). Having said this, it is worth to keep in mind that physiological experiments in a slice to analyze synaptic plasticity cannot be used to predict the behavior of an animal in complex learning tasks. It is therefore not surprising that genetically modified animals that exhibit alterations in synaptic plasticity do not neccessarily show alterations in learning tasks.

However, a correlation of impaired LTD and learning deficits has been reported for few animal models but the roles of molecular mediators of synaptic plasticity are not fully understood (Kemp and Manahan-Vaughan, 2007). For instance, EphB2 KO animals show impaired LTD, reduced depotentiation, and impaired spatial learning (Grunwald et al., 2001). Interestingly, expression of a carboxyterminally truncated form of EphB2 rescued these effects, indicating that EphB2 kinase signaling is not required for these functions. In addition, postsynaptic ephrinBs play a role in synaptic plasticity and affect LTP as well as LTD (Grunwald et al., 2004). However, the present study is the first to report that the loss of a synaptic molecule causes enhanced LTD and improved learning. As expected, the complementary effect was observed upon SynCAM1 overexpression, which resulted in loss of LTD and impaired spatial learning without affecting LTD.

4.4.3 SynCAM1 impacts spatial learning

In light of the dramatic changes of excitatory synapse number by alteration of SynCAM1 expression, it is surprising that these animals perform normally in other behavioral tasks except the Morris water maze (open field test, elevated plus maze, visual cliff, sensory and motor function, data not shown). However, the loss of SynCAM1 facilitates LTD and improves spatial learning (Fig. 3.10, 3.12). This correlation of LTD impairment and impaired spatial learning reported here for SynCAM1^{flag} overexpressing mice was also observed in a mouse mutant with impaired postsynaptic signaling that lacks LTD (Nicholls et al., 2008). Different from this thesis, however, those animals learn and remember normally, but fail to be flexible when the task is altered. N-CAM, EphB2 and ephrinBs have also been implicated in LTD (Grunwald et al., 2001; Bukalo et al., 2004; Grunwald et al., 2004). One study demonstrated that blocking EphA receptors impairs learning (Gerlai et al., 1999) and ephrinA3 KO mice show impaired fear conditioning and object recogition (Carmona et al., 2009). More closely related to the phenotype described in this study, conditional N-CAM KO animals exhibit impaired LTD and impaired learning (Bukalo et al., 2004).

I cannot conclude that increased synaptic plasticity in LTD is the reason for improved spatial learning. However, the correlation of both experimental results is noteworthy and this study demonstrates for the first time that an adhesion molecule facilitates LTD and causes improved spatial learning.

4.5 Cell signaling by SynCAM proteins

In addition to the adhesive properties of SynCAM1, one question remains: Is SynCAM1 involved in cellular signaling and if so, what are the signaling mechanisms involved? Aside from the observation that excitatory synapse number depends on the expression level of SynCAM1, the mechanism regulating signaling downstream of SynCAM1 remains elusive. In which of the steps of synapse formation (see Fig. 1.1) is SynCAM1 involved? Does SynCAM1 trigger cell signalling, recruit other proteins or does the protein exclusively mediate its function by trans-synaptic adhesion?

Cell adhesion and synaptic signaling molecules contribute to synapse formation in two different ways: They can directly mediate cell signalling via their intracellular domain or

they can mediate protein interactions and protein scaffolding (Garner et al., 2002; Waites et al., 2005). For instance, the intracellular tyrosine kinase domain of EphB2 phosphorylates the small G protein Ras and thereby mediates cell signaling via tyrosine phosphorylation (Zou et al., 1999). SynCAM1 cannot directly mediate cell signaling with regard to catalytic activity due to the lack of a catalytic domain. Consequently, SynCAM1 presumably mediates protein scaffolding since all SynCAM family proteins posess intracellular binding motifs for FERM and for PDZ class II domains (Biederer, 2006). If SynCAM1 serves as a scaffolding protein that recruits signaling molecules to the synaptic membrane this raises the question: Which proteins are likely to interact with the cytoplasmic tail of SynCAM1 to mediate signaling and which proteins are likely to mediate the functions that have been reported for SynCAM1?

FERM domain proteins of the 4.1 subfamiliy are involved in protein scaffolding and in cell signaling. Whether the results described in this thesis are mediated by one of the proteins that are known to interact with SynCAM1, remains to be shown. However, some intracellular binding partners of SynCAM1 are more likely to account for the observed effects than others.

The family of 4.1 proteins belongs to the superfamily of proteins that are characterized by an amino-terminal FERM (**4**.1-**e**zrin-**r**adixin-**m**oesin) domain and often by a spectrin/actin-binding domain (SABD) (Diakowski et al., 2006). FERM domains are implicated in protein scaffolding and in the formation of synapse-organizing signaling complexes (Hoover and Bryant, 2000). The FERM domain proteins 4.1G, 4.1N and 4.1B are prominently expressed in the nervous system and control neuronal function and morphology (Walensky et al., 1998). For instance, the 4.1 family protein Talin mediates the interaction of integrins with the cytoskeleton (Ziegler et al., 2008). Protein 4.1 binding motifs are found in the membrane associated guanulyl kinase (MAGUK) protein CASK, in the small G protein Ras, in neurexins and in syndecans (Hoover and Bryant, 2000) which are implicated in cell signaling or in neuron morphogenesis (Lee et al., 2008). The protein 4.1 isoform 4.1N is a candidate to regulate synapse function since it is localized synaptically and colocalizes with PSD-95 and GluA1 (Walensky et al., 1999). In analogy to the learning deficits described in this study, it is worth mentioning that knockout mice lacking 4.1R show locomotor and learning deficits (Walensky et al., 1998). The 4.1 binding motif in the cytoplasmic tail of

SynCAM1 is predicted to recruit FERM proteins and thereby mediate protein scaffolding (Biederer, 2006) and the described colocalization with CASK and syntenin make such interactions likely (Biederer et al., 2002).

However, it remains unclear whether the interaction of SynCAM1 and CASK as well as the interaction of SynCAM1 and syntenin are mediated by the 4.1 binding motif or by the PDZ binding motif of SynCAM1 (Biederer, 2006). The abbreviation PDZ domain stems from the initials of the proteins in which these sequence motifs were originally identified: **P**SD-95, **d**iscs large, and **z**ona occludens1. PDZ domains are often found in multi-domain scaffolding proteins and have been implicated in synapse formation and in spine morphogenesis (Sheng and Sala, 2001; Hung and Sheng, 2002; Kim and Sheng, 2004). PDZ domains are grouped into three classes (I-III) that recognize distinct binding motifs at the carboxy terminus of their binding partner (Songyang et al., 1997). The C-terminal amino acid and the amino acid in position -2 of the PDZ binding motif as well as the structure of the PDZ domain itself are most important to define binding specificity (Elkins et al., 2007).

The PDZ domain of SynCAM1 belongs to class II (Biederer, 2006) and is thus implicated in signaling cascades that are distinct from those targeting PDZ class I proteins like PSD-95 (Sheng and Sala, 2001). PDZ class II binding motifs are also found in the synaptic molecules neurexin (Hata et al., 1996), syndecan (Hsueh et al., 1998), GluA2 (Xia et al., 1999) and in EphB2, Eph7A and ephrinB1 (Sheng and Sala, 2001). These proteins can be recognized by PDZ class II domain proteins that include prominent members like PICK1, GRIP1, Tiam-1, CASK, and syntenin that play central roles in the control of neuronal development, morphogenesis and function (Songyang et al., 1997; Sheng and Sala, 2001; Hung and Sheng, 2002). Neuron and spine morphogenesis are often mediated via interactions of PDZ proteins with the actin cytoskeleton (Hoover and Bryant, 2000; Zhang and Macara, 2006; Ziegler et al., 2008) and PDZ domain proteins can regulate synapse function via interactions with ion channels (Schuh et al., 2003; Xia et al., 1999).

The PDZ class II binding motif of SynCAM1 is homologous to that of the synaptic cell-surface proteins neurexins and syndecans, which bind to the PDZ-domain proteins CASK and syntenin (Hata et al., 1996; Hsueh et al., 1998). As described above, SynCAM1 also binds syntenin and recruits the MAGUK family protein CASK to the synaptic membrane but it remains unknown whether this colocalization is mediated by its PDZ- or by its protein

4.1 binding motif (Biederer et al., 2002). SynCAM1 also interacts with the PDZ domain proteins Mint1 (Munc-18-interacting protein 1) and Veli which have been proposed to act as a nucleation site for coupling cell adhesion molecules to synaptic vesicle exocytosis (Okamoto and Sudhof, 1997; Butz et al., 1998; Gerrow and El-Husseini, 2006). Other PDZ class II domain proteins include GRIP1 and p55, which are all putative interaction partners for SynCAM1 that could mediate cell signaling or the association of SynCAM1 with the actin cytoskeleton and thereby control the effect on synapse formation shown here.

Taken together, SynCAM1 has not been shown to interact with catalytically active proteins and cannot phosphorylate other molecules to trigger cell signaling. Instead, SynCAM1 is localized to sites of synapse formation via its adhesive properties conferred by its extracellular Ig domains (Fogel et al., 2007). At sites of synaptogenesis, SynCAM1 serves as an ideal candidate for the recruitment of synaptic proteins via its protein 4.1 and PDZ binding motifs and might thereby mediate the formation of synaptic protein scaffolds. These scaffolds include CASK, syntenin, Mint1, Velis and possibly other synaptic proteins like Tiam-1 and PICK1 that control synapse formation and synaptic plasticity (Kim and Sheng, 2004; Hsueh, 2006; Terashima et al., 2008).

4.6 Methodological aspects of studying synapse formation

Although enormous progress has been made in understanding synaptogenesis, the field faces technical limitations that preclude insights into the most fundamental processes underlying synaptogenesis. In general, two different approaches have been used to elucidate the mechanisms underlying synaptogenesis: The functional characterization of synapses and the morphological analysis of synapse structure and ultrastructure.

Functional characterizations by physiological measures face one intrinsic difficulty: They can only be applied once a synapse has become functional and are therefore not suitable to study very early steps of synaptogenesis. This restriction also applies to the measurement of presynatic vesicle release and vesicle recycling with styryl dyes (Gaffield and Betz, 2006).

Much of the current knowledge about the birth of synapses stems from morphological analyses. Different subtypes of synapses have been followed over development by microscopy and distinctions between immature and mature synapses were suggested based on the ul-

trastructure of the pre- and postsynapse (Miller and Peters, 1981; De Roo et al., 2008). Since electron microscopy requires tissue fixation, chronically following the development of individual synapses is not possible with this technique. The conclusions from these studies were thus based on alterations of the average of morphological parameters from different specimen over time. Following individual synapses during development has only become possible by the implementation of novel methods that have made many of these questions more accessible:

Video microscopy and time lapse imaging as well as multiphoton microscopy permit imaging fine neuronal structures in living tissue and in alive animals (Helmchen and Denk, 2005). Importantly, multiphoton microscopy enables improved tissue penetration that allows the use of living tissue or animals and also enables repetetive imaging of the same neuron or dendrite over time. For the first time, the birth of a synapse could be watched *in vivo* and structural changes of neurons during synaptogenesis could be analyzed in fluorescently labeled neurons thanks to this technique. Furthermore, optical measurements monitoring neuronal Ca^{2+} signals prior to completion of synapse formation have been used with great success to analyze very early stages of synapse formation (Lohmann et al., 2005). Additionally, optical indicators were designed to monitor changes in the neuronal membrane potential (Bedlack et al., 1992; Davidenko et al., 1992) but the experimental use proofed difficult. Recently, Holthoff and colleagues improved this method, which allows studying neuronal activity in very early phases of development, e.g. in synapse formation (Holthoff et al., 2010).

However, light microscopy has physical limits of resolution that are determined by the wavelength. Additionally, fluorescence microscopy of biological specimen or living animals suffers from phototoxicity. As a consequence, temporal and spatial resolution of this technique are limited. Despite the enormous potential of these novel ways to address synapse formation in the living organism, microscopy alone cannot elucidate the mechanisms underlying synapse formation. For instance, the role of individual molecules that mediate cell adhesion or cell signalling cannot be addressed by imaging neuronal morphology. Instead, the combination of a wide range of methods will be required to illuminate the mechanisms that control synapse formation and to characterize the function of SynCAM1 in more detail.

The functions of individual molecules in synaptogenesis have been addressed using a

simple yet elegant method: Non-neuronal cells (e.g. HEK293T cells) do not express neuronal surface proteins. To study the function of neuronal surface proteins, the proteins of interest were artificially expressed in non-neuronal cells and these cells were co-cultured with neurons. For instance, co-cultured neurons formed functional presynaptic terminals onto HEK cells that overexpressed SynCAM1 and NLGN1, demonstrating the synaptogenic potential of these two adhesion molecules (Scheiffele et al., 2000; Biederer et al., 2002; Sara et al., 2005). Combined with genetic modifications, even the function of individual protein domains can be answered, e.g. by modification or truncation of the proteins of interest. Although this method cannot answer how synaptogenesis is mediated *in vivo*, it provides a powerful and elegant tool to study the contribution of individual molecules to synapse formation. In addition, the use of genetically modified mice in combination with neuroimaging and physiological studies will be valuable to reveal the function of individual proteins in brain and synapse development.

Caveats of mEPSC analysis

Analysis of mEPSCs is an important method to assess alterations in synapse number physiologically. However, analysis of mEPSC recordings needs to follow some simple rules to permit valid interpretation of the data. This paragraph will not deal with basic methodology of physiological experiments, which is vital to obtain high quality data. Instead, this section focuses on the analysis of datasets with large sample sizes, which applies to the analysis of mEPSC frequency.

Briefly, mEPSC data is analyzed by measuring mEPSC amplitude and the interval between individual mEPSC events. Experience shows that a minimum of 150-200 mEPSC events per cell need to be analyzed to obtain reproducable results. As an example, let us assume that we need to analyze two mEPSC datasets: Dataset A contains bursts of mEPSCs whereas the events in dataset B are evenly distributed. The crucial point is that both classes of cells are clearly distinct (cell A with bursts of events, cell B with an event frequency that is constant over time) but show an identical number of events over the total recording time. Consequently, the average interval for the entire recording time is identical for both conditions although the cells have completely different properties. Thus, analysis

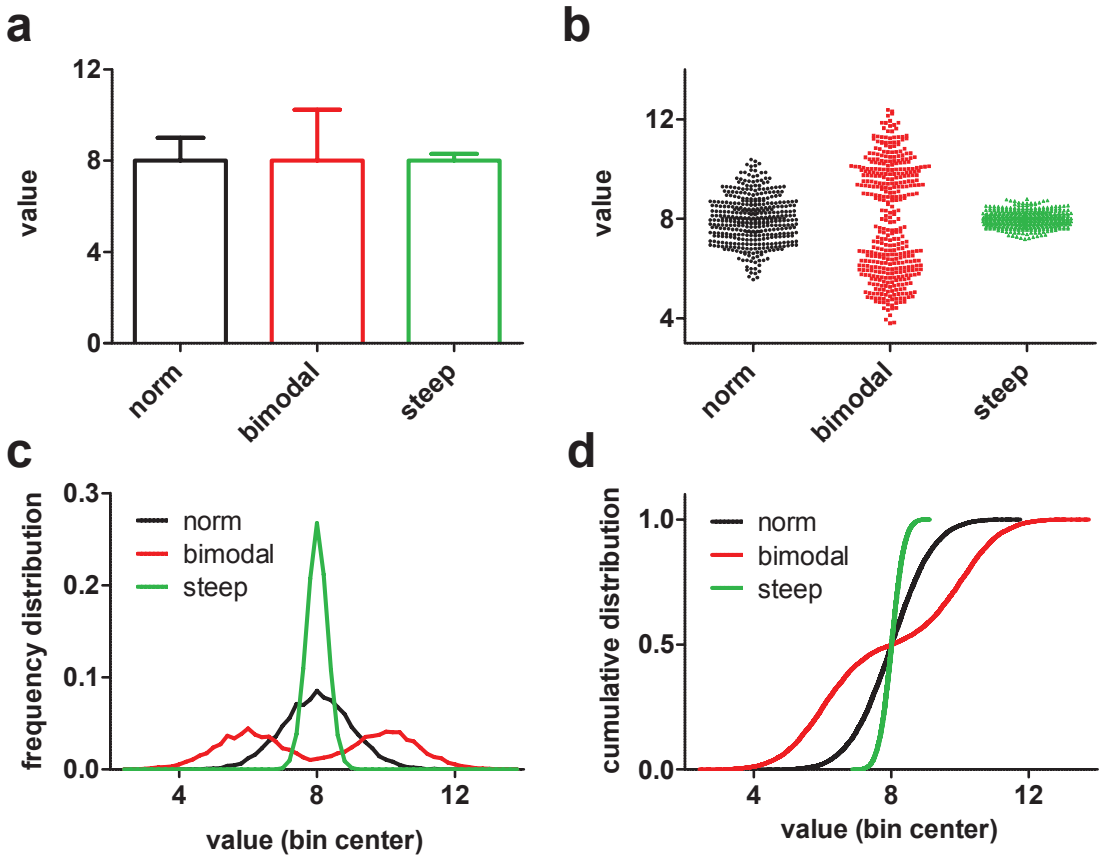

Figure 4.2: Presenting experimental data. Three datasets were generated to illustrate different possibilities of data analysis and presentation: One set of data that is normally distributed around $x = 8$ (norm), the identical dataset, compressed by a factor of three (steep) and a bimodal distribution with two maxima at $x = 8 \pm 2$ (bimodal). These datasets were plotted in four different ways. **a**. Bar graph with standard deviation. **b**. Scatter plot of raw data. **c**. Histogram (bin size: 0.2). **d**. Cumulative distribution.

of average event frequencies only reflects a very reduced view on the experimental data and can easily occlude important differences between datasets. Nevertheless, average mEPSC frequencies are often used as the only measure to describe this kind of experimental data (Flavell et al., 2006; Varoqueaux et al., 2006; Groffen et al., 2010).

Consequently, presenting this kind of data in a way that ideally reflects all information contained therein should be the goal of every unbiassed analysis. To illustrate the relevance of these considerations, three distinct datasets were generated. Fig. 4.2 depicts four possible ways to plot these datasets. Apart from having an average of $x = 8$ these datasets are quite distinct, which is not apparent from displaying average values in bar graphs (Fig. 4.2a).

In contrast, a scatter plot (Fig. 4.2b) reveals more information about the data. However, it is obvious that scatter plots are not suitable for large sample sizes and are not ideally suited to compare individual datasets since the number of distinguishable points that can be displayed is limited. The first plot that permits interpretation of the datasets is the standard histogram (Fig. 4.2c). Similar to the scatter plot, comparing datasets in histograms is difficult as information about the average of the dataset cannot be easily deducted. In contrast, presentation of the data in a cumulative histogram (Fig. 4.2d) contains all relevant information about the respective dataset and is ideally suited to compare datasets. In this case, the slope of the "norm" and "steep" datasets reflects the width of the normal distribution. Similarly, the bimodal distribution can be clearly identified and it is obvious that the median of all datasets is $x = 8$ as all distributions reach $y = 0.5$.

It is thus worth considering presenting this kind of data in cumulative histograms to solve these difficulties. The arguments presented above do not only relate to mEPSC frequency; identical considerations apply to the analysis of mEPSC amplitude and of virtually all datasets with large sample numbers. For the reasons named above, a central finding in neuroscience, would have been impossible if only averages of EPSCs had been analyzed: The quantal nature of transmitter release from the presynapse results in a multimodal distribution of PSC amplitdes, which would not have been detected by the comparison of average values (Fatt and Katz, 1952; del Castillo and Katz, 1954).

The objection that displaying data in cumulative distributions is not extremely common and cannot intuitively be interpreted is often raised. This dilemma comes down to balancing the content of information and comprehensiveness, which is of relevance as excellent scientific results that are not understood are just as bad as science that is incompletely presented. For the lack of an ideal solution to this problem, some of the results in this thesis are presentated as bar graphs and as histograms. The data presented in Fig. 3.8d illustrates another problem of the presentation of mean frequencies in bar graphs: The cumulative distributions for the conditions OE^{always} and OE^{late} are almost superimposed and are not significantly different from one another ($p_{KStest} = 1$, see Table 3.1a). Nevertheless, the means of both distributions are slightly different which causes a seeming difference of these conditions in the bar graph inset. However, nobody would argue that the distributions of both conditions differ, which underlines the necessity of this unbiassed way of data analysis using

cumulative distributions.

Along these lines, comparison of average mEPSC frequencies could possibly encourage quantitative comparison of experimental conditions at first sight. As outlined above, interpretations of the kind *"double average mEPSC frequency reflects an increase in excitatory synapse number by a factor of two"* do not appear to be valid. In this context, not mistaking average values for suitable parameters of quantification appears to be indicated. The more careful interpretation that shifts in the distribution demonstrate differences in synapse number (without quantifying them) appears to reflect this kind of result in a more realistic way.

In summary, important conlusions can easily be overlooked in data with large sample sizes if only average values are analyzed. Consequently, displaying data in histograms (see Carroll et al., 1999; Noel et al., 1999; Cingolani et al., 2008 for exapmples) appears to be more adequate to achieve a precise representation of the underlying phenomena although it might not meet the needs of a broader audience that might not be familiar with this kind of presentation. Having said this, it appeared extremely beneficial to provide a tool for the analysis of mEPSC data that takes these and more caveats into consideration. Hence, a powerful, MATLAB-based tool for mEPSC analysis was developed and used in the present study (see 2.2.7 for detailed description). This "MiniAnalysis" tool is now the standard for mEPSC analysis in our lab and combines semi-automatic event detection and *lege artis* data analysis.

4.7 Concluding remarks

Taken together, these results confirm the synaptogenic capacity of SynCAM1 for the first time in the intact brain and suggest that SynCAM1 acts early during synapse formation and is required to maintain a SynCAM1 induced increase in synapse number. I hypothesize that other trans-synaptic interactions subsequently instruct the formation of excitatory synapses and mediate synapse maturation. The neuroligin-neurexin adhesive pair regulates synapse maturation and might act in this later phase of synapse development. Furthermore, biochemical analyses revealed that SynCAM1 regulates synapse formation through transsynaptic interactions that can either be homo– or heterophilic. These interactions are mediated

by the Ig domains 1 and 2 and depend on glycosylation of the protein's extracellular domain (Fogel et al., 2007). The strongest heterophilic binding was detected between SynCAM1 and SynCAM2, which likely defines the dominant adhesive pair (Fogel et al., 2007).

Moreover, SynCAM1 regulates excitatory synapse number not only in cell culture, but also in the intact brain: Overexpression of SynCAM1 increases the number of excitatory synapses whereas SynCAM1 KO animals exhibit a decrease in excitatory synapse number. Synapse formation is a highly regulated process with different adhesion molecules acting in different phases of synapse development. Whether the function of SynCAM1 is restricted to a particular time of development was addressed using conditional SynCAM1^{flag} overexpression. It was demonstrated that SynCAM1 retains its synaptogenic potential from early to later stages of development. Furthermore, SynCAM1 is not only required to induce synapse formation but also to maintain an increase in excitatory synapse number over time. It is noteworthy that SynCAM1 neither affects basal synaptic transmission nor does it alter most parameters associated with synapse maturation.

In summary, these data support the hypothesis that SynCAM1 regulates synapse formation and maintenance without affecting synapse maturation. In addition, the synaptogenic capacity of SynCAM1 is not restricted to a particular time in brain development but rather serves as a universal regulator of excitatory synapse formation and maintenance.

The expression level of SynCAM1 had no effect on LTP but significantly altered LTD. Increasing synaptic adhesion by SynCAM1 overexpression impeded LTD whereas reduced synaptic adhesion in SynCAM1 KO animals resulted in enhanced LTD expression. These experiments demonstrate a decrease in synaptic plasticity upon SynCAM1 overexpression and an increase in synaptic plasticity in SynCAM1 KO animals.

Synaptic plasticity is required to adapt the brain to changes in the environment and is thought to be involved in learning. Spatial learning was assessed in the Morris water maze, which revealed that SynCAM1 overexpressing mice with impaired synaptic plasticity exhibit severe learning deficits. In contrast, SynCAM1 KO mice with enhanced synaptic plasticity learn better than control animals. In summary, these results demonstrate that SynCAM1 acts specifically in the brain as a synaptic cell adhesion molecule that regulates excitatory synapse number as well as synaptic plasticity and spatial learning.

5 Outlook

The mechanisms underlying the regulation of synapse number and of synaptic plasticity by SynCAM1 will be investigated in future studies. Two hyptheses underlying SynCAM1 function are conceivable and can be tested experimentally: SynCAM1 might stabilize nascent and existing synapses through its adhesive properties (see Fig. 4.1). Alternatively, SynCAM1 might mediate protein scaffolding and cell signaling via its cytosolic domain to control synapse number and synaptic plasticity.

The role of SynCAMs in early synaptogenesis and in contact stabilization will be addressed by analysis of the motility patterns of dendritic filopodia by video microscopy. According to the filopodia model (see Fig. 1.1), dendritic filopodia sense their environment for axonal partners. Once formed, contacts between filopodium and axon can either be transient or they can be stabilized and mature to become a synapse. Analysis of the number of filopodia per stretch of dendrite, of filopodia motility, and of filopodia dwell time at sites of contact will reveal the aspect of early synaptogenesis SynCAM proteins affect.

Investigating SynCAM1-dependent scaffolding and signaling will be another long-term goal since SynCAM proteins seem to be ideally suited as mediators of protein scaffolding at the synapse (see 4.5). Hence, identifying binding partners of SynCAM1 biochemically and validating their implication in SynCAM function will be a very promising project: Neuronal cultures will serve as an ideal system to characterize the function of proteins interacting with SynCAMs in more detail. Cultured neurons are well accessible to experimental manipulations and can be used to study the involvement of proteins interacting with SynCAM1 to mediate plasticity and synaptogenesis. Neurons with three possible background levels of SynCAM1 expression can be obtained from SynCAM1 KO, overexpressing, and wt mice. Additionally, knock down or mutagenesis of potentially interacting proteins will enable characterization of the mechanisms a particular interaction partner of SynCAM1 is involved

in.

It is of great interest to identify the role of SynCAM1 in synaptic plasticity. Hence, a third series of experiments will follow up on the modulation of LTD by SynCAM1. Synaptic plasticity involves trafficking of AMPA receptors as well as gain and loss of synapses. Again, SynCAM1 could either exert its effect by its adhesive properties and stabilize synapses serving as 'synaptic glue' to prevent synapse loss. Alternatively, SynCAM1 could anchor receptors at the synapse and thereby 'protect' synapses against receptor loss. This hypothesis will be tested experimentally by inducing LTD in whole cell recordings with subsequent analysis of the AMPAR content. This experiment will reveal whether SynCAM1 affects AMPAR removal from the synapse or whether synapse loss might account for the observed LTD effect.

Finally, the function of SynCAM1 in synaptogenesis will be studied *in vivo* by imaging the same stretch of dendrite of fluorescently labelled neurons at multiple timepoints using multiphoton microscopy. This chronic imaging will shed light on the contribution of SynCAM1 to the stability of individual synapses over time. Additionally, the temporal control of SynCAM1^{flag} overexpression afforded by the TET off transgenic design enables switching SynCAM1^{flag} overexpression on and off. By combining chronic imaging with conditional overexpression, the contribution of SynCAM1 to synapse formation and to synapse maturation can be distinguished *in vivo*.

Bibliography

Adesnik, H. and Nicoll, R. A. (2007). Conservation of glutamate receptor 2-containing ampa receptors during long-term potentiation. *J Neurosci*, 27(17):4598–602.

Akins, M. R. and Biederer, T. (2006). Cell-cell interactions in synaptogenesis. *Curr Opin Neurobiol*, 16(1):83–9.

Atasoy, D., Schoch, S., Ho, A., Nadasy, K. A., Liu, X., Zhang, W., Mukherjee, K., Nosyreva, E. D., Fernandez-Chacon, R., Missler, M., Kavalali, E. T., and Sudhof, T. C. (2007). Deletion of cask in mice is lethal and impairs synaptic function. *Proc Natl Acad Sci U S A*, 104(7):2525–30.

Banke, T. G., Bowie, D., Lee, H., Huganir, R. L., Schousboe, A., and Traynelis, S. F. (2000). Control of glur1 ampa receptor function by camp-dependent protein kinase. *J Neurosci*, 20(1):89–102.

Bastrikova, N., Gardner, G. A., Reece, J. M., Jeromin, A., and Dudek, S. M. (2008). Synapse elimination accompanies functional plasticity in hippocampal neurons. *Proceedings of the National Academy of Sciences*, 105(8):3123–3127.

Becker, N., Wierenga, C. J., Fonseca, R., Bonhoeffer, T., and Nagerl, U. V. (2008). Ltd induction causes morphological changes of presynaptic boutons and reduces their contacts with spines. *Neuron*, 60(4):590–7.

Bedlack, R. S., J., Wei, M., and Loew, L. M. (1992). Localized membrane depolarizations and localized calcium influx during electric field-guided neurite growth. *Neuron*, 9(3):393–403.

Benson, D. L. and Tanaka, H. (1998). N-cadherin redistribution during synaptogenesis in hippocampal neurons. *J Neurosci*, 18(17):6892–904.

Bernard-Trifilo, J. A., Kramar, E. A., Torp, R., Lin, C. Y., Pineda, E. A., Lynch, G., and Gall, C. M. (2005). Integrin signaling cascades are operational in adult hippocampal synapses and modulate nmda receptor physiology. *J Neurochem*, 93(4):834–49.

Biederer, T. (2006). Bioinformatic characterization of the syncam family of immunoglobulin-like domain-containing adhesion molecules. *Genomics*, 87(1):139–50.

Biederer, T., Sara, Y., Mozhayeva, M., Atasoy, D., Liu, X., Kavalali, E. T., and Sudhof, T. C. (2002). Syncam, a synaptic adhesion molecule that drives synapse assembly. *Science*, 297(5586):1525–31.

Biederer, T. and Sudhof, T. C. (2000). Mints as adaptors. direct binding to neurexins

and recruitment of munc18. *J Biol Chem*, 275(51):39803–6.

Blue, M. E. and Parnavelas, J. G. (1983). The formation and maturation of synapses in the visual cortex of the rat. i. qualitative analysis. *Journal of Neurocytology*, 12(4):599–616.

Bozdagi, O., Valcin, M., Poskanzer, K., Tanaka, H., and Benson, D. L. (2004). Temporally distinct demands for classic cadherins in synapse formation and maturation. *Mol Cell Neurosci*, 27(4):509–21.

Bredt, D. S. and Nicoll, R. A. (2003). Ampa receptor trafficking at excitatory synapses. *Neuron*, 40(2):361–79.

Budreck, E. C. and Scheiffele, P. (2007). Neuroligin-3 is a neuronal adhesion protein at gabaergic and glutamatergic synapses. *Eur J Neurosci*, 26(7):1738–48.

Bukalo, O., Fentrop, N., Lee, A. Y., Salmen, B., Law, J. W., Wotjak, C. T., Schweizer, M., Dityatev, A., and Schachner, M. (2004). Conditional ablation of the neural cell adhesion molecule reduces precision of spatial learning, long-term potentiation, and depression in the ca1 subfield of mouse hippocampus. *J Neurosci*, 24(7):1565–77.

Butz, S., Okamoto, M., and Sudhof, T. C. (1998). A tripartite protein complex with the potential to couple synaptic vesicle exocytosis to cell adhesion in brain. *Cell*, 94(6):773–82.

Carmona, M. A., Murai, K. K., Wang, L., Roberts, A. J., and Pasquale, E. B. (2009). Glial ephrin-a3 regulates hippocampal dendritic spine morphology and glutamate transport. *Proceedings of the National Academy of Sciences*, 106(30):12524–12529.

Carroll, R. C., Lissin, D. V., von Zastrow, M., Nicoll, R. A., and Malenka, R. C. (1999). Rapid redistribution of glutamate receptors contributes to long-term depression in hippocampal cultures. *Nat Neurosci*, 2(5):454–60.

Chan, C. S., Weeber, E. J., Kurup, S., Sweatt, J. D., and Davis, R. L. (2003). Integrin requirement for hippocampal synaptic plasticity and spatial memory. *J Neurosci*, 23(18):7107–16.

Chan, C. S., Weeber, E. J., Zong, L., Fuchs, E., Sweatt, J. D., and Davis, R. L. (2006). Beta 1-integrins are required for hippocampal ampa receptor-dependent synaptic transmission, synaptic plasticity, and working memory. *J Neurosci*, 26(1):223–32.

Chavis, P. and Westbrook, G. (2001). Integrins mediate functional pre- and postsynaptic maturation at a hippocampal synapse. *Nature*, 411(6835):317–21.

Chih, B., Engelman, H., and Scheiffele, P. (2005). Control of excitatory and inhibitory synapse formation by neuroligins. *Science*, 307(5713):1324–8.

Chubykin, A. A., Atasoy, D., Etherton, M. R., Brose, N., Kavalali, E. T., Gibson, J. R., and Sudhof, T. C. (2007). Activity-dependent validation of excitatory versus inhibitory

synapses by neuroligin-1 versus neuroligin-2. *Neuron*, 54(6):919–31.

Chun, D., Gall, C. M., Bi, X., and Lynch, G. (2001). Evidence that integrins contribute to multiple stages in the consolidation of long term potentiation in rat hippocampus. *Neuroscience*, 105(4):815–829.

Cingolani, L. A., Thalhammer, A., Yu, L. M. Y., Catalano, M., Ramos, T., Colicos, M. A., and Goda, Y. (2008). Activity-dependent regulation of synaptic ampa receptor composition and abundance by [beta]3 integrins. *Neuron*, 58(5):749–762.

Collingridge, G. L., Olsen, R. W., Peters, J., and Spedding, M. (2009). A nomenclature for ligand-gated ion channels. *Neuropharmacology*, 56(1):2–5.

Crusio, W. E. (2009). Troublesome variability in mouse studies. *Nat Neurosci*, 12(9):1075.

Dalva, M. B., McClelland, A. C., and Kayser, M. S. (2007). Cell adhesion molecules: signalling functions at the synapse. *Nat Rev Neurosci*, 8(3):206–20.

Dalva, M. B., Takasu, M. A., Lin, M. Z., Shamah, S. M., Hu, L., Gale, N. W., and Greenberg, M. E. (2000). Ephb receptors interact with nmda receptors and regulate excitatory synapse formation. *Cell*, 103(6):945–56.

Davidenko, J. M., Pertsov, A. V., Salomonsz, R., Baxter, W., and Jalife, J. (1992). Stationary and drifting spiral waves of excitation in isolated cardiac muscle. *Nature*, 355(6358):349–51.

Daw, M. I., Chittajallu, R., Bortolotto, Z. A., Dev, K. K., Duprat, F., Henley, J. M., Collingridge, G. L., and Isaac, J. T. (2000). Pdz proteins interacting with c-terminal glur2/3 are involved in a pkc-dependent regulation of ampa receptors at hippocampal synapses. *Neuron*, 28(3):873–86.

De Roo, M., Klauser, P., Mendez, P., Poglia, L., and Muller, D. (2008). Activity-dependent psd formation and stabilization of newly formed spines in hippocampal slice cultures. *Cereb. Cortex*, 18(1):151–161.

Dean, C., Scholl, F. G., Choih, J., DeMaria, S., Berger, J., Isacoff, E., and Scheiffele, P. (2003). Neurexin mediates the assembly of presynaptic terminals. *Nat Neurosci*, 6(7):708–16.

del Castillo, J. and Katz, B. (1954). Quantal components of the end-plate potential. *The Journal of Physiology*, 124(3):560–573.

Diakowski, W., Grzybek, M., and Sikorski, A. F. (2006). Protein 4.1, a component of the erythrocyte membrane skeleton and its related homologue proteins forming the protein 4.1/ferm superfamily. *Folia Histochem Cytobiol*, 44(4):231–48.

DiCiommo, D. P. and Bremner, R. (1998). Rapid, high level protein production using dna-based semliki forest virus vectors. *J Biol Chem*, 273(29):18060–6.

Dillon, C. and Goda, Y. (2005). The actin cytoskeleton: Integrating form and function at the synapse. *Annual Review of Neuroscience*, 28(1):25–55.

Drescher, U., Kremoser, C., Handwerker, C., Loschinger, J., Noda, M., and Bonhoeffer, F. (1995). In vitro guidance of retinal ganglion cell axons by rags, a 25 kda tectal protein related to ligands for eph receptor tyrosine kinases. *Cell*, 82(3):359–70.

Dudek, S. M. and Bear, M. F. (1992). Homosynaptic long-term depression in area ca1 of hippocampus and effects of n-methyl-d-aspartate receptor blockade. *Proc Natl Acad Sci U S A*, 89(10):4363–7.

Durand, G. M., Kovalchuk, Y., and Konnerth, A. (1996). Long-term potentiation and functional synapse induction in developing hippocampus. *Nature*, 381(6577):71–5.

Ehlers, M. D. (2000). Reinsertion or degradation of ampa receptors determined by activity-dependent endocytic sorting. *Neuron*, 28(2):511–25.

Elkins, J. M., Papagrigoriou, E., Berridge, G., Yang, X., Phillips, C., Gileadi, C., Savitsky, P., and Doyle, D. A. (2007). Structure of pick1 and other pdz domains obtained with the help of self-binding c-terminal extensions. *Protein Sci*, 16(4):683–94.

Engert, F. and Bonhoeffer, T. (1999). Dendritic spine changes associated with hippocampal long-term synaptic plasticity. *Nature*, 399(6731):66–70.

Ethell, I. M., Irie, F., Kalo, M. S., Couchman, J. R., Pasquale, E. B., and Yamaguchi, Y. (2001). Ephb/syndecan-2 signaling in dendritic spine morphogenesis. *Neuron*, 31(6):1001–13.

Fatt, P. and Katz, B. (1952). Spontaneous subthreshold activity at motor nerve endings. *The Journal of Physiology*, 117(1):109–128.

Filosa, A., Paixao, S., Honsek, S. D., Carmona, M. A., Becker, L., Feddersen, B., Gaitanos, L., Rudhard, Y., Schoepfer, R., Klopstock, T., Kullander, K., Rose, C. R., Pasquale, E. B., and Klein, R. (2009). Neuron-glia communication via epha4/ephrin-a3 modulates ltp through glial glutamate transport. *Nat Neurosci*.

Flavell, S. W., Cowan, C. W., Kim, T. K., Greer, P. L., Lin, Y., Paradis, S., Griffith, E. C., Hu, L. S., Chen, C., and Greenberg, M. E. (2006). Activity-dependent regulation of mef2 transcription factors suppresses excitatory synapse number. *Science*, 311(5763):1008–12.

Fogel, A. I., Akins, M. R., Krupp, A. J., Stagi, M., Stein, V., and Biederer, T. (2007). Syncams organize synapses through heterophilic adhesion. *J Neurosci*, 27(46):12516–30.

Forster, E., Tielsch, A., Saum, B., Weiss, K. H., Johanssen, C., Graus-Porta, D., Muller, U., and Frotscher, M. (2002). Reelin, disabled 1, and beta 1 integrins are required for the formation of the radial glial scaffold in the hippocampus. *Proc Natl Acad Sci U S A*, 99(20):13178–83.

Fujita, E., Kouroku, Y., Ozeki, S., Tanabe, Y., Toyama, Y., Maekawa, M., Kojima, N., Senoo, H., Toshimori, K., and Momoi, T. (2006). Oligo-astheno-teratozoospermia in mice lacking ra175/tslc1/syncam/igsf4a, a

cell adhesion molecule in the immunoglobulin superfamily. *Mol Cell Biol*, 26(2):718–26.

Futai, K., Kim, M. J., Hashikawa, T., Scheiffele, P., Sheng, M., and Hayashi, Y. (2007). Retrograde modulation of presynaptic release probability through signaling mediated by psd-95-neuroligin. *Nat Neurosci*, 10(2):186–95.

Gaffield, M. A. and Betz, W. J. (2006). Imaging synaptic vesicle exocytosis and endocytosis with fm dyes. *Nat Protoc*, 1(6):2916–21.

Galuska, S., Rollenhagen, M., Kaup, M., Eggers, K., Oltmann-Norden, I., Schiff, M., Hartmann, M., Weinhold, B., Hildebrandt, H., Geyer, R., Muhlenhoff, M., and Geyer, H. (2010). Synaptic cell adhesion molecule syncam 1 is a target for polysialylation in postnatal mouse brain. *Proc Natl Acad Sci U S A*.

Garner, C. C., Waites, C. L., and Ziv, N. E. (2006). Synapse development: still looking for the forest, still lost in the trees. *Cell Tissue Res*, 326(2):249–62.

Garner, C. C., Zhai, R. G., Gundelfinger, E. D., and Ziv, N. E. (2002). Molecular mechanisms of cns synaptogenesis. *Trends Neurosci*, 25(5):243–51.

Gerlai, R., Shinsky, N., Shih, A., Williams, P., Winer, J., Armanini, M., Cairns, B., Winslow, J., Gao, W., and Phillips, H. S. (1999). Regulation of learning by epha receptors: a protein targeting study. *J Neurosci*, 19(21):9538–49.

Gerrow, K. and El-Husseini, A. (2006). Cell adhesion molecules at the synapse. *Front Biosci*, 11:2400–19.

Gleeson, J. G. and Walsh, C. A. (2000). Neuronal migration disorders: from genetic diseases to developmental mechanisms. *Trends Neurosci*, 23(8):352–9.

Graf, E. R., Zhang, X., Jin, S. X., Linhoff, M. W., and Craig, A. M. (2004). Neurexins induce differentiation of gaba and glutamate postsynaptic specializations via neuroligins. *Cell*, 119(7):1013–26.

Gray, E. G. (1959). Axo-somatic and axo-dendritic synapses of the cerebral cortex: an electron microscope study. *J Anat*, 93:420–33.

Groffen, A. J., Martens, S., Diez Arazola, R., Cornelisse, L. N., Lozovaya, N., de Jong, A. P., Goriounova, N. A., Habets, R. L., Takai, Y., Borst, J. G., Brose, N., McMahon, H. T., and Verhage, M. (2010). Doc2b is a high-affinity ca2+ sensor for spontaneous neurotransmitter release. *Science*, 327(5973):1614–8.

Grunwald, I. C., Korte, M., Adelmann, G., Plueck, A., Kullander, K., Adams, R. H., Frotscher, M., Bonhoeffer, T., and Klein, R. (2004). Hippocampal plasticity requires postsynaptic ephrinbs. *Nat Neurosci*, 7(1):33–40.

Grunwald, I. C., Korte, M., Wolfer, D., Wilkinson, G. A., Unsicker, K., Lipp, H. P., Bonhoeffer, T., and Klein, R. (2001). Kinase-independent requirement of ephb2 receptors

in hippocampal synaptic plasticity. *Neuron*, 32(6):1027–40.

Han, K. and Kim, E. (2008). Synaptic adhesion molecules and psd-95. *Prog Neurobiol*, 84(3):263–83.

Hanley, J. G. and Henley, J. M. (2005). Pick1 is a calcium-sensor for nmda-induced ampa receptor trafficking. *Embo J*, 24(18):3266–78.

Hata, Y., Butz, S., and Sudhof, T. C. (1996). Cask: a novel dlg/psd95 homolog with an n-terminal calmodulin-dependent protein kinase domain identified by interaction with neurexins. *J Neurosci*, 16(8):2488–94.

Hebb, D. (1949). *The Organization of Behavior: A neuropsychological theory*. Lawrence Erlbaum Associates, Mahwah.

Helmchen, F. and Denk, W. (2005). Deep tissue two-photon microscopy. *Nat Methods*, 2(12):932–40.

Henkemeyer, M., Itkis, O. S., Ngo, M., Hickmott, P. W., and Ethell, I. M. (2003). Multiple ephb receptor tyrosine kinases shape dendritic spines in the hippocampus. *J Cell Biol*, 163(6):1313–26.

Hollmann, M. and Heinemann, S. (1994). Cloned glutamate receptors. *Annu Rev Neurosci*, 17:31–108.

Holt, C. E. and Harris, W. A. (1998). Target selection: invasion, mapping and cell choice. *Curr Opin Neurobiol*, 8(1):98–105.

Holthoff, K., Zecevic, D., and Konnerth, A. (2010). Rapid time course of action potentials in spines and remote dendrites of mouse visual cortex neurons. *J Physiol*, 588(Pt 7):1085–96.

Hoover, K. B. and Bryant, P. J. (2000). The genetics of the protein 4.1 family: organizers of the membrane and cytoskeleton. *Curr Opin Cell Biol*, 12(2):229–34.

Houshmandi, S. S., Surace, E. I., Zhang, H. B., Fuller, G. N., and Gutmann, D. H. (2006). Tumor suppressor in lung cancer-1 (tslc1) functions as a glioma tumor suppressor. *Neurology*, 67(10):1863–6.

Hsueh, Y. P. (2006). The role of the maguk protein cask in neural development and synaptic function. *Curr Med Chem*, 13(16):1915–27.

Hsueh, Y. P., Yang, F. C., Kharazia, V., Naisbitt, S., Cohen, A. R., Weinberg, R. J., and Sheng, M. (1998). Direct interaction of cask/lin-2 and syndecan heparan sulfate proteoglycan and their overlapping distribution in neuronal synapses. *J Cell Biol*, 142(1):139–51.

Huang, Z., Shimazu, K., Woo, N. H., Zang, K., Muller, U., Lu, B., and Reichardt, L. F. (2006). Distinct roles of the beta 1-class integrins at the developing and the mature hippocampal excitatory synapse. *J Neurosci*, 26(43):11208–19.

Hung, A. Y. and Sheng, M. (2002). Pdz domains: structural modules for protein complex assembly. *J Biol Chem*, 277(8):5699–702.

Jo, K., Derin, R., Li, M., and Bredt, D. S. (1999). Characterization of mals/velis-1, -2, and -3: a family of mammalian lin-7 ho-

mologs enriched at brain synapses in association with the postsynaptic density-95/nmda receptor postsynaptic complex. *J Neurosci*, 19(11):4189–99.

Jones, D. H. and Matus, A. I. (1974). Isolation of synaptic plasma membrane from brain by combined flotation-sedimentation density gradient centrifugation. *Biochim Biophys Acta*, 356(3):276–87.

Jontes, J. D., Emond, M. R., and Smith, S. J. (2004). In vivo trafficking and targeting of n-cadherin to nascent presynaptic terminals. *J Neurosci*, 24(41):9027–34.

Kakunaga, S., Ikeda, W., Itoh, S., Deguchi-Tawarada, M., Ohtsuka, T., Mizoguchi, A., and Takai, Y. (2005). Nectin-like molecule-1/tsll1/syncam3: a neural tissue-specific immunoglobulin-like cell-cell adhesion molecule localizing at non-junctional contact sites of presynaptic nerve terminals, axons and glia cell processes. *J Cell Sci*, 118(Pt 6):1267–77.

Kandler, K., Katz, L. C., and Kauer, J. A. (1998). Focal photolysis of caged glutamate produces long-term depression of hippocampal glutamate receptors. *Nat Neurosci*, 1(2):119–23.

Kattenstroth, G., Tantalaki, E., Sudhof, T. C., Gottmann, K., and Missler, M. (2004). Postsynaptic n-methyl-d-aspartate receptor function requires alpha-neurexins. *Proc Natl Acad Sci U S A*, 101(8):2607–12.

Kayser, M. S., McClelland, A. C., Hughes, E. G., and Dalva, M. B. (2006). Intracellular and trans-synaptic regulation of glutamatergic synaptogenesis by ephb receptors. *J Neurosci*, 26(47):12152–64.

Kayser, M. S., Nolt, M. J., and Dalva, M. B. (2008). Ephb receptors couple dendritic filopodia motility to synapse formation. *Neuron*, 59(1):56–69.

Kelleher, R. J., r., Govindarajan, A., and Tonegawa, S. (2004). Translational regulatory mechanisms in persistent forms of synaptic plasticity. *Neuron*, 44(1):59–73.

Kemp, A. and Manahan-Vaughan, D. (2007). Hippocampal long-term depression: master or minion in declarative memory processes? *Trends Neurosci*, 30(3):111–118.

Kerchner, G. A. and Nicoll, R. A. (2008). Silent synapses and the emergence of a postsynaptic mechanism for ltp. *Nat Rev Neurosci*, 9(11):813–25.

Kim, C.-H., Chung, H. J., Lee, H.-K., and Huganir, R. L. (2001). Interaction of the ampa receptor subunit glur2/3 with pdz domains regulates hippocampal long-term depression. *Proc Natl Acad Sci U S A*, 98(20):11725–11730.

Kim, E. and Sheng, M. (2004). Pdz domain proteins of synapses. *Nat Rev Neurosci*, 5(10):771–81.

Kim, J., Jung, S. Y., Lee, Y. K., Park, S., Choi, J. S., Lee, C. J., Kim, H. S., Choi, Y. B., Scheiffele, P., Bailey, C. H., Kandel, E. R., and Kim, J. H. (2008). Neuroligin-1 is required for normal expression of ltp and associative fear memory in the amygdala of

adult animals. *Proc Natl Acad Sci U S A*, 105(26):9087–92.

Klein, R. (2009). Bidirectional modulation of synaptic functions by eph/ephrin signaling. *Nat Neurosci*, 12(1):15–20.

Knott, G. W., Holtmaat, A., Wilbrecht, L., Welker, E., and Svoboda, K. (2006). Spine growth precedes synapse formation in the adult neocortex in vivo. *Nat Neurosci*, 9(9):1117–24.

Kramar, E. A., Bernard, J. A., Gall, C. M., and Lynch, G. (2003). Integrins modulate fast excitatory transmission at hippocampal synapses. *Journal of Biological Chemistry*, 278(12):10722–10730.

Kuramochi, M., Fukuhara, H., Nobukuni, T., Kanbe, T., Maruyama, T., Ghosh, H. P., Pletcher, M., Isomura, M., Onizuka, M., Kitamura, T., Sekiya, T., Reeves, R. H., and Murakami, Y. (2001). Tslc1 is a tumor-suppressor gene in human non-small-cell lung cancer. *Nat Genet*, 27(4):427–30.

Lambert, M., Choquet, D., and Mege, R. M. (2002). Dynamics of ligand-induced, rac1-dependent anchoring of cadherins to the actin cytoskeleton. *J Cell Biol*, 157(3):469–79.

Lee, H.-K. (2006). Synaptic plasticity and phosphorylation. *Pharmacology and Therapeutics*, 112(3):810–832.

Lee, H. K., Kameyama, K., Huganir, R. L., and Bear, M. F. (1998). Nmda induces long-term synaptic depression and dephosphorylation of the glur1 subunit of ampa receptors in hippocampus. *Neuron*, 21(5):1151–62.

Lee, H. W., Choi, J., Shin, H., Kim, K., Yang, J., Na, M., Choi, S. Y., Kang, G. B., Eom, S. H., Kim, H., and Kim, E. (2008). Preso, a novel psd-95-interacting ferm and pdz domain protein that regulates dendritic spine morphogenesis. *J. Neurosci.*, 28(53):14546–14556.

Lee, S. H., Liu, L., Wang, Y. T., and Sheng, M. (2002). Clathrin adaptor ap2 and nsf interact with overlapping sites of glur2 and play distinct roles in ampa receptor trafficking and hippocampal ltd. *Neuron*, 36(4):661–74.

Li, C., Brake, W. G., Romeo, R. D., Dunlop, J. C., Gordon, M., Buzescu, R., Magarinos, A. M., Allen, P. B., Greengard, P., Luine, V., and McEwen, B. S. (2004). Estrogen alters hippocampal dendritic spine shape and enhances synaptic protein immunoreactivity and spatial memory in female mice. *Proc Natl Acad Sci U S A*, 101(7):2185–90.

Li, Z. and Sheng, M. (2003). Some assembly required: the development of neuronal synapses. *Nat Rev Mol Cell Biol*, 4(11):833–41.

Liao, D., Scannevin, R. H., and Huganir, R. (2001). Activation of silent synapses by rapid activity-dependent synaptic recruitment of ampa receptors. *J. Neurosci.*, 21(16):6008–6017.

Lin, B., Arai, A. C., Lynch, G., and Gall, C. M. (2003). Integrins regulate nmda receptor-

mediated synaptic currents. *J Neurophysiol*, 89(5):2874–8.

Lohmann, C., Finski, A., and Bonhoeffer, T. (2005). Local calcium transients regulate the spontaneous motility of dendritic filopodia. *Nat Neurosci*, 8(3):305–12.

Lyckman, A. W., Horng, S., Leamey, C. A., Tropea, D., Watakabe, A., Van Wart, A., McCurry, C., Yamamori, T., and Sur, M. (2008). Gene expression patterns in visual cortex during the critical period: synaptic stabilization and reversal by visual deprivation. *Proc Natl Acad Sci U S A*, 105(27):9409–14.

Malenka, R. C. (2003). Synaptic plasticity and ampa receptor trafficking. *Annals of the New York Academy of Sciences*, 1003(GLUTAMATE AND DISORDERS OF COGNITION AND MOTIVATION):1–11.

Malenka, R. C. and Bear, M. F. (2004). Ltp and ltd: an embarrassment of riches. *Neuron*, 44(1):5–21.

Malinow, R. and Malenka, R. C. (2002). Ampa receptor trafficking and synaptic plasticity. *Annu Rev Neurosci*, 25:103–26.

Mansuy, I. M. and Bujard, H. (2000). Tetracycline-regulated gene expression in the brain. *Curr Opin Neurobiol*, 10(5):593–6.

Mao, X., Seidlitz, E., Ghosh, K., Murakami, Y., and Ghosh, H. P. (2003). The cytoplasmic domain is critical to the tumor suppressor activity of tslc1 in non-small cell lung cancer. *Cancer Res*, 63(22):7979–85.

Maurel, P., Einheber, S., Galinska, J., Thaker, P., Lam, I., Rubin, M. B., Scherer, S. S., Murakami, Y., Gutmann, D. H., and Salzer, J. L. (2007). Nectin-like proteins mediate axon schwann cell interactions along the internode and are essential for myelination. *J Cell Biol*, 178(5):861–74.

Mayford, M., Bach, M. E., Huang, Y. Y., Wang, L., Hawkins, R. D., and Kandel, E. R. (1996). Control of memory formation through regulated expression of a camkii transgene. *Science*, 274(5293):1678–83.

McClelland, A. C., Sheffler-Collins, S. I., Kayser, M. S., and Dalva, M. B. (2009). Ephrin-b1 and ephrin-b2 mediate ephb-dependent presynaptic development via syntenin-1. *Proceedings of the National Academy of Sciences*, 106(48):20487–20492.

Miller, M. and Peters, A. (1981). Maturation of rat visual cortex. ii. a combined golgi-electron microscope study of pyramidal neurons. *J Comp Neurol*, 203(4):555–73.

Mulkey, R. M., Herron, C. E., and Malenka, R. C. (1993). An essential role for protein phosphatases in hippocampal long-term depression. *Science*, 261(5124):1051–5.

Nagerl, U. V., Eberhorn, N., Cambridge, S. B., and Bonhoeffer, T. (2004). Bidirectional activity-dependent morphological plasticity in hippocampal neurons. *Neuron*, 44(5):759–67.

Nicholls, R. E., Alarcon, J. M., Malleret, G., Carroll, R. C., Grody, M., Vronskaya, S., and Kandel, E. R. (2008). Transgenic mice

lacking nmdar-dependent ltd exhibit deficits in behavioral flexibility. *Neuron*, 58(1):104–17.

Noel, J., Ralph, G. S., Pickard, L., Williams, J., Molnar, E., Uney, J. B., Collingridge, G. L., and Henley, J. M. (1999). Surface expression of ampa receptors in hippocampal neurons is regulated by an nsf-dependent mechanism. *Neuron*, 23(2):365–376.

Okamoto, M. and Sudhof, T. C. (1997). Mints, munc18-interacting proteins in synaptic vesicle exocytosis. *J Biol Chem*, 272(50):31459–64.

Oliet, S. H., Malenka, R. C., and Nicoll, R. A. (1997). Two distinct forms of long-term depression coexist in ca1 hippocampal pyramidal cells. *Neuron*, 18(6):969–82.

Pastalkova, E., Serrano, P., Pinkhasova, D., Wallace, E., Fenton, A. A., and Sacktor, T. C. (2006). Storage of spatial information by the maintenance mechanism of ltp. *Science*, 313(5790):1141–1144.

Piccinin, S., Cinque, C., Calo, L., Molinaro, G., Battaglia, G., Maggi, L., Nicoletti, F., Melchiorri, D., Eusebi, F., Massey, P. V., and Bashir, Z. I. (2010). Interaction between ephrins and mglu5 metabotropic glutamate receptors in the induction of long-term synaptic depression in the hippocampus. *J. Neurosci.*, 30(8):2835–2843.

Pietri, T., Easley-Neal, C., Wilson, C., and Washbourne, P. (2008). Six cadm/syncam genes are expressed in the nervous system of developing zebrafish. *Dev Dyn*, 237(1):233–46.

Plant, K., Pelkey, K. A., Bortolotto, Z. A., Morita, D., Terashima, A., McBain, C. J., Collingridge, G. L., and Isaac, J. T. (2006). Transient incorporation of native glur2-lacking ampa receptors during hippocampal long-term potentiation. *Nat Neurosci*, 9(5):602–4.

Rabenstein, R. L., Addy, N. A., Caldarone, B. J., Asaka, Y., Gruenbaum, L. M., Peters, L. L., Gilligan, D. M., Fitzsimonds, R. M., and Picciotto, M. R. (2005). Impaired synaptic plasticity and learning in mice lacking beta-adducin, an actin-regulating protein. *J Neurosci*, 25(8):2138–45.

Raghavachari, S. and Lisman, J. E. (2004). Properties of quantal transmission at ca1 synapses. *J Neurophysiol*, 92(4):2456–67.

Rosahl, T. W., Spillane, D., Missler, M., Herz, J., Selig, D. K., Wolff, J. R., Hammer, R. E., Malenka, R. C., and Sudhof, T. C. (1995). Essential functions of synapsins i and ii in synaptic vesicle regulation. *Nature*, 375(6531):488–93.

Rudenko, G., Nguyen, T., Chelliah, Y., Sudhof, T. C., and Deisenhofer, J. (1999). The structure of the ligand-binding domain of neurexin ibeta: regulation of lns domain function by alternative splicing. *Cell*, 99(1):93–101.

Sara, Y., Biederer, T., Atasoy, D., Chubykin, A., Mozhayeva, M. G., Sudhof, T. C., and Kavalali, E. T. (2005). Selective capabil-

ity of syncam and neuroligin for functional synapse assembly. *J Neurosci*, 25(1):260–70.

Scheiffele, P., Fan, J., Choih, J., Fetter, R., and Serafini, T. (2000). Neuroligin expressed in nonneuronal cells triggers presynaptic development in contacting axons. *Cell*, 101(6):657–69.

Schuh, K., Uldrijan, S., Gambaryan, S., Roethlein, N., and Neyses, L. (2003). Interaction of the plasma membrane ca2+ pump 4b/ci with the ca2+/calmodulin-dependent membrane-associated kinase cask. *Journal of Biological Chemistry*, 278(11):9778–9783.

Scoville, W. B. and Milner, B. (1957). Loss of recent memory after bilateral hippocampal lesions. *J Neurol Neurosurg Psychiatry*, 20(1):11–21.

Seidenman, K. J., Steinberg, J. P., Huganir, R., and Malinow, R. (2003). Glutamate receptor subunit 2 serine 880 phosphorylation modulates synaptic transmission and mediates plasticity in ca1 pyramidal cells. *J Neurosci*, 23(27):9220–8.

Setou, M., Nakagawa, T., Seog, D. H., and Hirokawa, N. (2000). Kinesin superfamily motor protein kif17 and mlin-10 in nmda receptor-containing vesicle transport. *Science*, 288(5472):1796–802.

Setou, M., Seog, D. H., Tanaka, Y., Kanai, Y., Takei, Y., Kawagishi, M., and Hirokawa, N. (2002). Glutamate-receptor-interacting protein grip1 directly steers kinesin to dendrites. *Nature*, 417(6884):83–7.

Shapira, M., Zhai, R. G., Dresbach, T., Bresler, T., Torres, V. I., Gundelfinger, E. D., Ziv, N. E., and Garner, C. C. (2003). Unitary assembly of presynaptic active zones from piccolo-bassoon transport vesicles. *Neuron*, 38(2):237–52.

Shapiro, L. and Colman, D. R. (1999). The diversity of cadherins and implications for a synaptic adhesive code in the cns. *Neuron*, 23(3):427–30.

Sheng, M. and Sala, C. (2001). Pdz domains and the organization of supramolecular complexes. *Annu Rev Neurosci*, 24:1–29.

Shi, Y. and Ethell, I. M. (2006). Integrins control dendritic spine plasticity in hippocampal neurons through nmda receptor and ca2+/calmodulin-dependent protein kinase ii-mediated actin reorganization. *J Neurosci*, 26(6):1813–22.

Shin, H., Wyszynski, M., Huh, K. H., Valtschanoff, J. G., Lee, J. R., Ko, J., Streuli, M., Weinberg, R. J., Sheng, M., and Kim, E. (2003). Association of the kinesin motor kif1a with the multimodular protein liprin-alpha. *J Biol Chem*, 278(13):11393–401.

Shingai, T., Ikeda, W., Kakunaga, S., Morimoto, K., Takekuni, K., Itoh, S., Satoh, K., Takeuchi, M., Imai, T., Monden, M., and Takai, Y. (2003). Implications of nectin-like molecule-2/igsf4/ra175/sgigsf/tslc1/syncam1 in cell-cell adhesion and transmembrane protein localization in epithelial cells. *J Biol Chem*, 278(37):35421–7.

Song, J. Y., Ichtchenko, K., Sudhof, T. C., and Brose, N. (1999). Neuroligin 1 is a postsynaptic cell-adhesion molecule of excitatory synapses. *Proc Natl Acad Sci U S A*, 96(3):1100–5.

Songyang, Z., Fanning, A. S., Fu, C., Xu, J., Marfatia, S. M., Chishti, A. H., Crompton, A., Chan, A. C., Anderson, J. M., and Cantley, L. C. (1997). Recognition of unique carboxyl-terminal motifs by distinct pdz domains. *Science*, 275(5296):73–7.

Sotelo, C. (1990). Cerebellar synaptogenesis: what we can learn from mutant mice. *J Exp Biol*, 153:225–49.

Spacek, J. (1985). Relationships between synaptic junctions, puncta adhaerentia and the spine apparatus at neocortical axo-spinous synapses. a serial section study. *Anat Embryol (Berl)*, 173(1):129–35.

Spiegel, I., Adamsky, K., Eshed, Y., Milo, R., Sabanay, H., Sarig-Nadir, O., Horresh, I., Scherer, S. S., Rasband, M. N., and Peles, E. (2007). A central role for necl4 (syncam4) in schwann cell-axon interaction and myelination. *Nat Neurosci*, 10(7):861–9.

Sprouston, N. and McBain, C. J. (2007). Structural and functional properties of hippocampal neurons. *The Hippocampus Book*, page 315.

Sudhof, T. C. (2004). The synaptic vesicle cycle. *Annu Rev Neurosci*, 27:509–47.

Sudhof, T. C. (2008). Neuroligins and neurexins link synaptic function to cognitive disease. *Nature*, 455(7215):903–11.

Sudhof, T. C. and Rothman, J. E. (2009). Membrane fusion: grappling with snare and sm proteins. *Science*, 323(5913):474–7.

Taniguchi, H., Gollan, L., Scholl, F. G., Mahadomrongkul, V., Dobler, E., Limthong, N., Peck, M., Aoki, C., and Scheiffele, P. (2007). Silencing of neuroligin function by postsynaptic neurexins. *J Neurosci*, 27(11):2815–24.

Terashima, A., Cotton, L., Dev, K. K., Meyer, G., Zaman, S., Duprat, F., Henley, J. M., Collingridge, G. L., and Isaac, J. T. (2004). Regulation of synaptic strength and ampa receptor subunit composition by pick1. *J Neurosci*, 24(23):5381–90.

Terashima, A., Pelkey, K. A., Rah, J. C., Suh, Y. H., Roche, K. W., Collingridge, G. L., McBain, C. J., and Isaac, J. T. (2008). An essential role for pick1 in nmda receptor-dependent bidirectional synaptic plasticity. *Neuron*, 57(6):872–82.

Thomas, L. A., Akins, M. R., and Biederer, T. (2008). Expression and adhesion profiles of syncam molecules indicate distinct neuronal functions. *J Comp Neurol*, 510(1):47–67.

Thorsen, T. S., Madsen, K. L., Rebola, N., Rathje, M., Anggono, V., Bach, A., Moreira, I. S., Stuhr-Hansen, N., Dyhring, T., Peters, D., Beuming, T., Huganir, R., Weinstein, H., Mulle, C., Stromgaard, K., Ronn, L. C., and Gether, U. (2010). Identification of a small-molecule inhibitor of the pick1 pdz domain that inhibits hippocampal ltp and ltd. *Proc Natl Acad Sci U S A*, 107(1):413–8.

Togashi, H., Abe, K., Mizoguchi, A., Takaoka, K., Chisaka, O., and Takeichi, M. (2002). Cadherin regulates dendritic spine morphogenesis. *Neuron*, 35(1):77–89.

Tomita, S., Shenoy, A., Fukata, Y., Nicoll, R. A., and Bredt, D. S. (2007). Stargazin interacts functionally with the ampa receptor glutamate-binding module. *Neuropharmacology*, 52(1):87–91.

Treves, A., Tashiro, A., Witter, M. E., and Moser, E. I. (2008). What is the mammalian dentate gyrus good for? *Neuroscience*, 154(4):1155–72.

Ullrich, B., Ushkaryov, Y. A., and Sudhof, T. C. (1995). Cartography of neurexins: more than 1000 isoforms generated by alternative splicing and expressed in distinct subsets of neurons. *Neuron*, 14(3):497–507.

Urase, K., Soyama, A., Fujita, E., and Momoi, T. (2001). Expression of ra175 mrna, a new member of the immunoglobulin superfamily, in developing mouse brain. *Neuroreport*, 12(15):3217–21.

Ushkaryov, Y. A., Petrenko, A. G., Geppert, M., and Sudhof, T. C. (1992). Neurexins: synaptic cell surface proteins related to the alpha-latrotoxin receptor and laminin. *Science*, 257(5066):50–6.

van der Weyden, L., Arends, M. J., Chausiaux, O. E., Ellis, P. J., Lange, U. C., Surani, M. A., Affara, N., Murakami, Y., Adams, D. J., and Bradley, A. (2006). Loss of tslc1 causes male infertility due to a defect at the spermatid stage of spermatogenesis. *Mol Cell Biol*, 26(9):3595–609.

Varoqueaux, F., Aramuni, G., Rawson, R. L., Mohrmann, R., Missler, M., Gottmann, K., Zhang, W., Sudhof, T. C., and Brose, N. (2006). Neuroligins determine synapse maturation and function. *Neuron*, 51(6):741–54.

Waites, C. L., Craig, A. M., and Garner, C. C. (2005). Mechanisms of vertebrate synaptogenesis. *Annu Rev Neurosci*, 28:251–74.

Walensky, L. D., Blackshaw, S., Liao, D., Watkins, C. C., Weier, H. U., Parra, M., Huganir, R. L., Conboy, J. G., Mohandas, N., and Snyder, S. H. (1999). A novel neuron-enriched homolog of the erythrocyte membrane cytoskeletal protein 4.1. *J Neurosci*, 19(15):6457–67.

Walensky, L. D., Shi, Z. T., Blackshaw, S., DeVries, A. C., Demas, G. E., Gascard, P., Nelson, R. J., Conboy, J. G., Rubin, E. M., Snyder, S. H., and Mohandas, N. (1998). Neurobehavioral deficits in mice lacking the erythrocyte membrane cytoskeletal protein 4.1. *Curr Biol*, 8(23):1269–72.

Wang, J., Arora, A., Yang, L., Parelkar, N., Zhang, G., Liu, X., Choe, E., and Mao, L. (2005). Phosphorylation of ampa receptors. *Mol Neurobiol*, 32(3):237–249.

Wang, X., Weiner, J. A., Levi, S., Craig, A. M., Bradley, A., and Sanes, J. R. (2002). Gamma protocadherins are required for survival of spinal interneurons. *Neuron*, 36(5):843–54.

Wang, Y. T. and Linden, D. J. (2000). Ex-

pression of cerebellar long-term depression requires postsynaptic clathrin-mediated endocytosis. *Neuron*, 25(3):635–647.

Weiner, J. A., Wang, X., Tapia, J. C., and Sanes, J. R. (2005). Gamma protocadherins are required for synaptic development in the spinal cord. *Proc Natl Acad Sci U S A*, 102(1):8–14.

Wenthold, R. J., Petralia, R. S., Blahos, J., I., and Niedzielski, A. S. (1996). Evidence for multiple ampa receptor complexes in hippocampal ca1/ca2 neurons. *J Neurosci*, 16(6):1982–9.

Whitlock, J. R., Heynen, A. J., Shuler, M. G., and Bear, M. F. (2006). Learning induces long-term potentiation in the hippocampus. *Science*, 313(5790):1093–1097.

Wittenmayer, N., Korber, C., Liu, H., Kremer, T., Varoqueaux, F., Chapman, E. R., Brose, N., Kuner, T., and Dresbach, T. (2009). Postsynaptic neuroligin1 regulates presynaptic maturation. *Proc Natl Acad Sci U S A*, 106(32):13564–9.

Xia, J., Zhang, X., Staudinger, J., and Huganir, R. L. (1999). Clustering of ampa receptors by the synaptic pdz domain-containing protein pick1. *Neuron*, 22(1):179–87.

Yageta, M., Kuramochi, M., Masuda, M., Fukami, T., Fukuhara, H., Maruyama, T., Shibuya, M., and Murakami, Y. (2002). Direct association of tslc1 and dal-1, two distinct tumor suppressor proteins in lung cancer. *Cancer Res*, 62(18):5129–33.

Yuste, R. and Bonhoeffer, T. (2004). Genesis of dendritic spines: insights from ultrastructural and imaging studies. *Nat Rev Neurosci*, 5(1):24–34.

Zhang, H. and Macara, I. G. (2006). The polarity protein par-3 and tiam1 cooperate in dendritic spine morphogenesis. *Nat Cell Biol*, 8(3):227–237.

Zhou, Q., Homma, K. J., and Poo, M.-m. (2004). Shrinkage of dendritic spines associated with long-term depression of hippocampal synapses. *Neuron*, 44(5):749–757.

Ziegler, W. H., Gingras, A. R., Critchley, D. R., and Emsley, J. (2008). Integrin connections to the cytoskeleton through talin and vinculin. *Biochemical Society Transactions*, 036(2):235–239.

Ziff, E. B. (2007). Tarps and the ampa receptor trafficking paradox. *Neuron*, 53(5):627–633.

Ziv, N. E. and Garner, C. C. (2004). Cellular and molecular mechanisms of presynaptic assembly. *Nat Rev Neurosci*, 5(5):385–99.

Zou, J. X., Wang, B., Kalo, M. S., Zisch, A. H., Pasquale, E. B., and Ruoslahti, E. (1999). An eph receptor regulates integrin activity through r-ras. *Proc Natl Acad Sci U S A*, 96(24):13813–13818.

Acknowledgements

Foremost, I thank my supervisor Valentin Stein for the opportunity to work in his lab and take on this project. Valentin nourished my fascination for neuroscience and turned me into a neuroscientist and electrophysiologist. Without Valentin, I would not have learned programming much of the data analysis tools in MATLAB and it was great that he tought me the most basic and also more advanced programming. I am very thankful for having found a supervisor who has always taken his time to discuss, to help when needed and who has been very supportive altogether. Nancy Meyer, Andrea Gruschka and the animal house staff helped a lot with my colonies of mice and also helped to keep the lab running. I am thankful to all members of the Stein lab for the enjoyable lunch and coffee breaks. I am also thankful to Clara Essmann who helped with the preparation of dissociated neuronal cultures in the very first days of this project.

Special thanks go to Thomas Biederer, Elissa M. Robbins and Adam I. Fogel who have been great collaborators in the entire work presented here. Despite the big pond and a couple of hours time difference between us, I am still happy about the way this collaboration worked, about the knowledge we generated together, which finally resulted in a project at least I am still proud of (and I guess your are, too).

I thank Mark Hübener for serving as "Doktorvater". Rüdiger Klein and Alessandre Ferrao-Santos were members of my thesis committee who followed this project throughout and gave valuable advice. Helmut W. Klein and Denis I. Crane shared their fascination for science in general and for biochemistry in particular and took me by the hand when I did the first careful steps into the world of science. I am grateful to Herbert Schuster who has been a great mentor since we first met almost 10 years ago.

Above all I want to thank my family for their support and love. I am equally thankful to Friederike for making every single day special and for her admirable skill to compensate my moodiness caused by all the little scientific and non-scientific setbacks. The crowd of people who make life as good as it is would not be complete without these close friends who have shared my happiest and sadest moments. Thank you, Claus, Totti, Felix, Guido, Henna, Tina, Dani, Maize, Moe, and Natalie.

Publications

Articles

Fogel, A. I., **Krupp, A. J.**, Akins, M. R., Stagi,M., Stein, V., and Biederer, T. (2007). Syncams organize synapses through heterophilic adhesion. *J Neurosci 27(46):12516-30*

Krupp, A. J., Robbins, E.M., Ghosh, A. K., Fogel, A. I., Boucard, A., Südhof, T.C., Biederer, T., and Stein, V. (2010). SynCAM1 Adhesion Dynamically Regulates Synapse Number and Impacts Plasticity and Learning. *Neuron, manuscript accepted for publication*

Posters and Abstracts

Fogel, A. I., **Krupp, A. J.**, Akins, M. R., Stagi, M., Biederer, T., and Stein, V. (2007). SynCAMs Organize Nascent Synapses Through Heterophilic Adhesion. *2nd Westerburg Symposium "Molecular dynamics of the chemical synapse". Abstract, Westerburg, Germany*

Krupp, A. J., Fogel, A. I., Akins, M. R., Stagi, M., Biederer, T., and Stein, V. (2007). Make Me Think — A Putative Promoter of Synapse Formation. *Annual Meeting of the Munich Life Science Community. Abstract, Munich, Germany*

Krupp, A. J., Robbins, E.M., Südhof, T.C., Biederer, T., and Stein, V. (2009). SynCAM1 Controls Synapse Formation and Maintenance. *Annual Meeting of the German Society of Neuroscience. Abstract, Göttingen, Germany*

Krupp, A. J., Robbins, E.M., Ghosh, A. K., Fogel, A. I., Boucard, A., Südhof, T.C., Biederer, T., and Stein, V. (2010). SynCAM1 Adhesion Dynamically Regulates Synapse Number and Impacts Plasticity and Learning. *Annual Meeting of the Federation of European Neuroscience Societies (FENS). Abstract, Amsterdam, Netherlands*